ARIZONA GEOTHERMAL ENERGY APPRAISAL STUDIES FINAL REPORT

Arizona Geological Survey
Open-File Report 80-1

March, 1980

Arizona Geological Survey
416 W. Congress, Suite #100, Tucson, Arizona 85701

BUREAU OF GEOLOGY AND MINERAL TECHNOLOGY
GEOLOGICAL SURVEY BRANCH GEOTHERMAL GROUP

NEW MEXICO STATE UNIVERSITY
DEPARTMENT OF PHYSICS AND EARTH SCIENCES

UNIVERSITY OF TEXAS-EL PASO
DEPARTMENT OF GEOLOGICAL SCIENCES
KIDD MEMORIAL SEISMIC OBSERVATORY

UNIVERSITY OF ARIZONA GEOSCIENCES DEPARTMENT

Prepared for the U.S. Department of the Interior
Water and Power Resource Service, and in conjunction with the
Department of Energy, Division of Geothermal Energy, under
Contract EG-77-S-02-4362

This report is preliminary and has not been edited
or reviewed for conformity with Arizona Geological Survey standards

TABLE OF CONTENTS

Executive Summary W. R. Hahman, Sr.	ii, iii, iv
Analysis of Short Term Microearthquake Activity Related to Potential Geothermal Areas in Arizona Dr. Marc L. Sbar University of Arizona	v, vi, 1
Geochemical Studies in Arizona Dr. Chandler A. Swanberg New Mexico State University	12
Geoelectrical Studies Near Springerville, Arizona Dr. Charles T. Young New Mexico State University	16
Interim Technical Report: Implications of a Refraction Profile Study for Geothermal Potential, Eastern and Central Arizona Dr. Marc L. Sbar and Don M. Gish University of Arizona	58
Potential for Geothermal Desalination in the Southwest United States Dr. Chandler A. Swanberg Sandra M. Rybarczyk New Mexico State University	67
A List of all Waters in Arizona with Temperatures in Excess of 30°C: Compiled from the WATSTORE File Dr. Chandler A. Swanberg New Mexico State University	77
Springerville, Arizona: Results of Heatflow Drilling Claudia Stone Bureau of Geology & Mineral Technology Geology Survey Branch, Geothermal Group	100
Heat Flow and the Thermal Regime in the Clifton, Arizona Area James C. Witcher and Claudia Stone Bureau of Geology & Mineral Technology Geological Survey Branch, Geothermal Group	117

Executive Summary

This text presents the results of the investigations for geothermal energy resources in the Springerville and Clifton areas of Arizona. The investigations focused on identifying potential geothermal resources with temperatures suitable for use in desalination plants. The resulting purified water would be used to augment Arizona's water supply.

The result of geological, geochemical and geophysical investigations in the two areas, as well as the results of preliminary heat-flow studies are presented. Two additional studies are included in this report to augment the site-specific data. These latter two studies are a refraction profile survey for geothermal energy in eastern and central Arizona and a tabulation of all waters in Arizona with temperatures in excess of 30°C. The water-temperature data were extracted from the U.S. Geological Survey WATSTORE file.

One of the geophysical investigations was a passive seismic survey for the detection of microearthquakes, one of the generalized characteristics of most moderate to high temperature (in excess of 150°C) geothermal resource areas. No microearthquake activity was recorded in either Springerville or Clifton during the two week study time in each area. Because microearthquakes usually occur in swarms, and an area can be totally quiet for months during the time between swarms, our conclusion is that the two-week monitoring period was of insufficient duration to determine whether microearthquake activity is in fact occurring in either area.

It is recommended that future microseismic investigations be of at least twelve months' duration.

Geoelectrical studies near Springerville, Arizona, produced favorable results. Saline water (high total dissolved solids) is an excellent conductor of electricity and can be reflected in a geoelectrical study as a d.c. resistivity low. Since geothermal waters generally have higher salinity than nongeothermal waters, electrical studies are often useful in geothermal exploration. In the Springerville area a saline-fresh groundwater interface is known to occur between Springerville and St. Johns to the north. A d.c. resistivity low was identified near Greer, west of Springerville, which could be indicative of geothermal fluids. In addition, a broad d.c. resistivity low coincident with a telluric current low and a Bouguer gravity low was identified south of Springerville near Alpine, Arizona. Preliminary exploration of these anomalies was then undertaken. The results of these further studies, primarily heat flow drilling, are very promising but inconclusive. The data show an anomaly is present but the resource intensity, magnitude, and reservoir have yet to be determined.

Hot springs in the Clifton area are the hottest in Arizona, 66-82°C (150-180°F), and they have some of the highest calculated geothermometers, 130-180°C (265-356°F), in the southwestern United States. Only the Jamez Mountains, New Mexico, and Imperial Valley, California, exceed these values. Arizona's two KGRAs, Clifton Hot Springs and Gillard Hot Springs, are located in this area.

The hot springs discharge sodium chloride water and deteriotate the chemical quality of the San Francisco and Gila rivers, making the Clifton area a prime target for geothermal desalination and water supply augmentation. A thriving and expanding mining industry in the area could use the excess water. Farmers downstream in the Safford Valley would benefit from the improved chemical quality of the Gila River.

The heat flow investigations at Clifton were undertaken to assist the geological exploration program for resource definition. Three heat flow measurements are detailed in the Clifton section of this report. Analysis of the data shows that the regional heat flow, believed to be 2.25 HFU in this area, is masked by the movement of large volumes of near-surface groundwater. The lower values measured in this study, compared to the regional heat flow, probably result from lateral or downward flow of ground water, which may recharge the hot spring-geothermal convection system(s). The convection systems are apparently heated by regional heat flow, although a hypothetical magmatic heat source masked by groundwater flow has not been ruled out.

In summary, the preliminary resource evaluations in both the Springerville and Clifton areas are most favorable. Both areas warrant feasibility studies to define the resources, prior to the preproduction and production stages of development.

AMERICAN INSTITUTE OF PROFESSIONAL GEOLOGISTS
CERTIFICATE NUMBER
2764
AIPG
W. R. HAHMAN, SR.

W. Richard Hahman, Sr. CPGS
Geologist
Geothermal Project Manager

ANALYSIS OF SHORT TERM MICROEARTHQUAKE ACTIVITY RELATED TO POTENTIAL GEOTHERMAL AREAS IN ARIZONA

Technical Report

to

Geothermal Group
State of Arizona
Bureau of Geology and Mineral Technology

by

Marc L. Sbar
Assistant Professor, Dept. of Geosciences
University of Arizona

May 8, 1979

The views and conclusions contained in this document are those of the author and should not be interpreted as necessarily representing the official policies, either expressed or implied of the Arizona Bureau of Geology and Mineral Technology.

Interpretations and conclusions in this report are those of the consultant and do not necessarily coincide with those of the staff of the Bureau of Geology and Mineral Technology.

ABSTRACT

A minimum of twelve high sensitivity microearthquake instruments were operated for two week periods in the San Bernardino, Clifton-Safford - Morenci, and Springerville - St. Johns areas of Arizona during the Summer of 1978. The purpose of this program was to assess the seismicity of these areas and to relate any earthquakes detected to faulting and the regional tectonics of the areas. Only one earthquake, which was located in the southern part of the San Bernardino area, was recorded. This activity is less than that observed during the same summer in Prescott, Arizona and in the southern extension of the San Bernardino valley, into northern Sonora. It is evident that a two week period is not adequate to properly assess the seismicity of these areas.

ANALYSIS OF SHORT TERM MICROEARTHQUAKE ACTIVITY RELATED TO POTENTIAL GEOTHERMAL AREAS IN ARIZONA

INTRODUCTION

Shallow microearthquake activity of the swarm type (no single large event but rather many events of the maximum size observed), is often associated with geothermal areas. Yellowstone and the Imperial valley in California are examples of this behavior. The activity is shallow (5 km or less) because the temperature below this depth is thought to be high enough to enable rocks to yield by ductile failure rather than in a brittle mode. Earthquake swarm behavior may be related to the heterogeniety of the stress field, which in turn may be controlled by repeated failure of the rocks due to high thermal gradients. A heterogeneous stress field does not provide a sufficiently large uniform area of high stress for large earthquakes to occur. Instead local regions of stress concentration fail separately, triggering nearby regions into failure and so on, producing a swarm of earthquakes. Earthquake swarms are commonly found in volcanic areas. An association with geothermal regions is therefore logical and expected.

Nonetheless, not all geothermal areas exhibit microearthquake activity. We can rationalize this within the above model by simply stating that these areas are (1) too hot at all depths for earthquakes to occur, (2) the regional tectonic stresses are too low, or (3) these are not pre-existing faults of the proper orientation to permit failure.

The second possibility seems most reasonable for Arizona. If microearthquake activity were identified in an area, we could use it to locate active faults. These in turn might act as conduits for hot fluids. We would also be in a position to interpret the local stress

field and evaluate the seismic hazard to any development in the region.

With this background in mind, we embarked on a study of potential geothermal areas in Arizona. A glance at the historic seismicity of the State (Figure 1) and reference to other microearthquake work done in the northern part of Arizona (Sbar et al., 1972) indicate that we might be able to record one event every one or two days on the average. We also assumed that it was possible for areas of swarm type seismicity to exist, but to have had no earthquake large enough to have been felt or recorded by the sparse distribution of seismic stations in this area.

PROGRAM

Three areas of interest were outlined by the Geothermal Group of the Arizona Bureau of Geology and Mineral Technology: San Bernardino, Clifton - Safford - Morenci, and Springerville - St. Johns. Since we only have eight portable seismographs, it was decided to join forces with groups from the University of New Mexico at Las Cruces and the University of Texas at El Paso. They were under contract with Los Alamos Scientific Laboratory to investigate other potential geothermal areas in Arizona and New Mexico, namely the Aquarius Mountains area and an area to the east of St. Johns (see Figure 2). We also assisted them with refraction profiles in New Mexico. A schedule of the areas studied and the number of instruments used in each is shown in Figure 3.

We operated for approximately two-week intervals in each of the areas of interest to the Arizona Bureau of Geology. Because of the UTEP group's prior commitments, we had twelve instruments available for the San Bernardino area. Nineteen instruments were then deployed in both the Clifton and Springerville - St. Johns area. During late July and early August, the instruments were divided between the

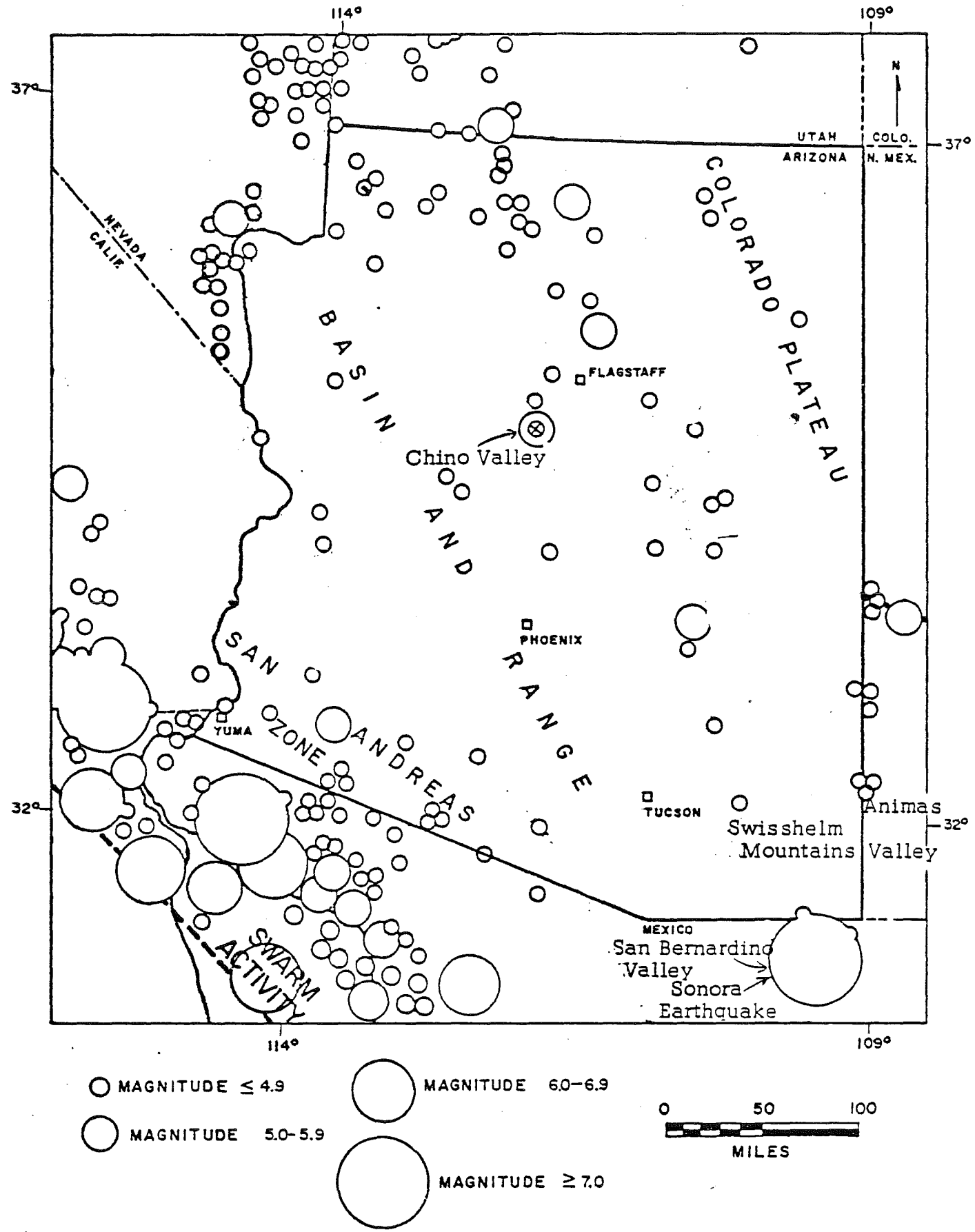

Figure 1. Seimicity of Arizona from 1850 to 1976.

Adapted from Sumner, 1976.

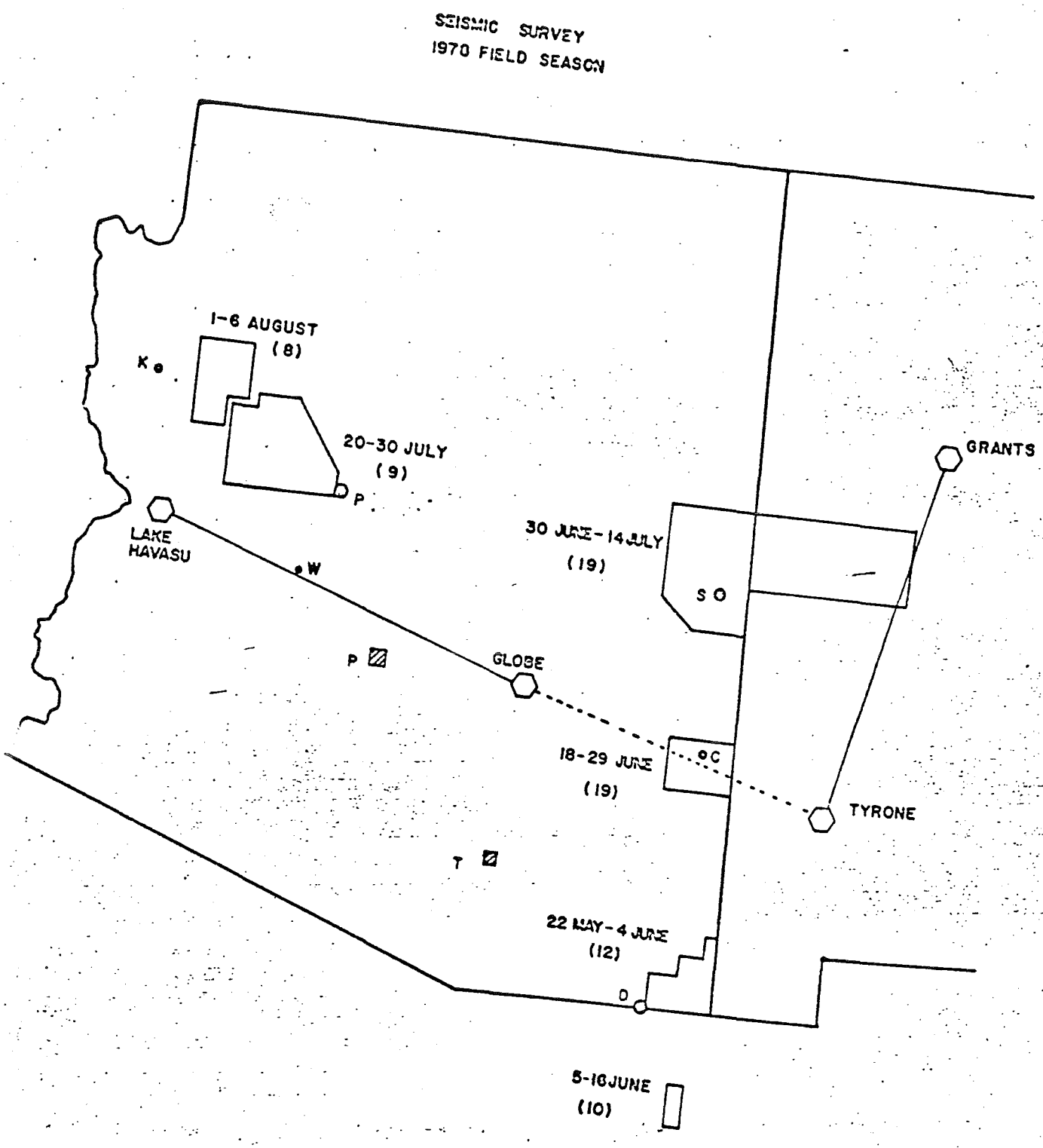

Figure 2. Areas surveyed during summer 1978. Cities are shown by letters. D - Douglas, C - Clifton, S - Springerville, T - Tucson, P - Phoenix (square), P - Prescott (circle), K - Kingman, and W - Wickenburg. The San Bernardo area is east of Douglas and the Aquarius Mountains are just east of Kingman. The refraction lines completed during the summer is between Grants and Tyrone.

Aquarius Mountains microearthquake study and a refraction profile between Tyrone and Grants, New Mexico.

As a separate project funded by the National Science Foundation, ten instruments were used to monitor the residual activity associated with northern Sonora's magnitude 7-7 1/2 earthquake of 1887. The monitoring (6-16 June, 1978) occurred a mere 60 km south of Arizona's San Bernardino Geothermal Prospect. The significantly higher level of seismic activity will be compared in this paper with the other areas studied.

INSTRUMENTATION

Both Sprengnether MEQ 800's and Geotech Portacorders were used as the primary instruments for microearthquake detection. Under optimum conditions, the recorded traces on these smoked-drum recorders magnified ground motion by 5 million times at a frequency of 10 Hz. At lower frequencies (1 Hz), this gain typically rolled off to between 300,000 and 600,000 times ground displacement. Most of the seismic signal generated by micro-earthquakes occurs in this frequency band (between 1 and 10 Hz). To provide high-resolution information that can be readily analyzed by computer, five Sprengnether and one Terra-Technology three-component digital recorders were operated alongside smoked-drum recorders.

The instruments were spaced about 10 to 15 km apart in the San Bernardino and Clifton areas and about 20 km apart in Springerville. It is difficult to accurately determine the detection capability of the networks at such short hypocentral distances, since the attenuation characteristics of the local region are unknown. We estimate, using a formula from Brune and Allen (1967), that a single station operating at a gain of 2.5 million can detect a magnitude 0

event at a distance of 10 km. Thus, at the above station spacing, a magnitude 0 is an approximate threshold for the detection capability of the networks operated.

RESULTS

Of the three areas of interest, San Bernardino, Clifton and Springerville, only one microearthquake was recorded, and that was in the southern part of the San Bernardino area near the Mexican border (Figure 4). The seismogram and location are shown in Figure 5. This is in marked contrast to the San Bernardino valley's southern extension into Sonora, Mexico. Along the 1887 Fault scarp, sixteen events were recorded during a ten-day period. This tremendous variation in seismic activity within the same valley is puzzling, and remains to be explained. Furthermore, in the Aquarius Mountains region near Prescott, six events were recorded by the nine-station network during an eleven-day period. Three of these were outside the networks and were poorly located (Figure 6). At all of the stations mine blasts were routinely recorded indicating proper operation of the equipment. Precise depths cannot be determined from the available data, since the velocity structure of the region is poorly known. They appear, however, to be in the normal range for earthquakes in the Basin and Range Province (0-15 km).

Before trying to make some statements about the implications of these results, it should be noted that microearthquake activity in the western United States is sporadic and that two weeks of recording is not sufficient to characterize the activity of a region. For the short time interval of the sample the three areas of interest are essentially aseismic. They are certainly less active than the Prescott and San

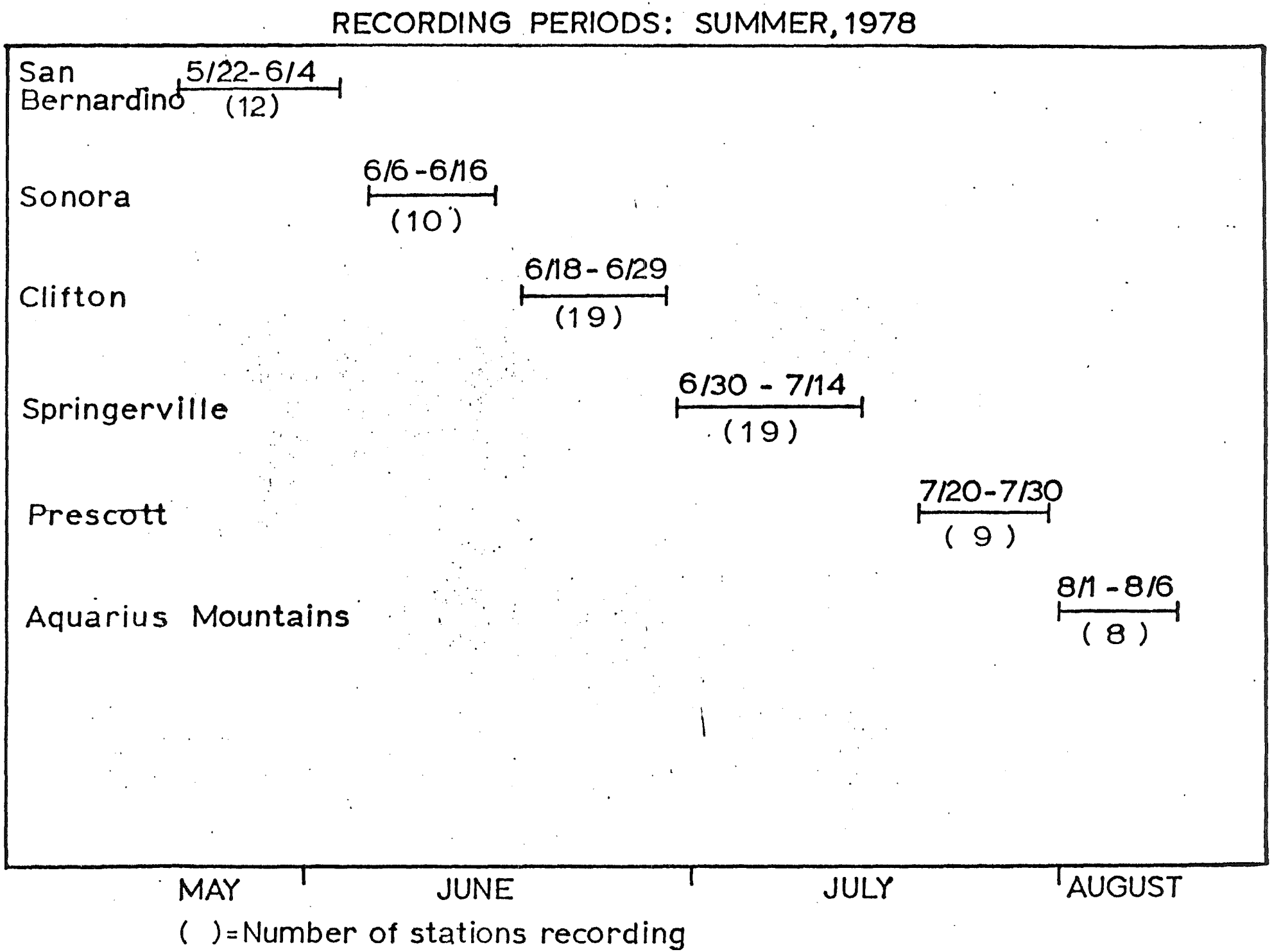
RECORDING PERIODS: SUMMER, 1978
San Bernardino
5/22-6/4
(12)
Sonora
6/6-6/16
(10)
Clifton
6/18-6/29
(19)
Springerville
6/30 - 7/14
(19)
Prescott
7/20-7/30
(9)
Aquarius Mountains
8/1 - 8/6
(8)
MAY
JUNE
JULY
AUGUST
( )=Number of stations recording

Fig. 3.

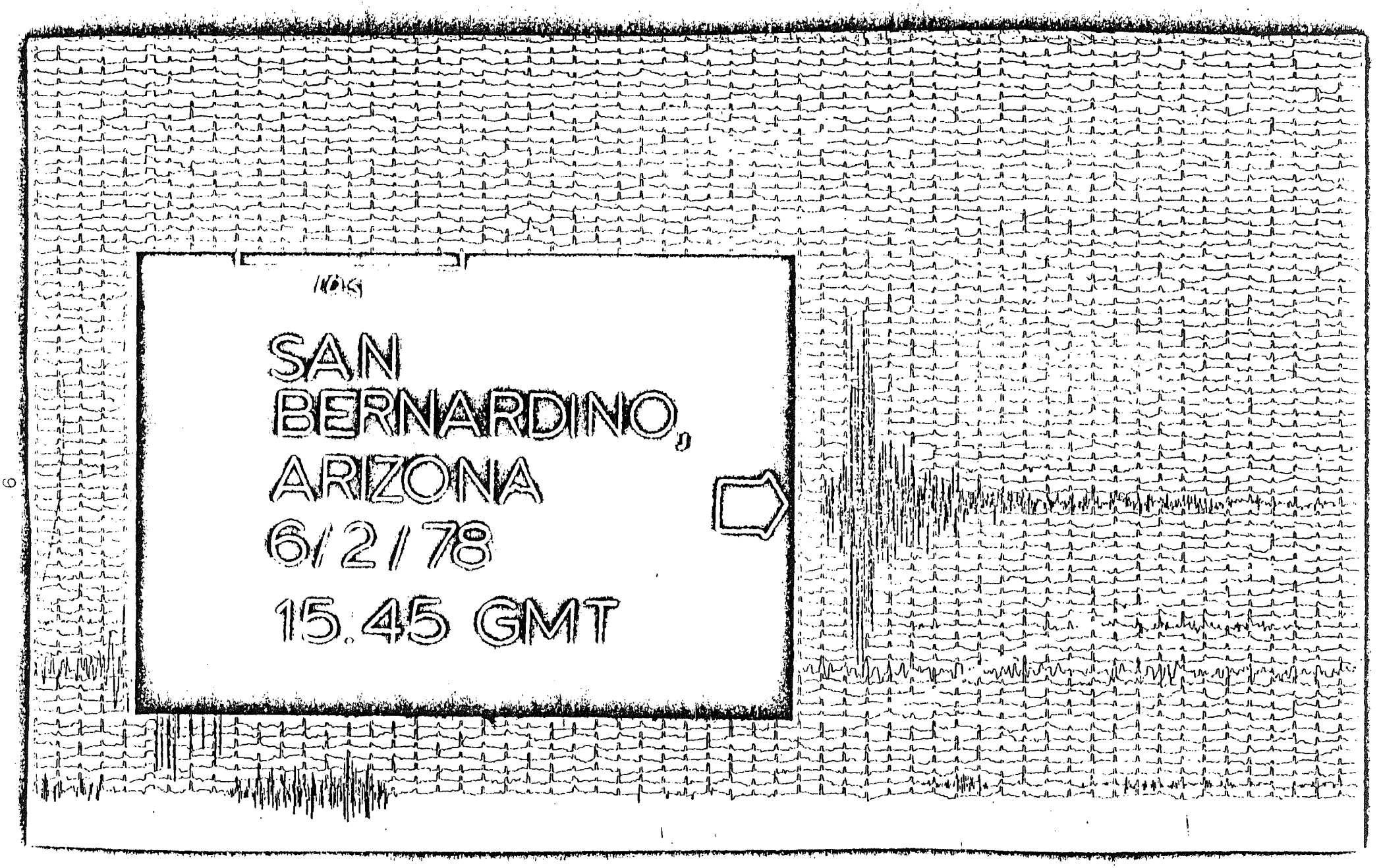

Figure 5. Earthquake recorded on Station MGF in San Bernardino Valley, Arizona. See Figure 4 for location of event.

Fig. 4.

SAN BERNARDINO VALLEY, ARIZONA

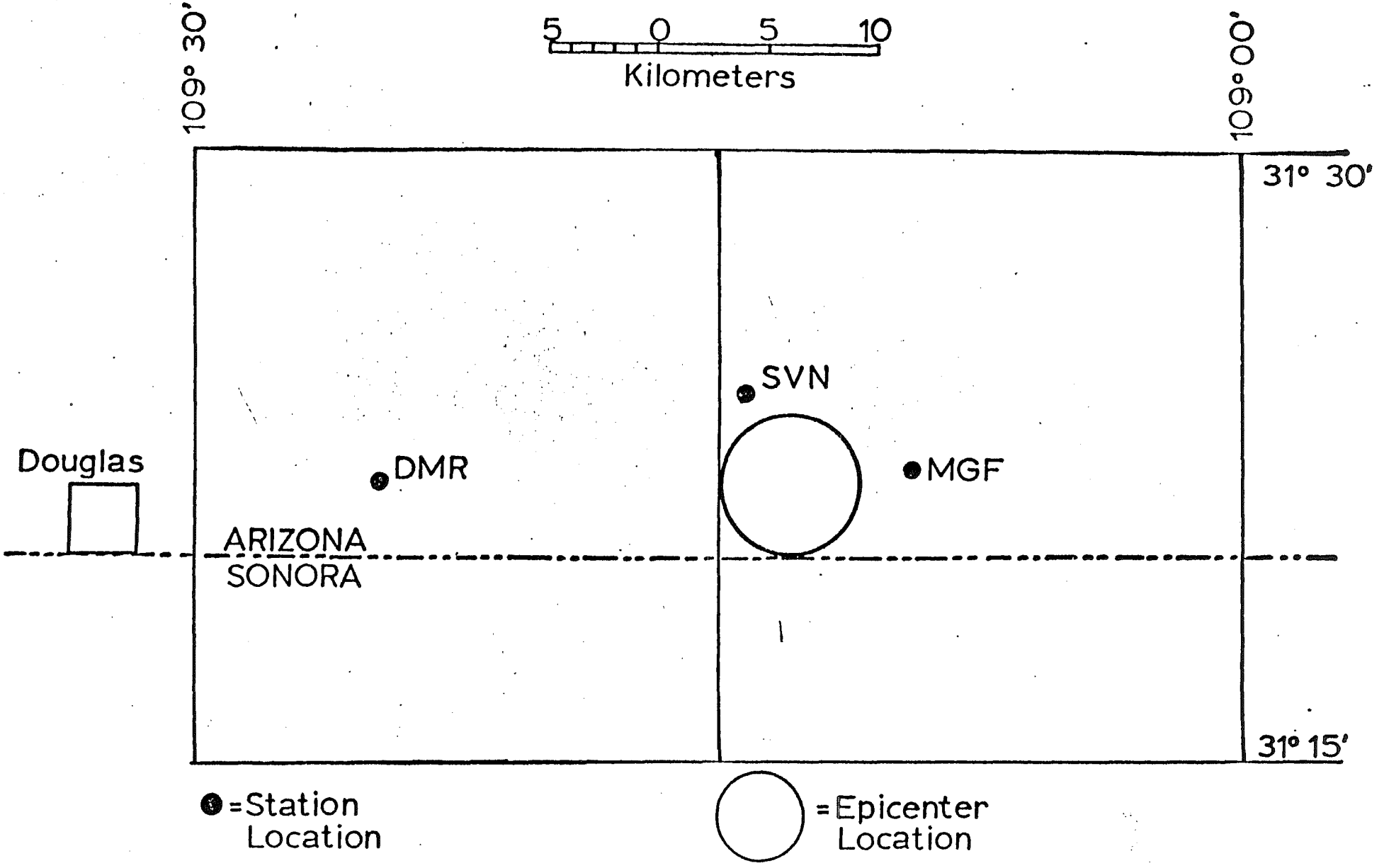

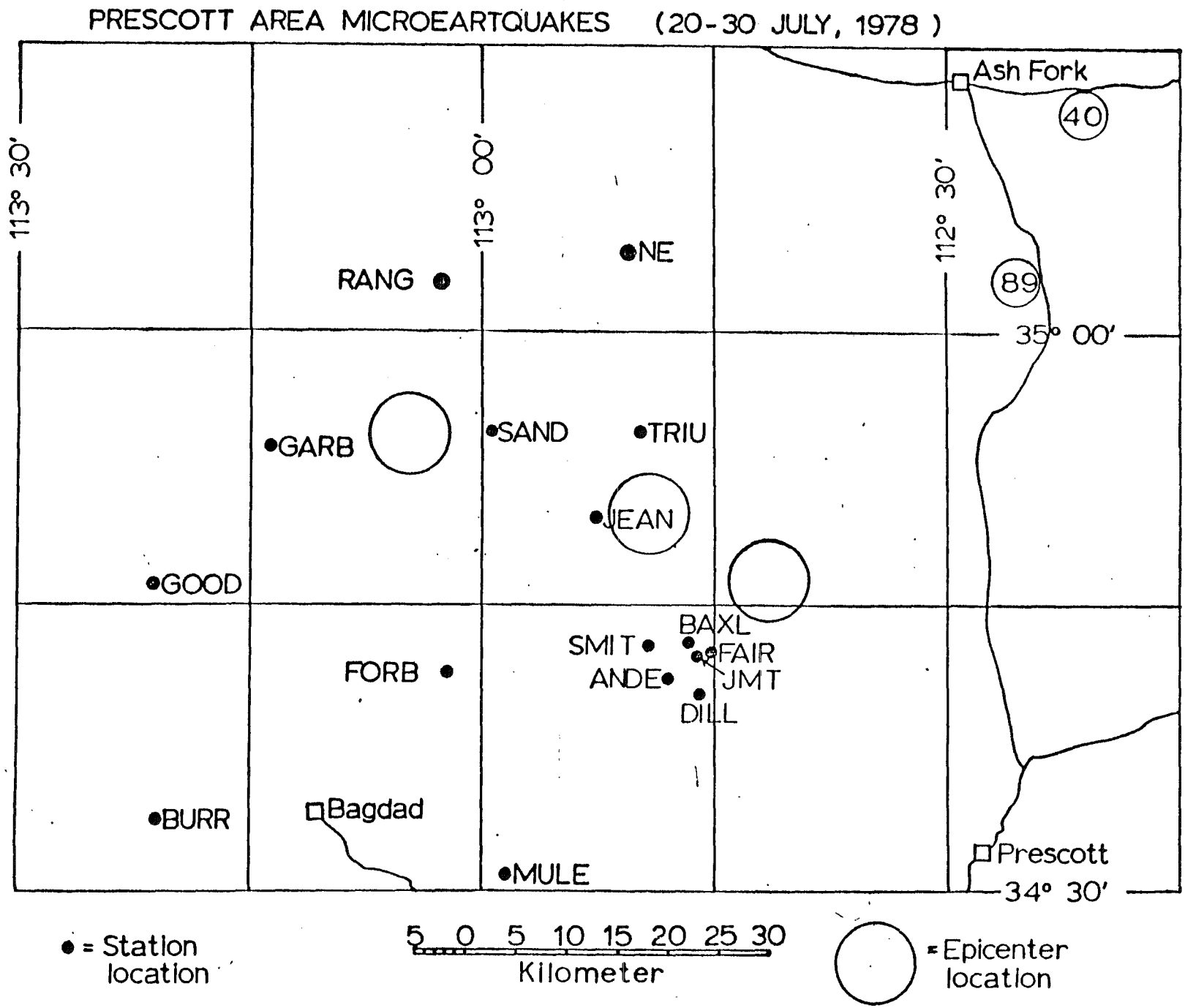

Figure 6. Prescott network and well-located epicenters.

Bernardino, Sonora areas which are in the same geologic province.

In both the Prescott and San Bernardino, Sonora areas significant earthquakes have occurred during the 100 year record in Arizona. Essentially no earthquakes were reported in any of the three potential geothermal areas studied. Tectonically there may be fundamental differences in these areas, although at this time we cannot identify these differences.

At this stage to do anything useful from the microearthquake point of view, it appears necessary to spend a considerably longer time recording in each of the above areas with a network at least as dense as used in this study. In this way, enough events might be detected to map faults and determine the tectonics of the region.

ACKNOWLEDGEMENTS

Peder Dahlgren, Debra Feist, Dan Gish, Steve Natali, and Talal Mokhtar all assisted in the field work and data reduction associated with this project.

REFERENCES

Brune, J.N. and C.R. Allen, 1967, A microearthquake survey of the San Andreas Fault System in Southern California, Bull. Seism., Soc. Am. V. 57, 277-296.

Sbar, Marc L., M. Barazangi, J. Dorman, C.H. Scholz, and R.B. Smith, 1972, Tectonics of the Intermountain seismic belt, western United States: Microearthquake seismicity and composite fault plane solutions, Bull. Geol. Soc. Am. V. 83, 13 - 28.

Sumner, J.S., 1976, Earthquakes in Arizona, Fieldnotes, Arizona Bureau of Mines, v. 6, no. 1, p. 1-8.

GEOCHEMICAL STUDIES IN ARIZONA

by

Chandler A. Swanberg

Interpretations and conclusions in this report are those of the consultant and do not necessarily coincide with those of the staff of the Bureau of Geology and Mineral Technology.

GEOCHEMICAL STUDIES IN ARIZONA

Geochemical studies in Arizona include the application of the NaKCa Mg geothermometer to thermal and non-thermal groundwaters to evaluate the State's geothermal resources and to field-test the application of this newly developed geothermometer. The study also includes application of the silica geothermometer to the same data set with the good of using the silica heat flow interpretation technique to prepare a new heat flow map of Arizona. Roughly half of the geothermal areas delineated by Swanberg et al. (1977) on the basis of chemical geothermometry also can be characterized as having anomalously high NaKCa Mg geotemperatures (see figure 1). Of particular note is the new potential geothermal area located near the Salt River in the Apache Indian Reservation. Heat flow in the Colorado Plateau region of Arizona is typically 1.5 HFU, whereas the Basin and Range heat flow is typically about 2.5 HFU (see figure 2). The Basin and Range shows considerably more variability with respect to regional heat flow than does the Colorado Plateau.

This study was funded in part by U.S. Department of Energy, Division of Geothermal Energy, Contract no. EG-77-S-02-4362.

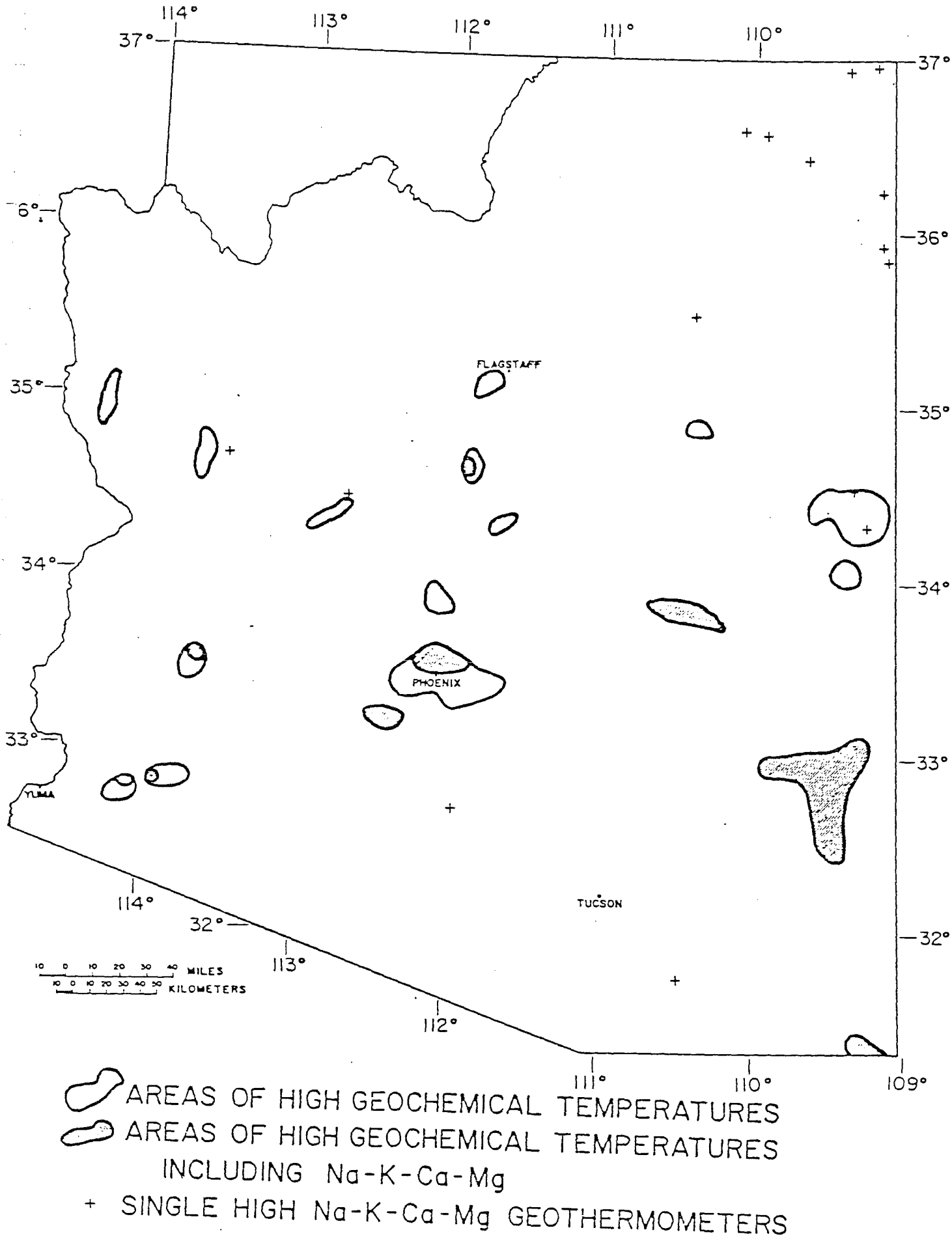
114°
113°
112°
111°
110°
37°
36°
35°
34°
33°
32°
109°
FLAGSTAFF
PHOENIX
TUCSON
YUMA
MILES
KILOMETERS
AREAS OF HIGH GEOCHEMICAL TEMPERATURES
AREAS OF HIGH GEOCHEMICAL TEMPERATURES
INCLUDING Na-K-Ca-Mg
+ SINGLE HIGH Na-K-Ca-Mg GEOTHERMOMETERS

Figure 1.

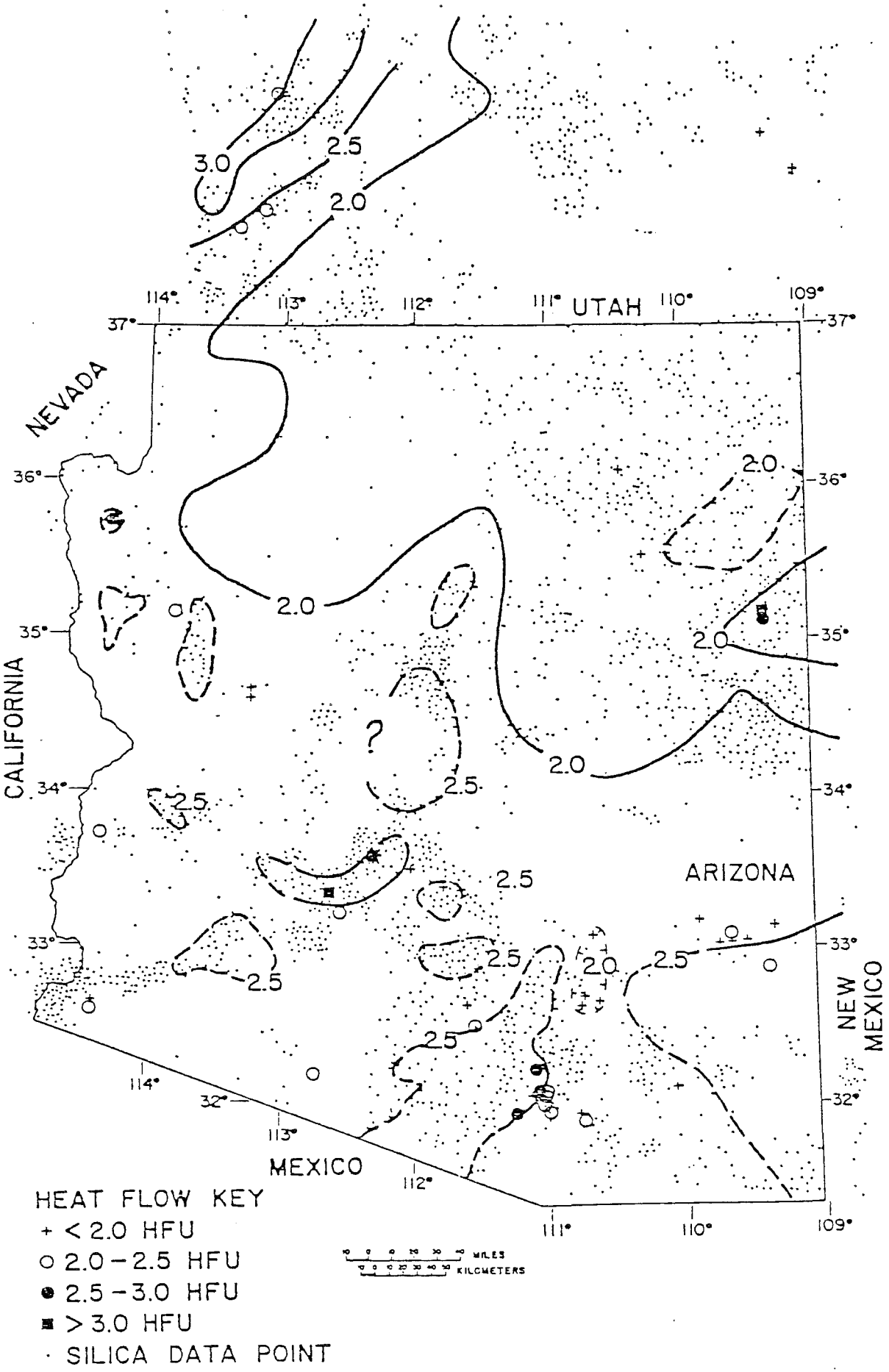
UTAH
NEVADA
CALIFORNIA
ARIZONA
NEW MEXICO
MEXICO
114°
113°
112°
111°
110°
109°
37°
36°
35°
34°
33°
32°
3.0
2.5
2.0
?
HEAT FLOW KEY
+ < 2.0 HFU
○ 2.0 – 2.5 HFU
● 2.5 – 3.0 HFU
■ > 3.0 HFU
· SILICA DATA POINT
MILES
KILOMETERS

Figure 2.

Reference

Swanberg, C.A., Morgan, P. Stoyer, C.H., and Witcher, J.C., Regions of High Geothermal Potential, An Appraisal Study of the Geothermal Resources of Arizona and Adjacent Areas in New Mexico and Utah and Their Value for Desalination and Other Uses, NMEI Report No. 6, July 1977.

GEOELECTRICAL STUDIES NEAR SPRINGERVILLE, ARIZONA

Final Report

Contract 8-01-3011 820

Prepared for

Arizona Bureau of Geology and Mineral Technology

Geologic Survey Branch

Geothermal Group

by

Charles T. Young

Physics Department

New Mexico State University

Las Cruces, New Mexico 88003

June 1979

Interpretations and conclusions in this report are those of the consultant and do not necessarily coincide with those of the staff of the Bureau of Geology and Mineral Technology.

GEOELECTRICAL STUDIES NEAR
SPRINGERVILLE, ARIZONA

Abstract

Evaluation of geothermal potential of lands near Springerville was conducted with d.c. resistivity and telluric current measurements. Geological, geochemical and geophysical evidence suggests a possible hot water or deep dry rock resource in the study area. We found:

1. Low d.c. resistivity values associated with known high total dissolved solids values north and south of Springerville. Further exploration of the zones might locate hot rock which would be the source of the high TDS values, or locate faults or brecciated zones which act as conduits for the high TDS water;

2. A low d.c. resistivity zone near Greer, Arizona, that does not show up in the TDS data. This could be a high TDS or hot water zone. If possible, a heat flow hole should be drilled here:

3. A telluric current low southwest of Springerville. This low is near a Los Alamos Scientific Laboratory (LASL) magnetotelluric site, where conductive material is anomalously close to the earth's surface, 12 km deep as opposed to 24 km elsewhere. The LASL station is on the edge of the telluric current low; both coincide roughly with a several-hundred-square kilometer gravity low. The region could be either a hot dry rock resource or it could be hot wet rock affecting deeply circulating groundwater which is detected as high TDS values to the north. Additional geoelectrical measurements over the telluric current low would be desirable to determine the boundaries more accurately and find the depth to the conductive material.

GEOELECTRICAL STUDIES NEAR SPRINGERVILLE, ARIZONA

by CHARLES T. YOUNG

Introduction

This research was conducted to coordinate with geological and other geophysical studies to evaluate potential geothermal resources near Springerville, Arizona. The study area is located on an index map of Arizona in Figure 1. Stone, in Hahman, 1979, discusses geothermal potential of the area in terms of geology, geochemical data and earlier geophysical studies. The review of gravity, magnetic and teleseismic P_n velocity data, suggest a crustal hot spot in the study area. Los Alamos Scientific Laobratory (LASL) magnetotelluric data discussed below, agree with this prediction.

Los Alamos Scientific Laboratories is in the process of completing two large-scale deep-penetration magnetotelluric profiles across Arizona and New Mexico, (Mark Ander, personal communication). The profile includes four stations along a north-south line passing through our research area. The stations are numbered L28, L29, L30 and L31 (shown on Figure 2, along with our stations). Data are now available from stations L28 and L30. Preliminary modelling of site 28 data indicates resistive material overlying a conductive half-space at a depth of about 12 km, however, the data are of too poor quality to indicate layer resistivities. The site 31 preliminary model has four layers:

1. A top layer of 119 Ω-m material 1 km thick,
2. A second layer of 18 Ω-m material 1 km thick,
3. A third layer of 1120 Ω-m material 22 km thick,
4. An underlying conductive half-space of 29 Ω-m material.

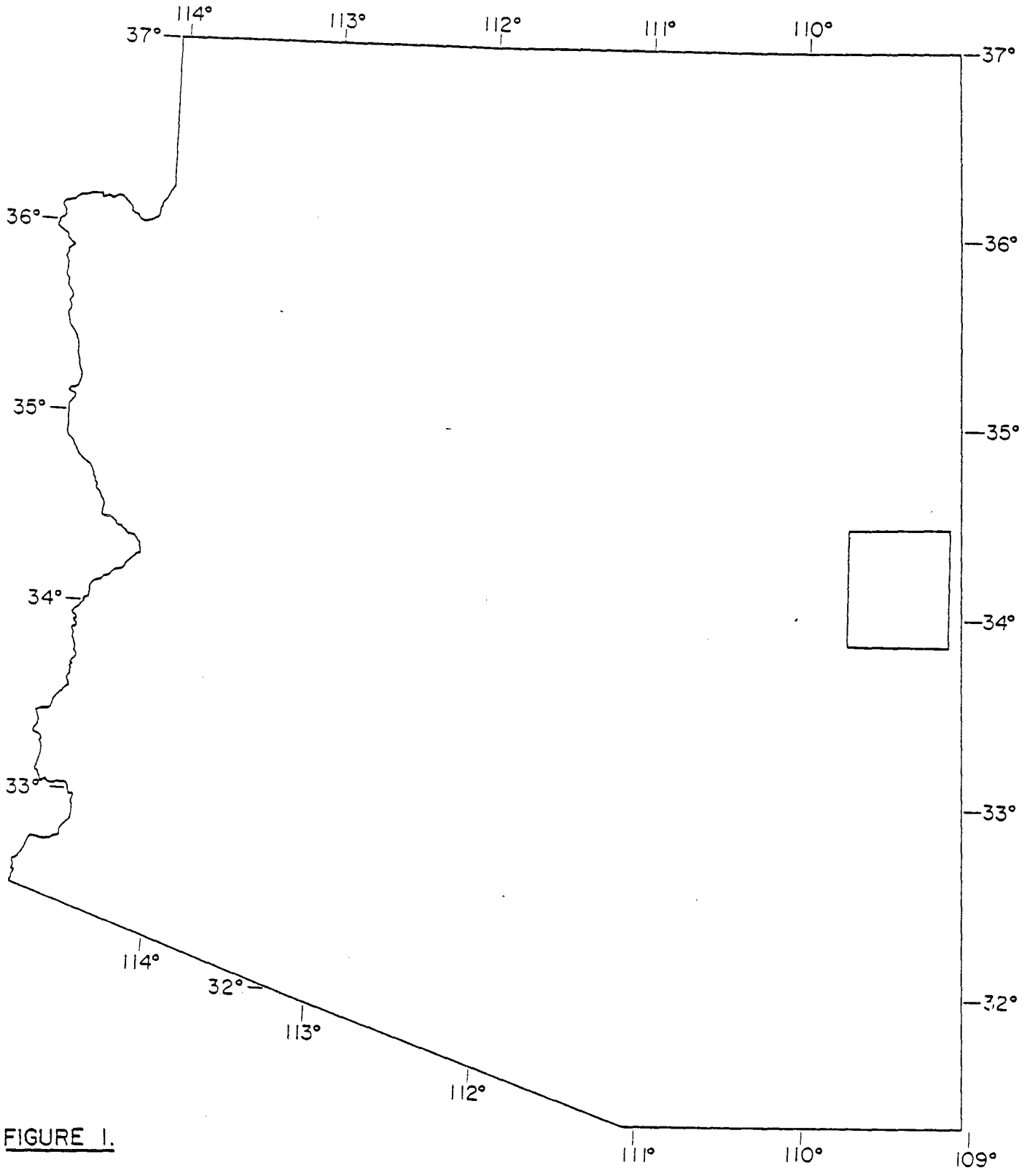
114°
113°
112°
111°
110°
37°
37°
36°
36°
35°
35°
34°
34°
33°
33°
114°
32°
32°
113°
112°
111°
110°
109°

FIGURE 1.

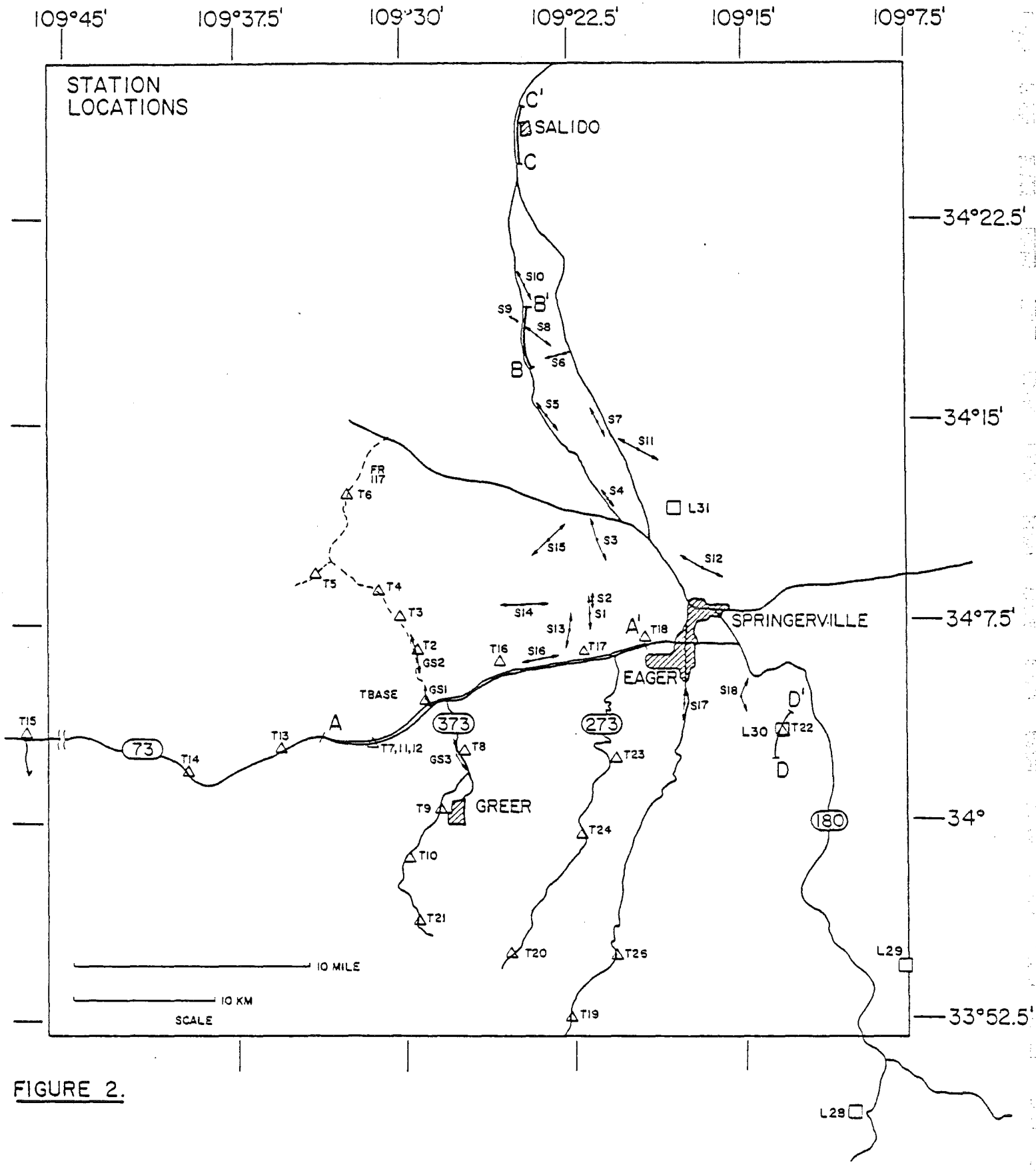
109°45'
109°37.5'
109°30'
109°22.5'
109°15'
109°7.5'
34°22.5'
34°15'
34°7.5'
34°
33°52.5'
STATION LOCATIONS
C'
SALIDO
C
S10
B'
S9
S8
S6
B
S5
S7
S11
S4
L31
S3
S15
S12
FR 117
T6
T5
T4
T3
S14
S2
S1
S13
A'
T18
SPRINGERVILLE
T2
GS2
T16
S16
T17
EAGER
TBASE
GS1
S18
S17
D'
T15
A
373
273
L30
T22
73
T13
T7,11,12
T8
T23
T14
GS3
D
T9
GREER
180
T24
T10
T21
T20
T25
L29
10 MILE
10 KM
SCALE
T19
L28

FIGURE 2.

SCHLUMBERGER
PROFILE A-A'

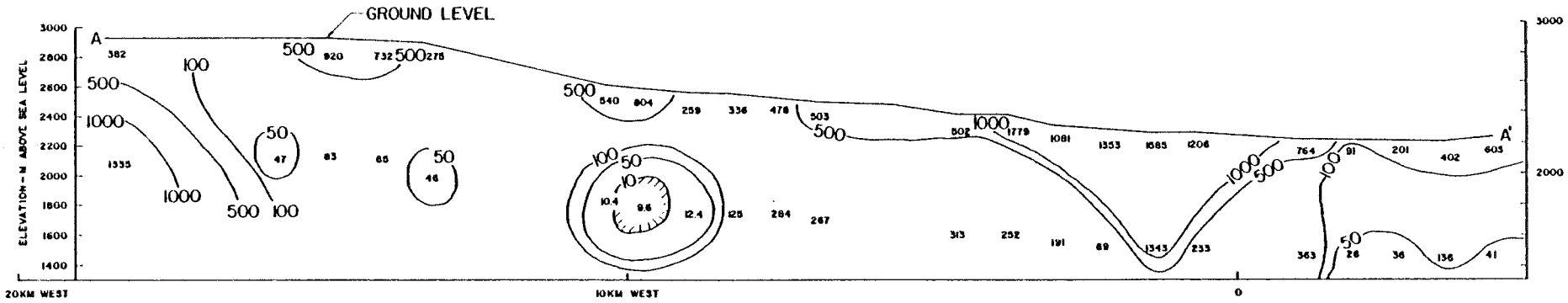

PROFILE B-B'

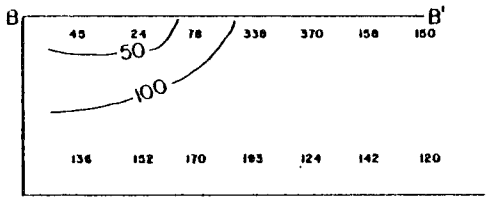

ELEVATION
1920M ±20M

PROFILE C-C'

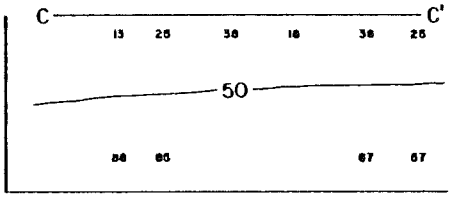

ELEVATION
1780M ±20M

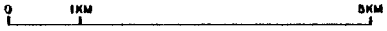

FIGURE 2a.

The significant difference between the two models is the shallower depth to the conductive layer at site 28 to the south, which agrees with our telluric current work described below.

Telluric Current Measurements

The Telluric Current Method measures natural alternating current voltages in the earth at a base and remote station to determine relative electric field strength over the survey area. The square-root of the ratio of electric fields is proportional to the ratio of magnetotelluric apparent resistivities at the base and remote sites. Thus, low telluric current voltages mean low resistivities at that site, relative to the base station. The data can also be analyzed to show direction of the earth's currents at the base and remote sites, possibly showing current channeling in conductive bodies.

The depth of penetration of the telluric current signals is approximately equal to the skin depth of the electromagnetic wave being detected, that is, the depth at which the wave amplitude drops to 1/4 or 37% of its value at the surface. Skin depth, δ, in meters, is calulated according to $\delta = 500\ (\rho/f)^{\frac{1}{2}}$, where ρ = resistivity of the orck in ohm-meters, f = frequency in Hz. The signals we recorded, with frequencies of .01 to .05 Hz, penetrate several kilometers.

Our data were analyzed by calculating broadband voltage power ratio (BPR): simultaneous base and remote records that exhibit high visual coherency are selected, several cycles are hand digitized and the power ratio between base and remote site are calculated by

$$BPR = \frac{\sum_{j=1}^{N} [(e^r_{xj} - \bar{e}^r_x)^2 + (e^r_{yi} - \bar{e}^r_y)^2]}{\sum_{j=1}^{N} [(e^b_{xj} - \bar{e}^b_x)^2 + (e^b_{yi} - \bar{e}^b_y)^2]} \qquad (1)$$

where, for example, e^r_{xj} refers to the jth data point of the electric (x or NS) component recorded at the remote (r) site, $\bar{e}^r_x$ is the mean value of those data and N is the number of data sampled. The summation over squares is proportional to the square of the standard deviation of the data. The function is available on sophisticated pocket calculators. Hermance, Thayer and Bjornsson (1975), show by example that the BPR values are just as effective as more complicated scalar data analysis techniques in locating low resistivity zones.

The telluric current apparatus used in this work is described in "Construction of Telluric Current Recording Apparatus", 1978, a report by C. T. Young to the Arts and Science Research Center of New Mexico State University. The report is available from the author.

Figure 2 shows the locations of all the geoelectric stations. The Schlumberger stations will be discussed later.

Figure 3 shows the BPR ratios. The lowest values are within the 0.5 contour, approximately 20 kilometers southwest of Springerville. The highest values are generally north of the base station. Since these signals penetrate several kilometers, the low voltages south of Springerville could represent a several-kilometer-deep, low resistivity zone, in general agreement with the Los Alamos magnetotelluric data, discussed above. If one considers the earth beneath the telluric current stations to be a resistive layer (cold rocks) over a conductor (hot rocks), then the low telluric current voltages represent either a decrease of second layer resistivity or a reduction of first layer thickness, or both.

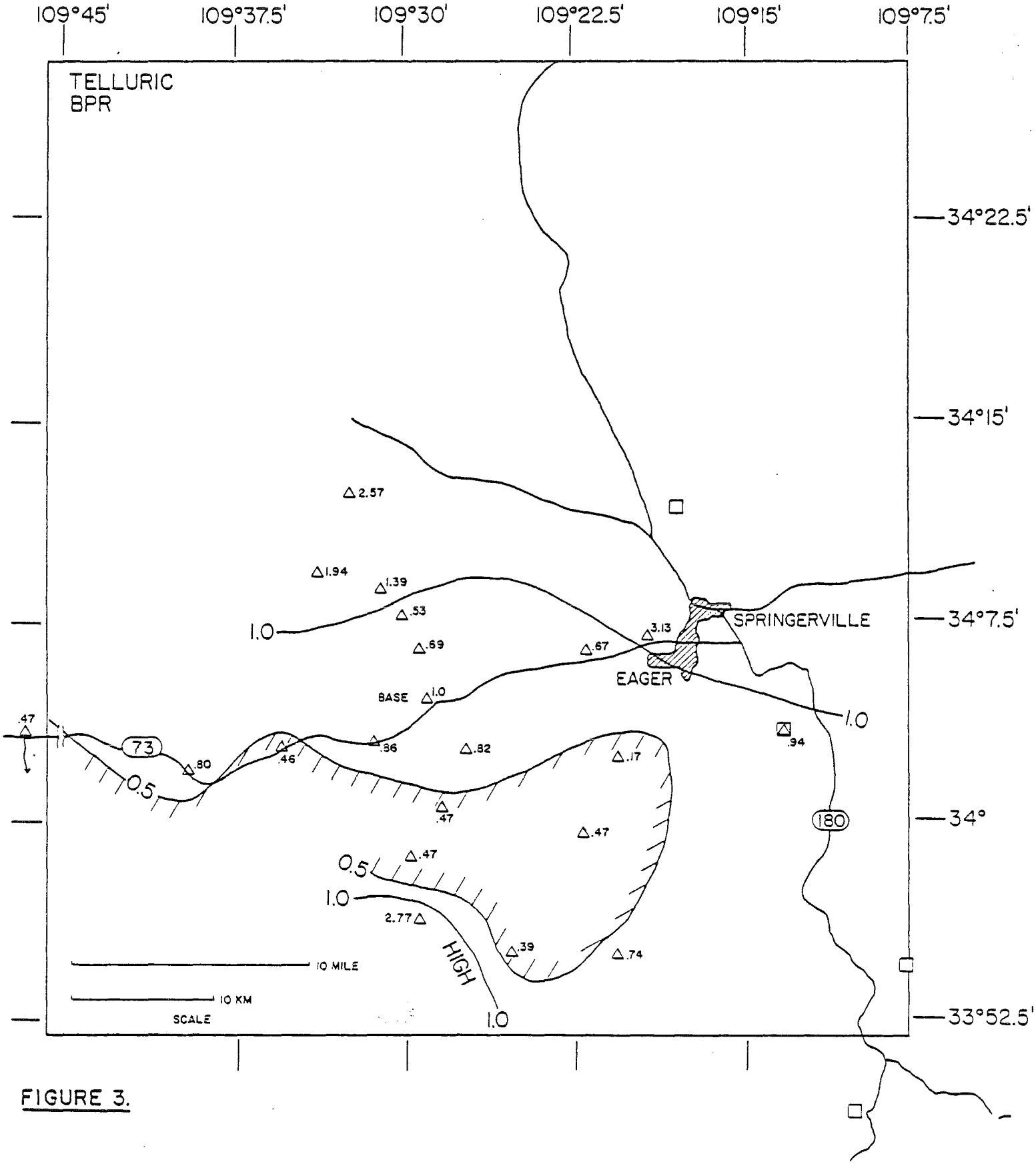
109°45'
109°37.5'
109°30'
109°22.5'
109°15'
109°7.5'
34°22.5'
34°15'
34°7.5'
34°
33°52.5'
TELLURIC
BPR
2.57
1.94
1.39
.53
1.0
.69
3.13
.67
SPRINGERVILLE
EAGER
BASE
1.0
.47
73
.80
.46
.36
.82
.17
.94
1.0
0.5
.47
.47
180
.47
0.5
1.0
2.77
HIGH
.39
.74
10 MILE
10 KM
SCALE
1.0

FIGURE 3.

Schlumberger Resistivity Measurements

Vertical Electric Soundings determine the resistivity and thickness of layers within the earth. Four electrodes are set up in a line on the earth's surface, direct current of a few amperes or tenths of amperes is introduced through the outer two electrodes, and the resultant voltage is measured at the inner two electrodes. One can calculate the apparent resistivity of the earth from the voltage and current readings and the electrode spacings. Deeper penetration is achieved by increasing the separation between the outer two current electrodes. The set of resistivities thus obtained for a set of increasing current electrode spacings, called a vertical electric sounding curve, is compared with handbook or computer-generated models to determine the thickness and resistivity of layers beneath the sounding site. We do cut-and-try modelling with an interactive APL language program on an Amdahl 470. The program is an APL translation of a BASIC language program from Sternberg, 1977, based on the convolution filtering technique of Ghosh, 1971.

The depth to which a sounding can detect layers depends on the layers present, and is always less than AB/2, half the distance between the outer two electrodes.

In addition to Schlumberger soundings, we also carried out Schlumberger profiling. In profiling, apparent resistivities are measured at only one or two electrode spacings along a survey line. Although it is not possible to construct layered models from these data, it is possible to map changes in subsurface resistivity, and roughly estimate the depth of these resistivities. If the AB/2 spacing is equal to the station interval, it is possible to "leap-frog"

along a survey line. We used AB/2 = 800 m and 100 m and spaced our stations 800 m apart, obtaining penetration of hundreds of meters and covering several kilometers per day of profiling.

The location of Schlumberger soundings are shown as double-ended arrows, and the profile locations are shown as lines A-A', B-B', C-C' and D-D' on Figure 2. The data and models are given in the Appendix. A summary of sounding models and profile data is given in Figure 4. Most Schlumberger soundings show:

1) high resistivity surface layers,
2) a low resistivity middle layers, presumably an aquifer,
3) a high resistivity electrical basement.

The low resistivity middle layer is of the greatest interest in the present study. In Figure 4, alongside the circles marking the Schlumberger stations, there are three numbers separated by slash marks showing

1) the layer resistivity of the aquifer in ohm-m
2) the depth from the surface to the bottom of the aquifer in meters,
3) the elevation above sea-level of the bottom of the aquifer, in meters.

Most soundings show an aquifer that is several hundred meters thick. The layer resistivities are contoured along with apparent resistivities for profile data for AB/2 = 800 m. Even though this seems like mixing two kinds of data, the combination is useful in indicating trends in subsurface resistivity. The contours should indicate changes in water quality, rock permeability, temperature, or all three.

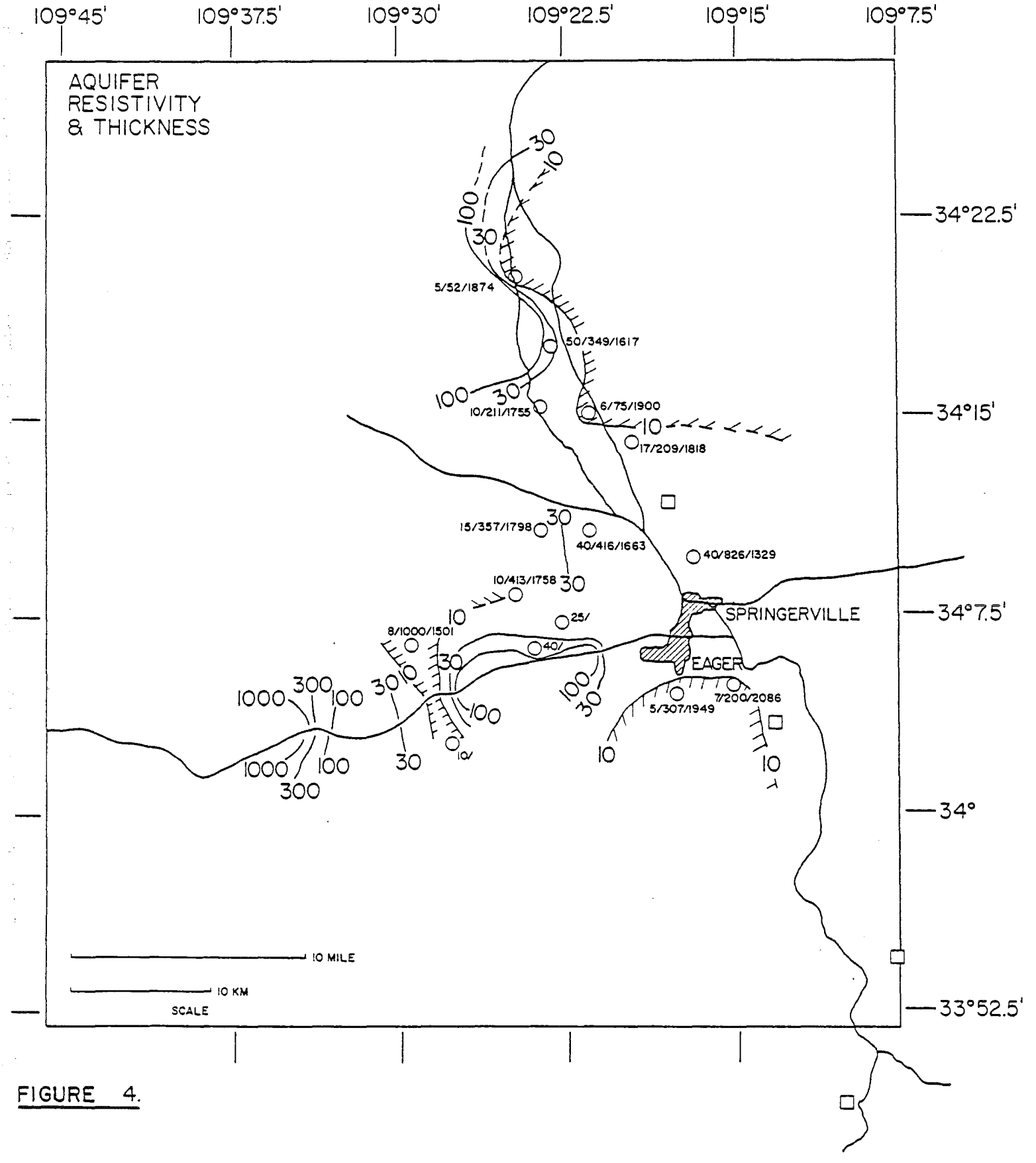
AQUIFER
RESISTIVITY
& THICKNESS
109°45'
109°37.5'
109°30'
109°22.5'
109°15'
109°7.5'
34°22.5'
34°15'
34°7.5'
34°
33°52.5'
SPRINGERVILLE
EAGER
5/52/1874
50/349/1617
10/211/1755
6/75/1900
17/209/1818
15/357/1798
40/416/1663
40/826/1329
10/413/1758
8/1000/1501
5/307/1949
7/200/2086
10 MILE
10 KM
SCALE

FIGURE 4.

Groundwater total dissolved solids (TDS) data, from the U.S. Geologic Survey WATSTORE file, contoured in Figure 5, give a clue to the interpretation of the low resistivities in Figure 3. High TDS values, which give rise to low resistivity, are present both north and south of Springerville. However, the narrow north-south zone of low resistivity west of Springerville has TDS values generally less than 75 ppm. It is surprising that there would be a zone of low TDS and low resistivity. The only explanation that comes to minds is that the well water samples all come from shallow wells which are recharged with low TDS rainwater, while the resistivity values represent deeper, more conductive, hot or higher TDS water. We made Schlumberger soundings G1, G2 and G3 in this low resistivity zone. Of the three, only G2 detected the bottom of the zone at a depth of 1024 meters. In fact, the bottom may be deeper, since a Schlumberger sounding can register a false electrical basement due to resistive material off to the side of the sounding. We know from the profile data that highly resistive material does exist off to the side, so, is possible that the low resistivity zone extends deeper than the measurement can detect.

Conclusions

Using telluric current measurements, we have found a low resistivity zone, which could be as much as several kilometers deep. This could be a crustal scale hot-spot which heats water and causes high geochemical temperatures and high dissolved solids values. Further deep penetration electrical work, either tellurics or magnetotellurics, would be desirable to map the zone more accurately and to determine the depth to the hot material.

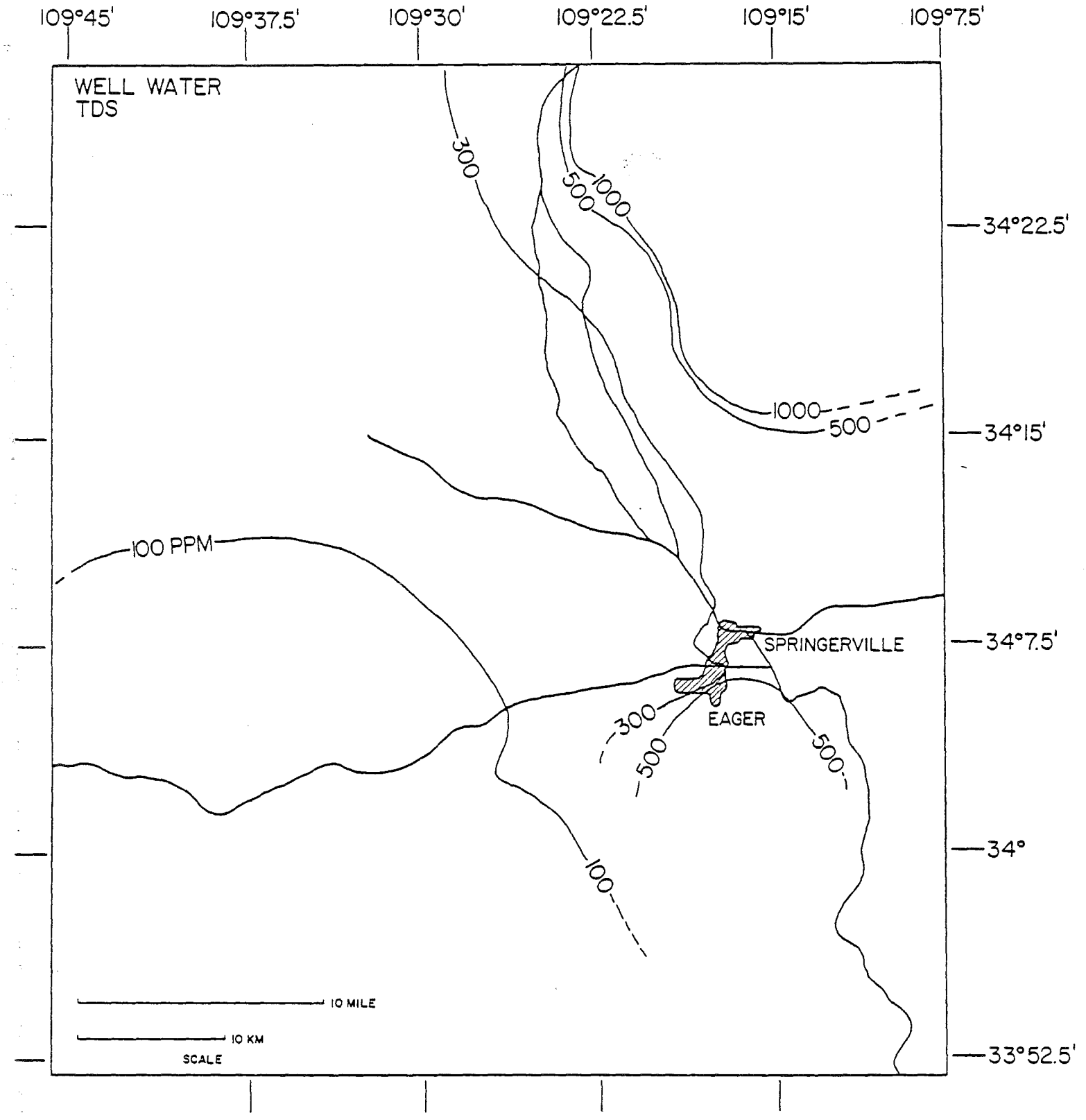
109°45'
109°37.5'
109°30'
109°22.5'
109°15'
109°7.5'
34°22.5'
34°15'
34°7.5'
34°
33°52.5'
WELL WATER
TDS
300
500
1000
1000
500
100 PPM
SPRINGERVILLE
EAGER
300
500
500
100
10 MILE
10 KM
SCALE

FIGURE 5.

The DC resistivity measurements found a low resistivity layer present on all the soundings which we interpreted as an aquifer. The resistivity of this layer generally correlates well with total dissolved solids data. We found one low resistivity region which did not correlate with TDS values, which could be deep hot or high TDS water.

Combined telluric, resistivity, and gravity data are shown in Figure 6. The telluric and gravity lows are overlapped and indicate a deep source of heat. Groundwater may flow through or above this deep heat source and move north and north westward and come near the surface at the locations identified by low d.c. resistivities. A more complete interpretation will be possible when the heat flow data are available.

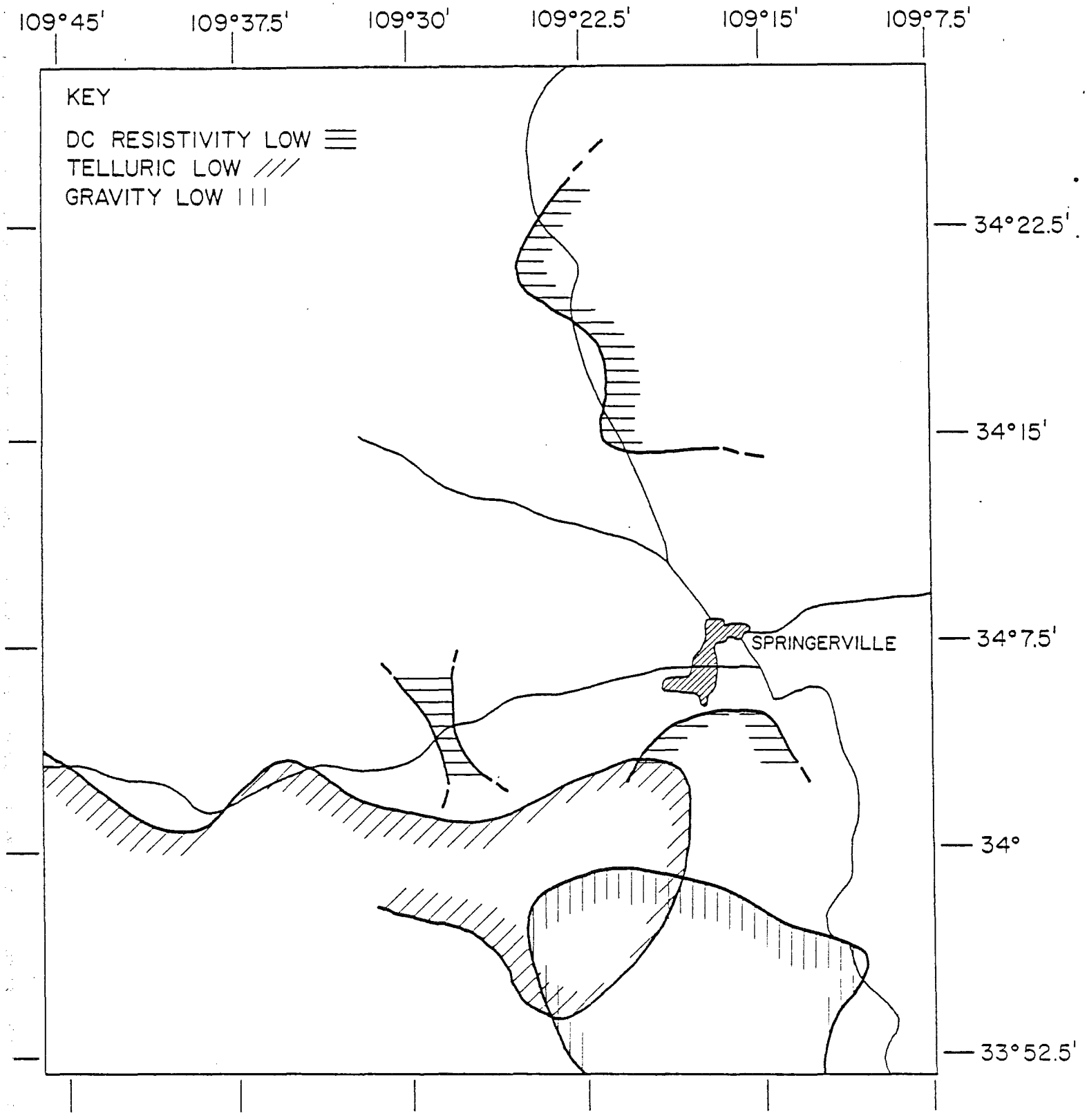
109°45'
109°37.5'
109°30'
109°22.5'
109°15'
109°7.5'
KEY
DC RESISTIVITY LOW
TELLURIC LOW
GRAVITY LOW
34°22.5'
34°15'
34°7.5'
34°
33°52.5'
SPRINGERVILLE

FIGURE 6.

ACKNOWLEDGEMENTS

The following students helped with the field work and data analysis; Thomas Rodke, Terry Templeman, James Moore, Douglas LaBrecque and John Benard.

The work was supported by the Arizona Bureau of Geology and Mineral Technology, Geological Survey Branch, Geothermal Group, under contract number 8-01-3011820.

Appendix

Sounding Curves and Models

The figures in the Appendix show for each Schlumberger site, 1) the measured apparent resistivity data as a function of electrode separation, plotted as crosses; 2) a layered earth model showing resistivities of layers and depths to interfaces; 3) an apparent resistivity curve calculated from the model, plotted as a continuous line, showing how well the model matches the data. The accuracy of the measurements range from about 1% at short electrode spacings to worst case of 20% at large electrode separations where the apparent resistivity is less than 10 ohm-meter. The inaccuracy is due to the fact that the low received voltages are masked by slowly varying telluric currents.

Some data show departures from the smooth sounding curves that would be predicted from layered model theory. Consistant offsets of several points usually indicate a lump of different resistivity material under the potential electrodes. An offset at a single point indicates some different material under the current electrode. In constructing layered models, we have assumed that such irregularities are due to lateral inhomogeneities, and calculated theoretical model curves that fit an imaginary smoothed version of the data. The models themselves are somewhat non-unique; a principle of equivalence holds for thin conductive and resistive beds:

1) For thin conductive beds, models with the bed having the same ratio of thickness to resistivity will give nearly the same sounding curve.

2) For a thin resistive bed, models with a bed having the same thickness-resistivities product will have nearly the same sounding curve.

Figure Captions

Figure 1. Location of study area on Arizona map.

Figure 2. Location of stations in study area. Triangles indicate telluric current stations. Double-ended arrows indicate Schlumberger soundings. Lines AA', BB',CC' and DD' are Schlumberger profiles, L28, L29, L30 and L31 are Los Alamos Scientific Laboratory magnetotelluric stations.

Figure 3. Telluric current broadband voltage power ratios.

Figure 4. Aquifer thickness and resistivity data. See text for key to numbers.

Figure 5. Total dissolved solids data from WATSTORE file.

Figure 6. Resistivity, Telluric Current and Gravity Data Summary.

1. D.C. resistivity low, from Figure 2, showing contour of aquifer resistivity or apparent resistivity at AB/2 = 800 m. Values less than 10 Ω-m.

2. Telluric current low, from Figure 3, showing contour of remote station broadband voltage powers ratios less than .5.

3. Bouger gravity low, from Hahman, 1979, showing -30 miligal contour.

References Cited

Ghosh, D.P., 1971, Application of linear filter theory to the direct interpretation of geoelectrical resistivity sounding measurements, Geophysical Prospecting, vol. 19, pp. 192-217.

Hahman, W.R., 1979, Geothermal reservoir site evaluation in Arizona, semiannual progress report for the period July 15, 1978 - January 15, 1979. Arizona Geological Survey, Tucson, Arizona.

Hermance, J., Thayer, R., Bjornsson, A., 1975, The telluric magnetotelluric method in the regional assessment of geothermal potentials, in United Nations 1975, Proceedings, Second United Nations Symposium on the Development and Use of Geothermal Resources, San Francisco, Calif., U.S.A., 20-29 May 1975, 3 volumes, 2500 pages, U.S. Government Printing Office.

Sternberg, Ben K., 1977, Interpretation of electromagnetic soundings data-numerical methods and computer program listings. University of Wisconsin Geophysical and Polar Research Center, Dept. of Geology and Geophysics, Madison, WI 53706. Wisconsin Report No. 77-1, Section B1 through B6.

Data for Schlumberger Profiles

A-A', B-B', and C-C'. For locations

and cross sections, see figures 2 and 2a.

*** START OF JOB CHY22377 TUESDAY MAY 22, 1979 21:26:53 ***

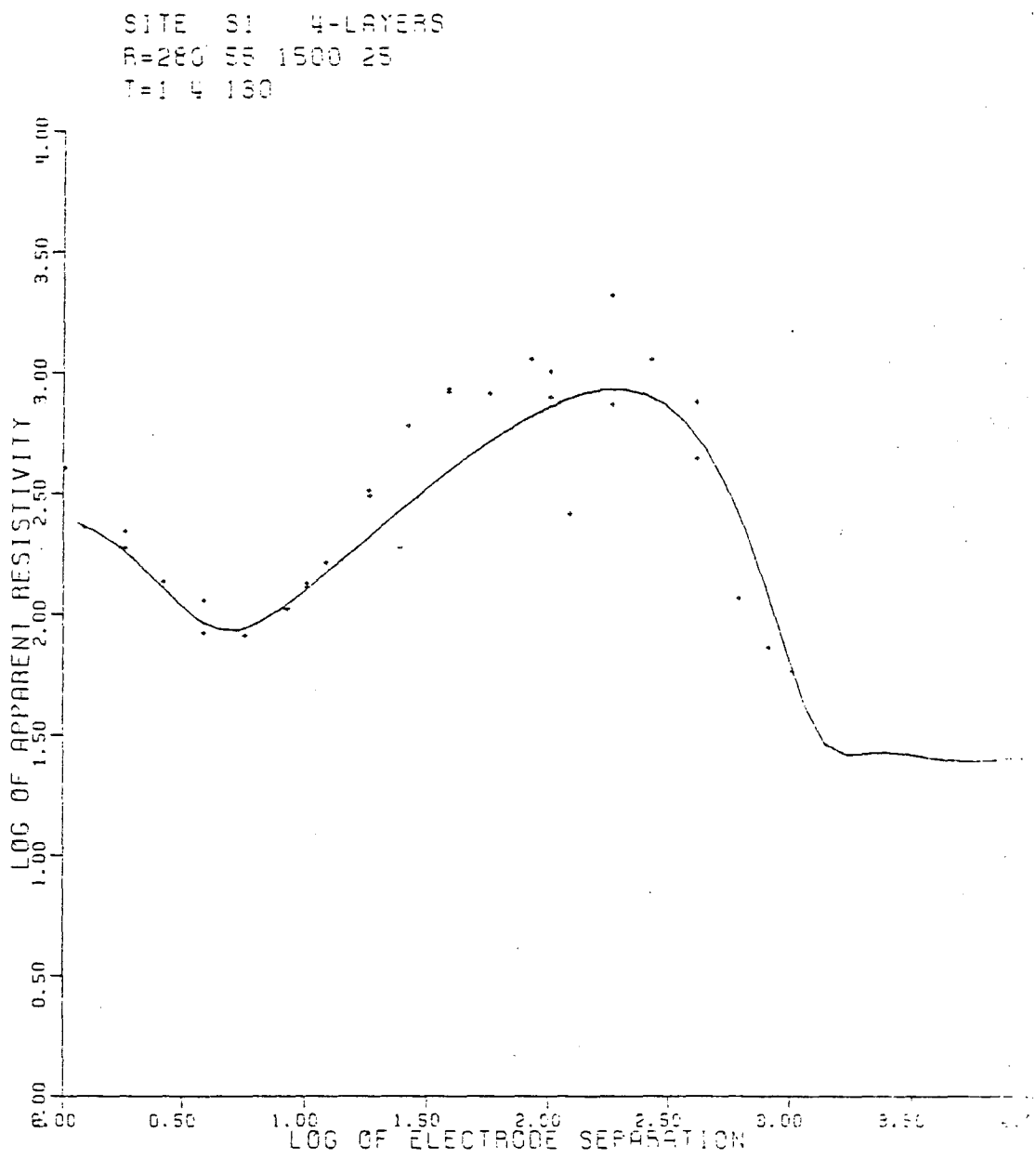

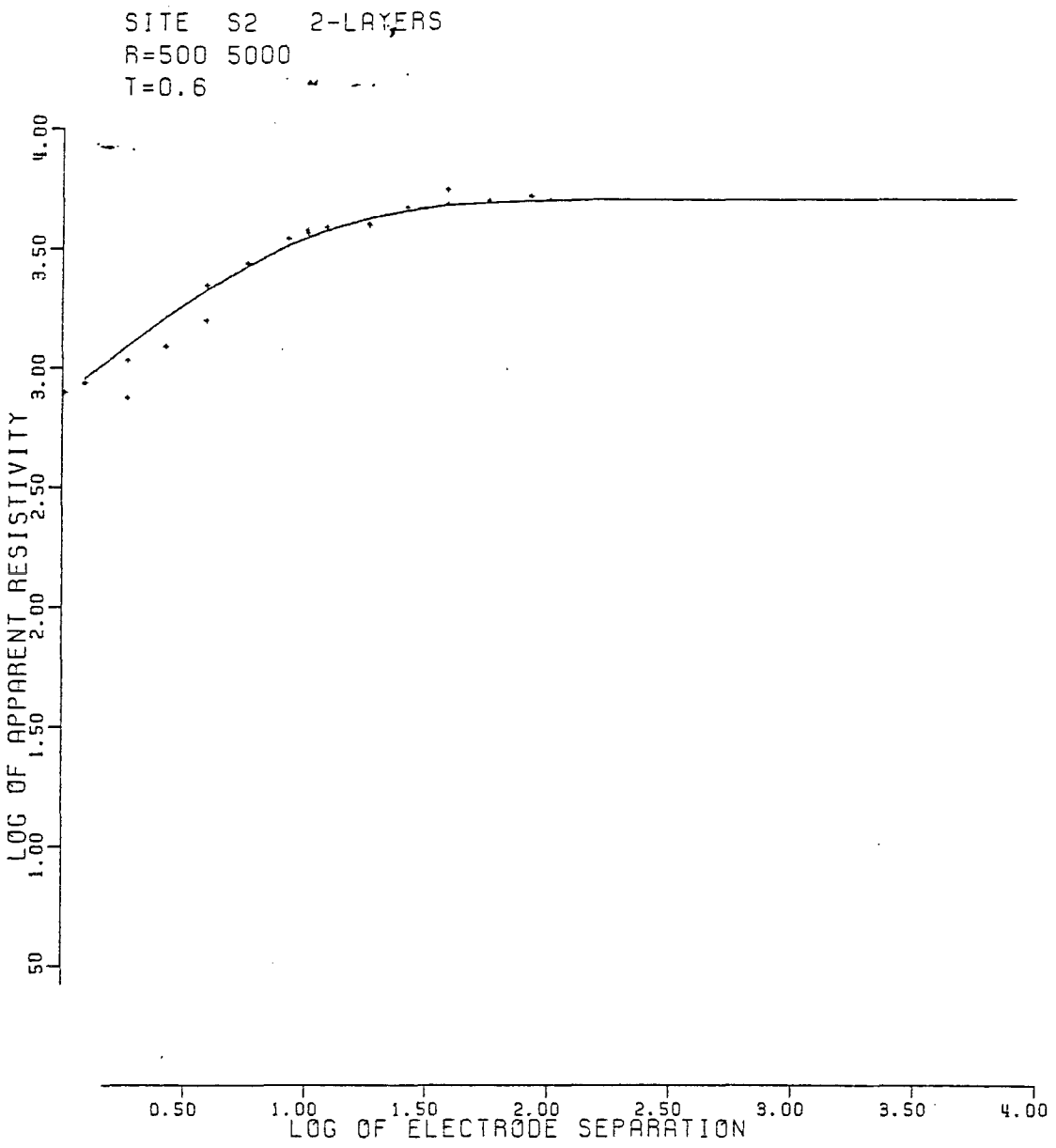

END OF PLOT CHY47562

SITE SITE 3 4-LAYERS
R=120 1700.40 150
T=0.85 95.320

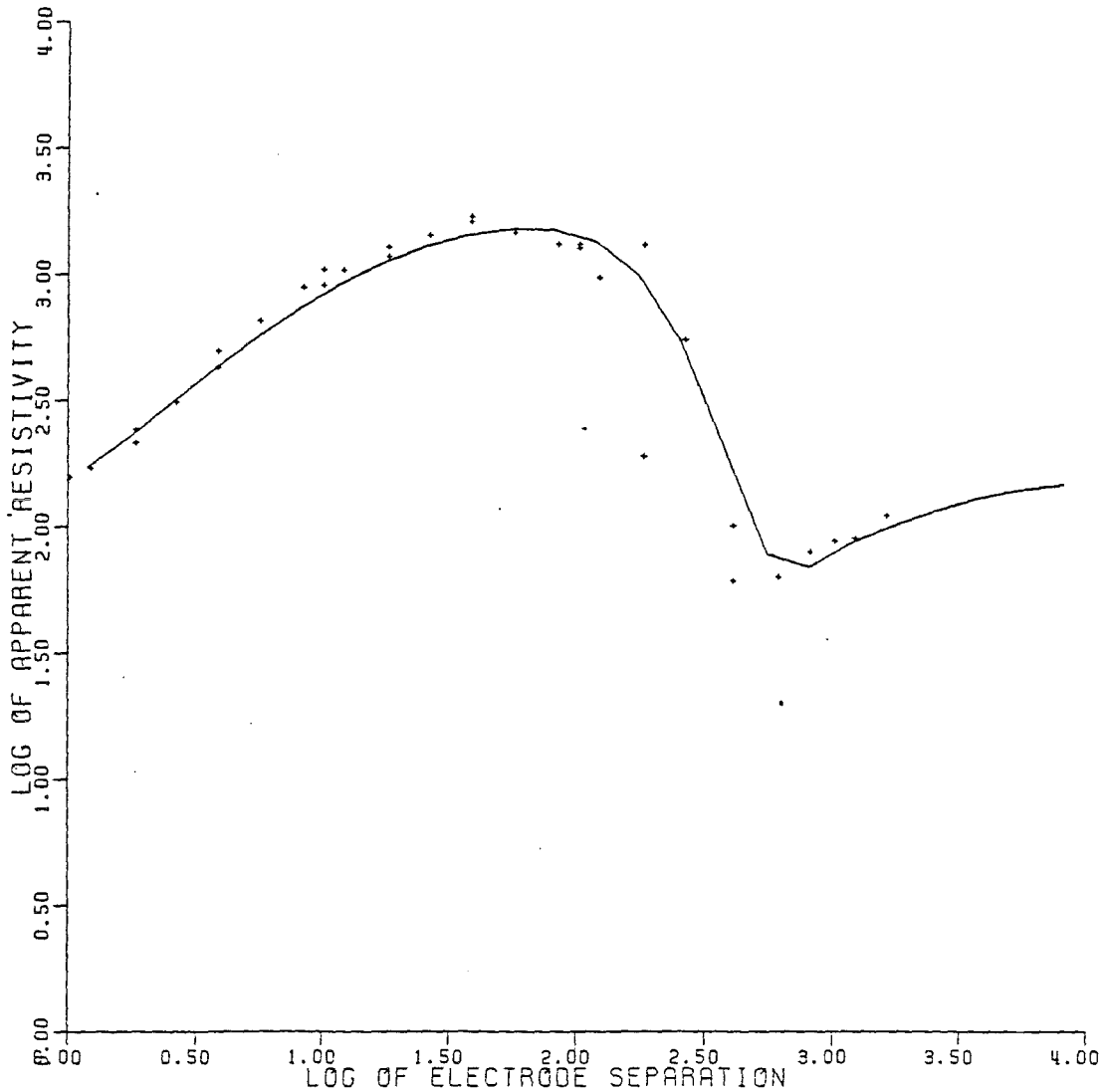

END OF PLOT CHY20007

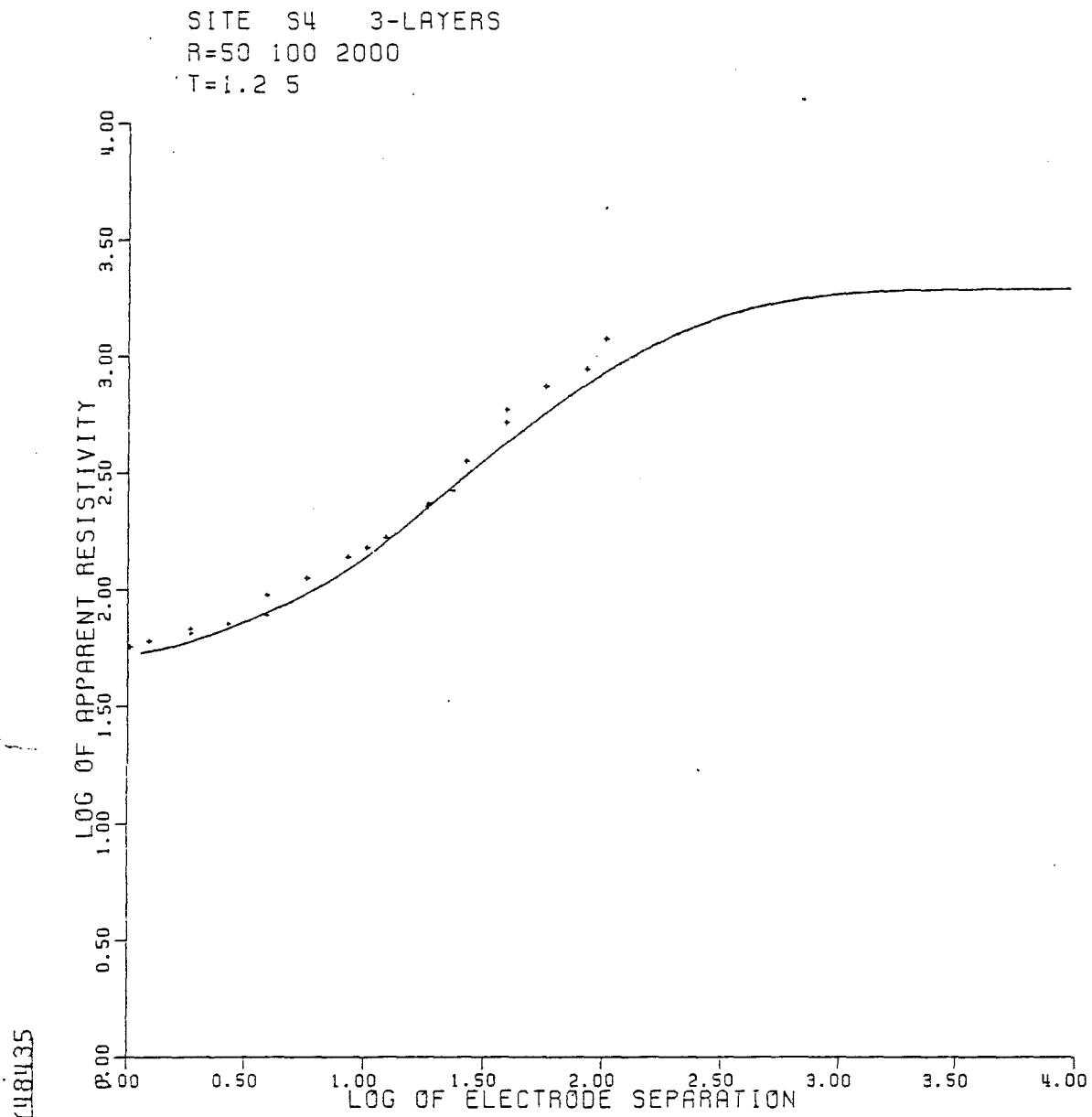

CHY18435

END OF PLOT CHY18435

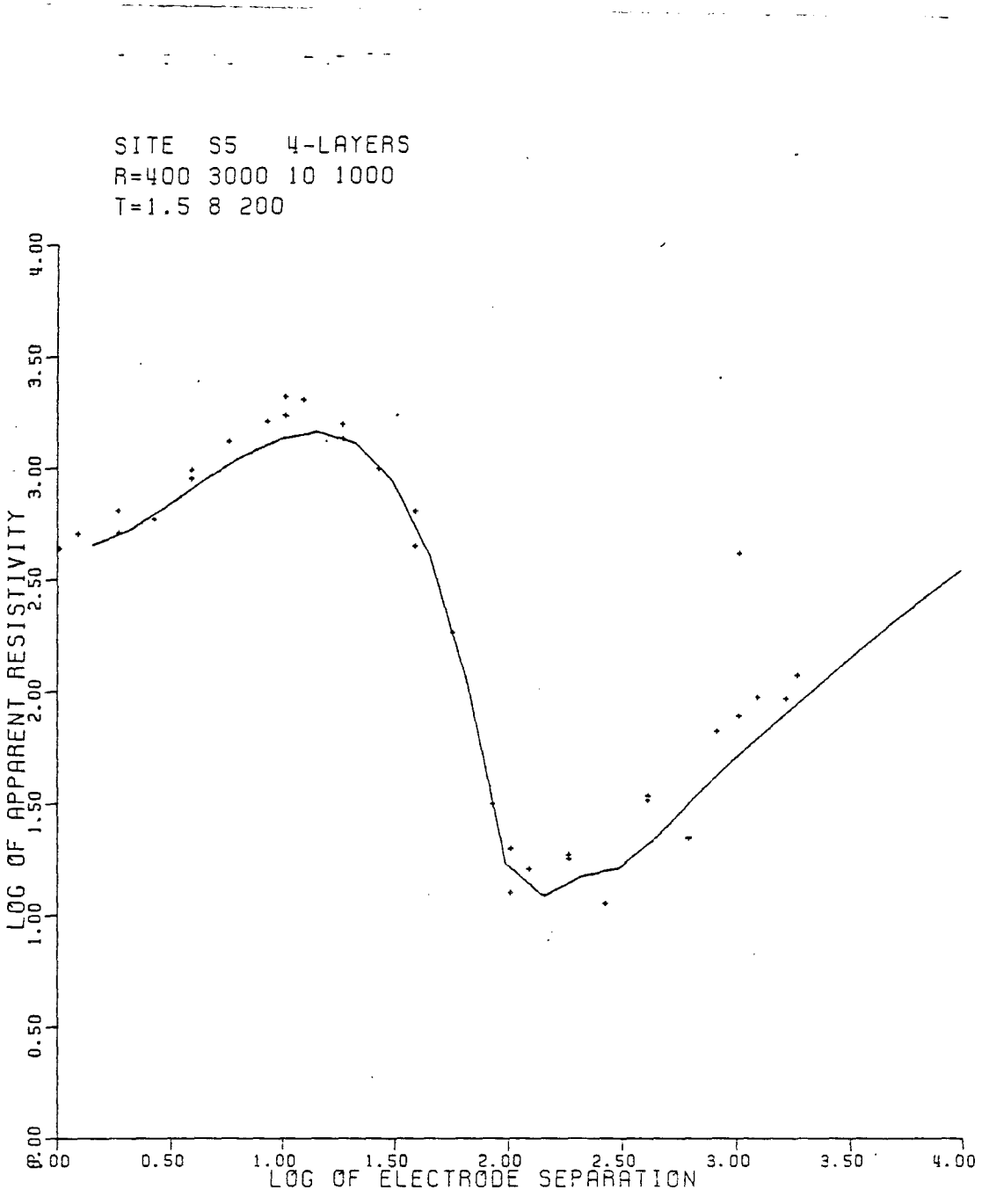

END OF PLOT CHY30188

CHY30188

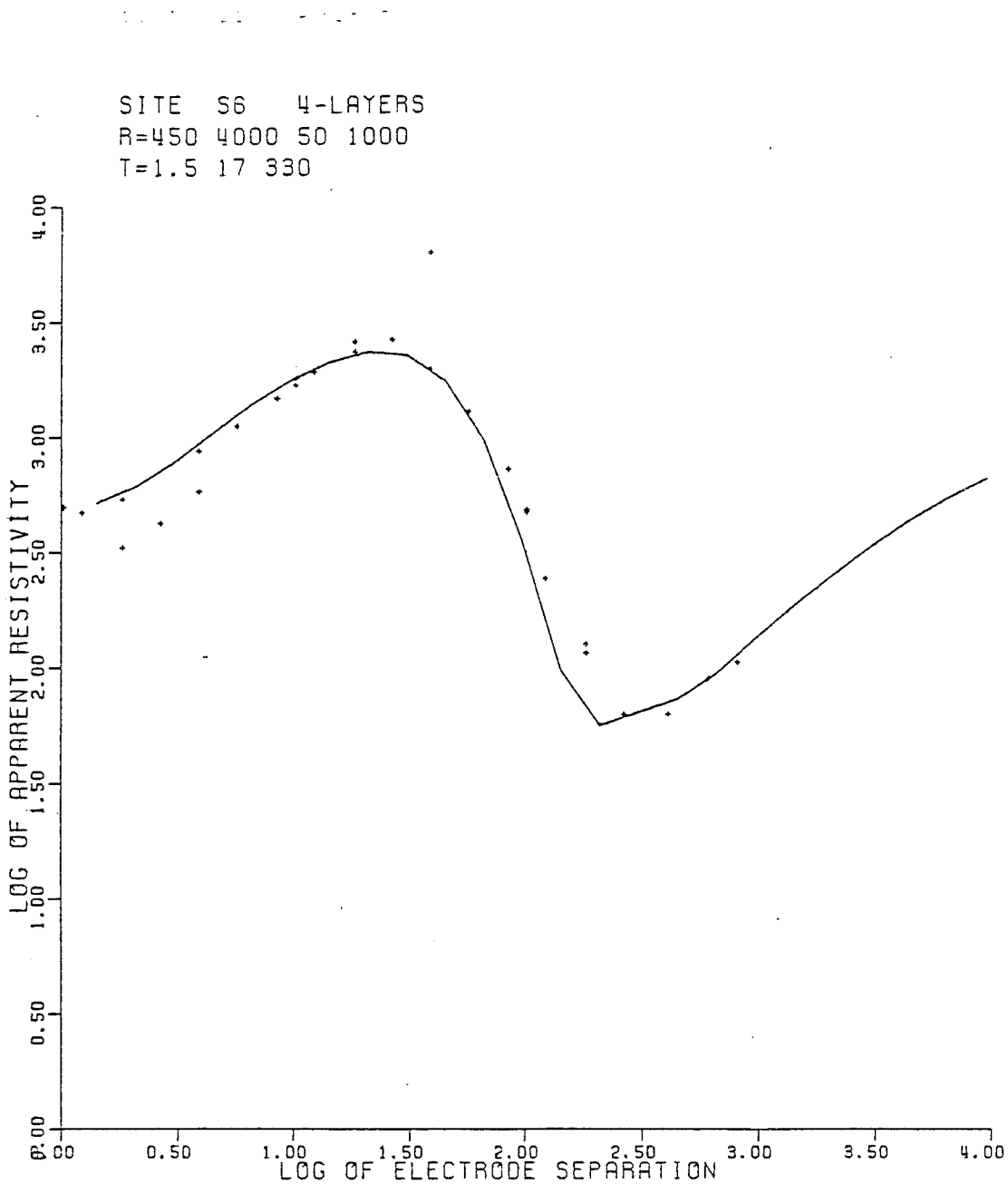

END OF PLOT CHY40074

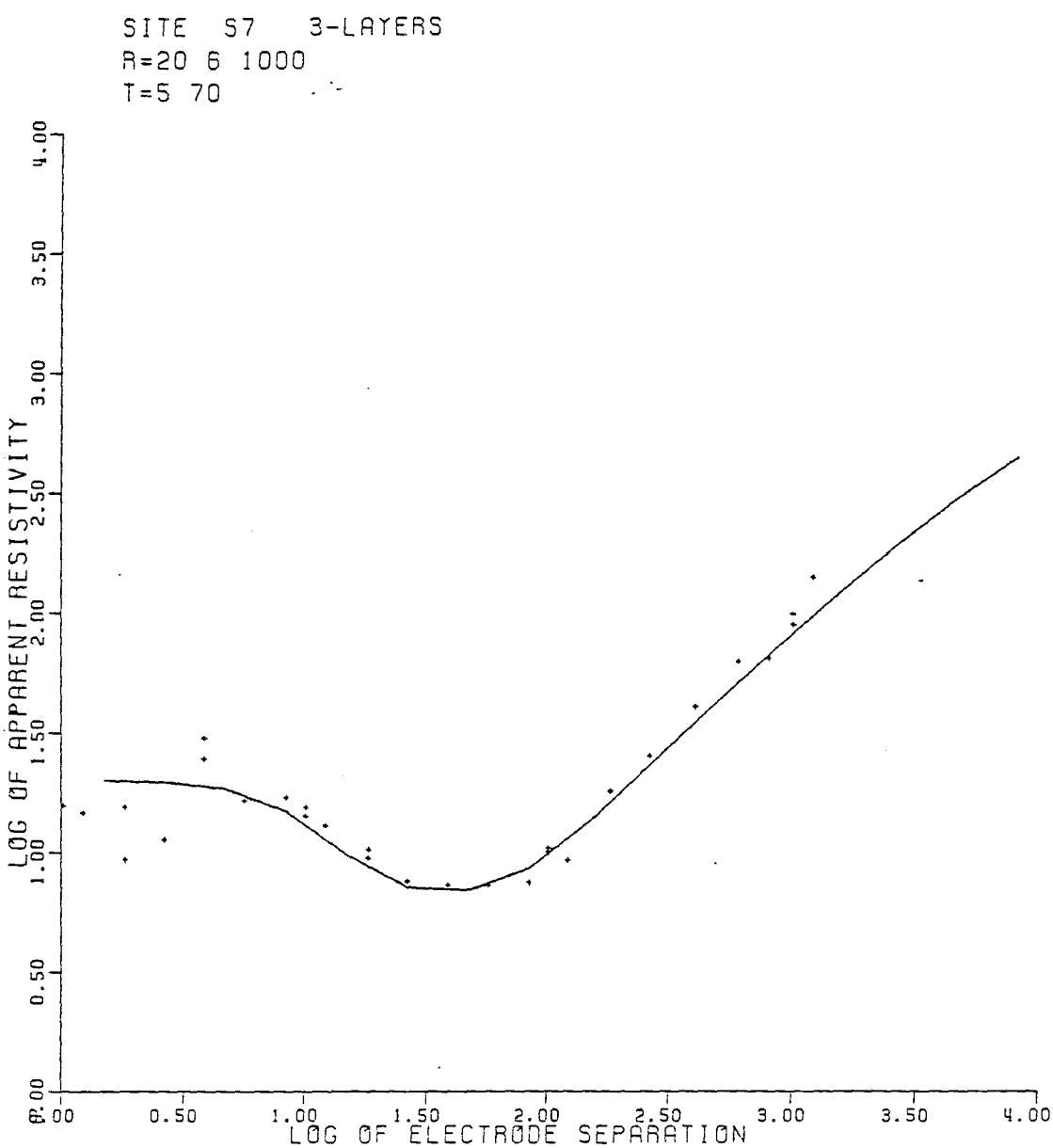

END OF PLOT CHY54373

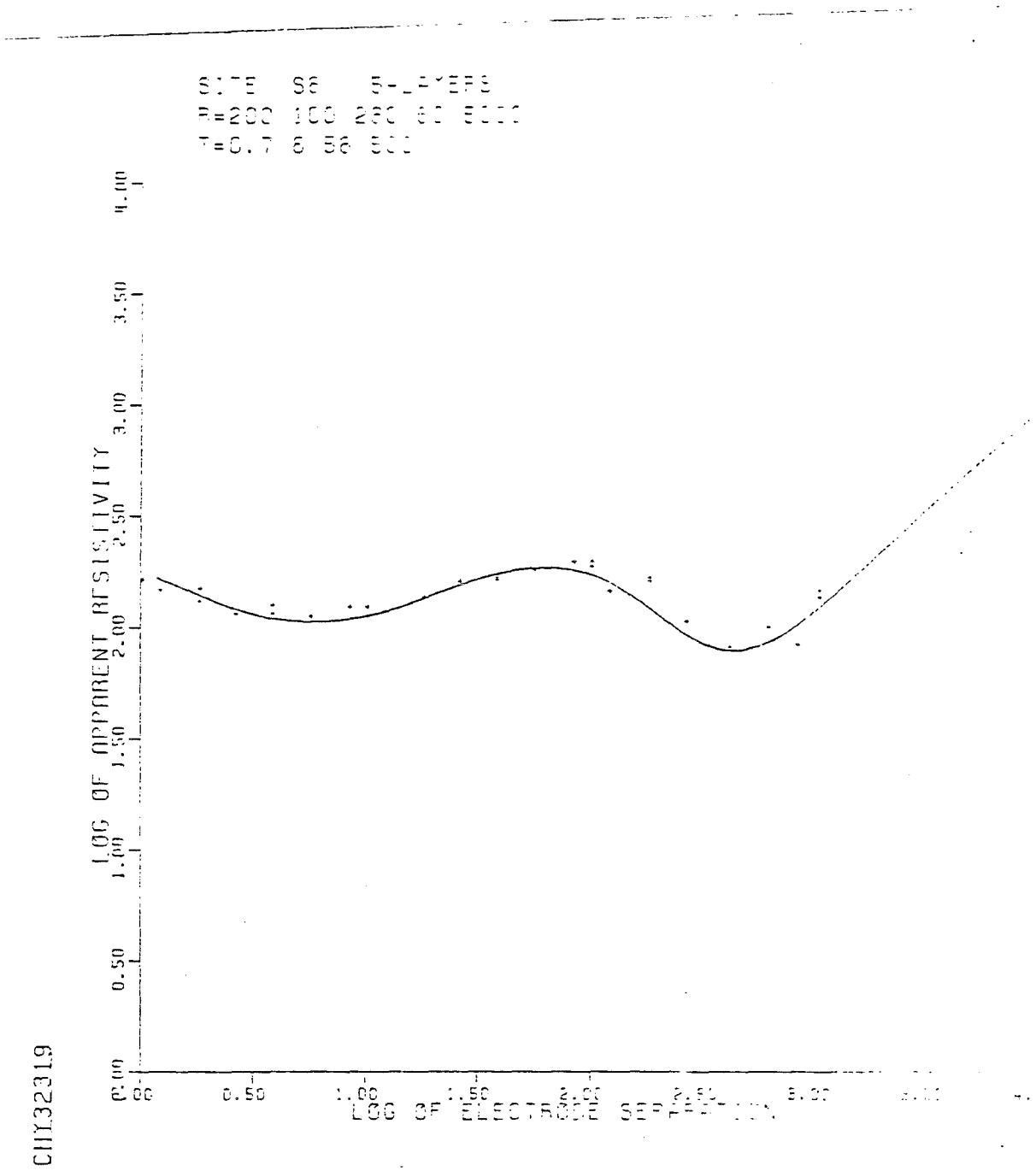
SITE S6 5-LAYERS
R=200 100 200 60 5000
T=0.7 6 56 500
LOG OF APPARENT RESISTIVITY
LOG OF ELECTRODE SEPARATION
0.00
0.50
1.00
1.50
2.00
2.50
3.00
3.50
4.00

CHY32319

CHY31564

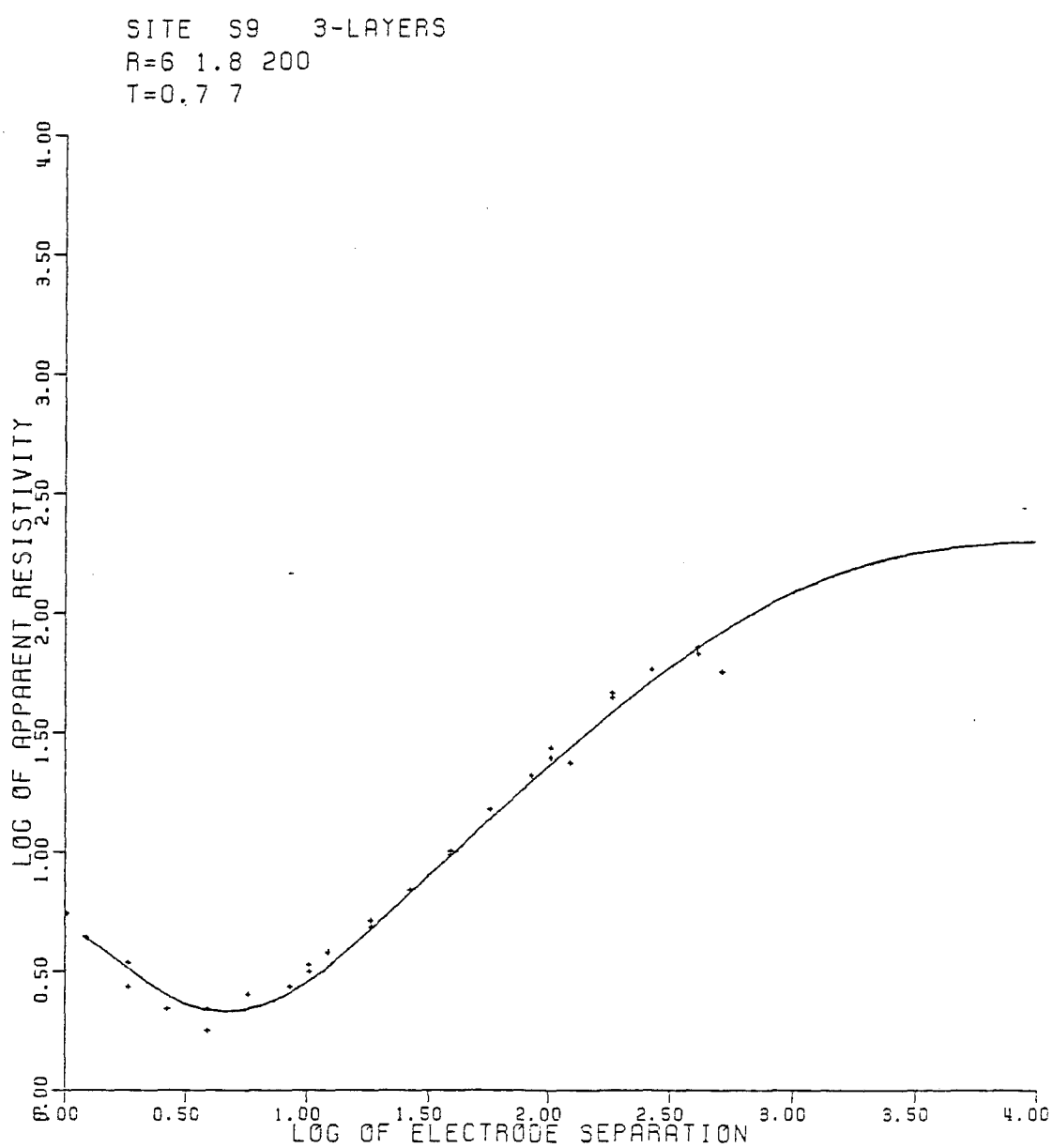

END OF PLOT CHY31564

SITE S10 5-LAYERS
R=100 30 80 5 300
T=0.6 2 25 25

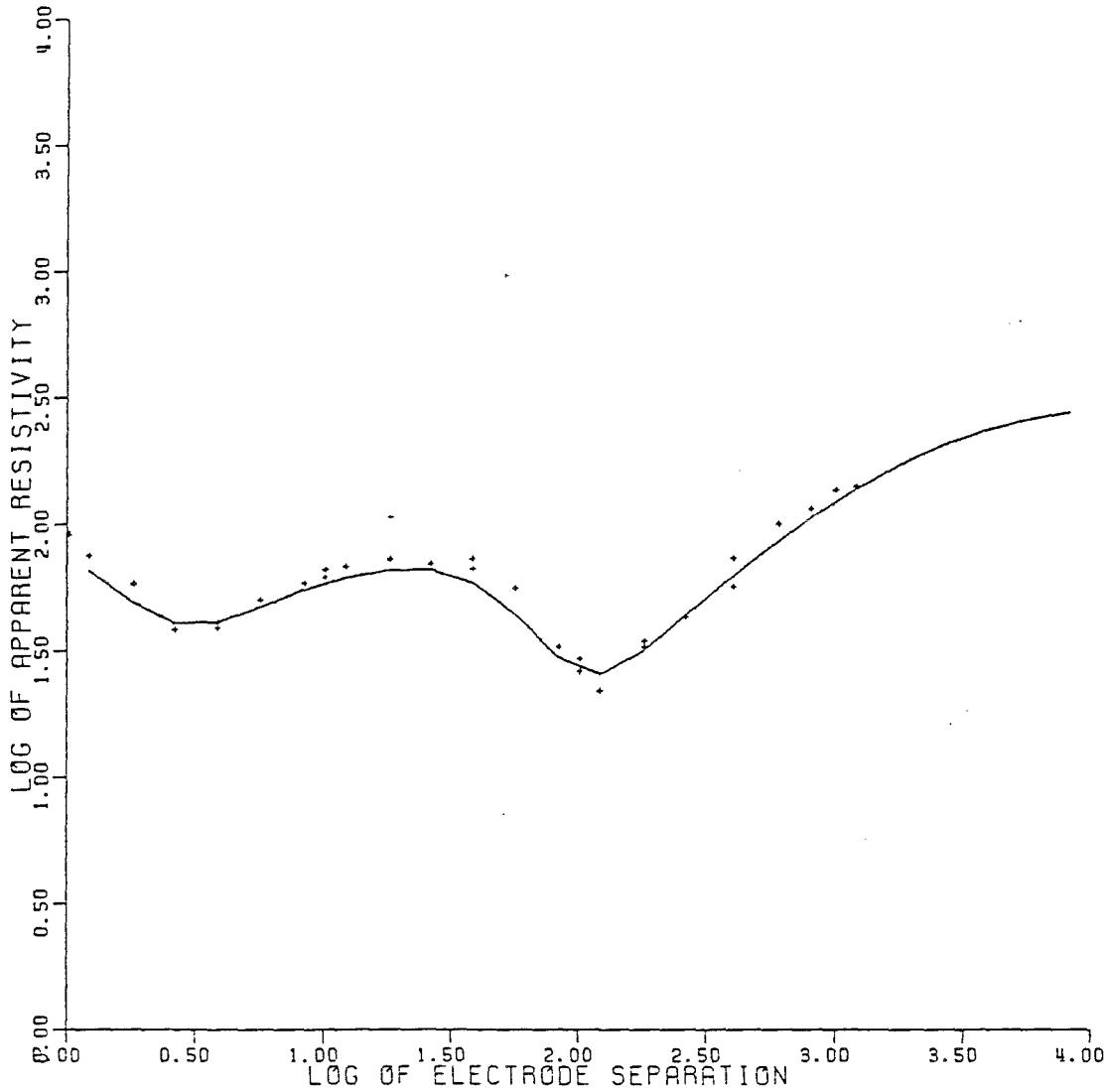

END OF PLOT CHY44538

CHY44538

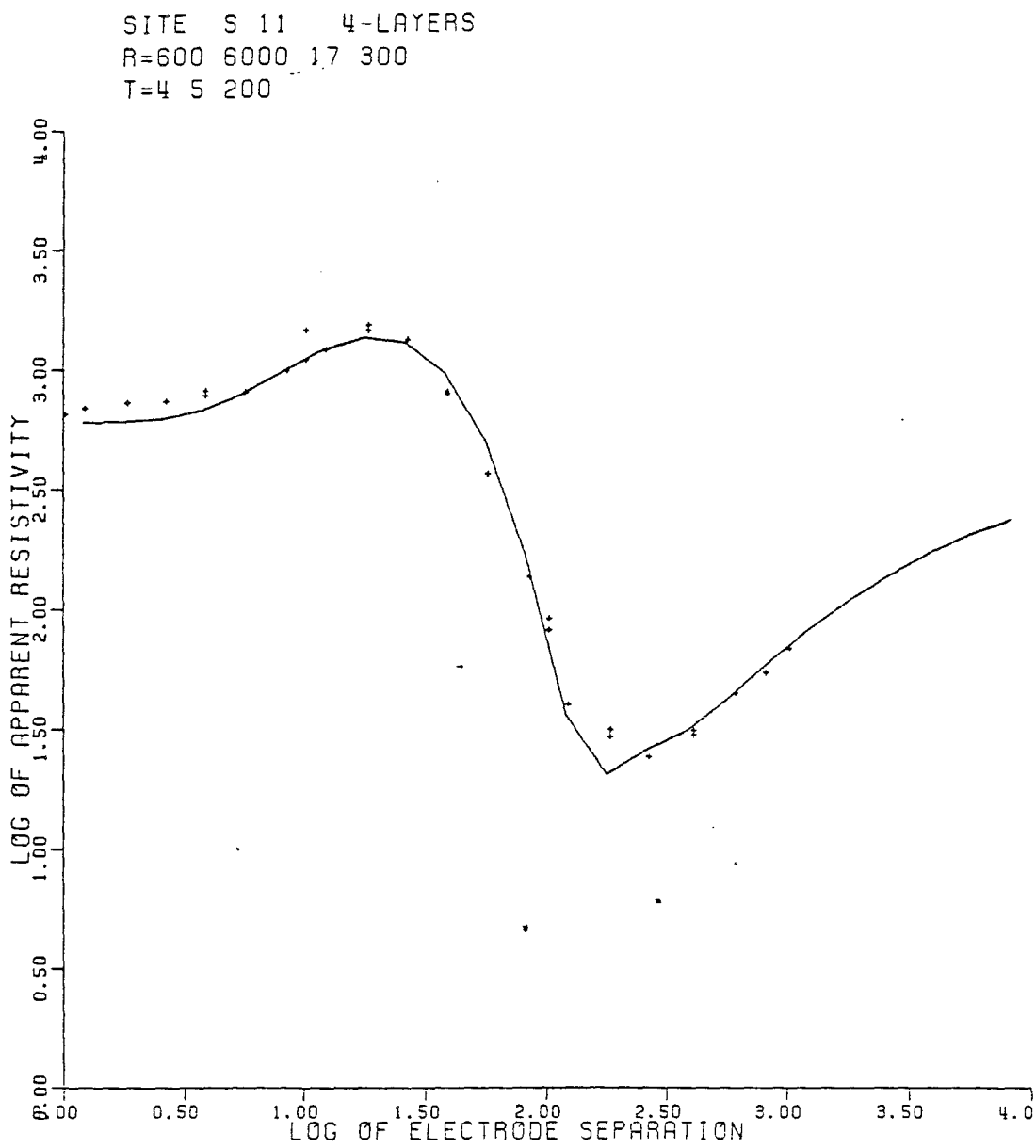

END OF PLOT CHY47451

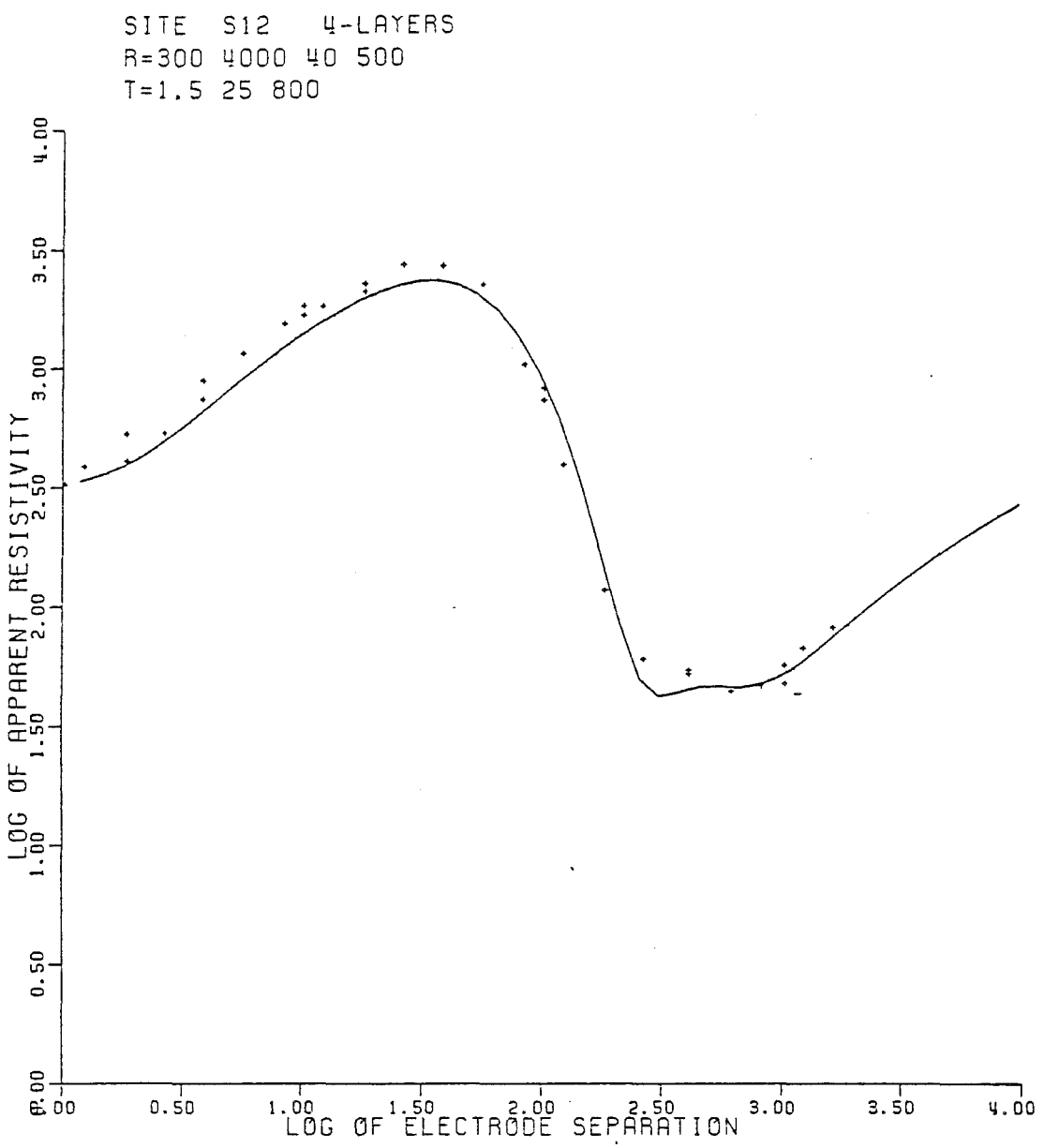

END OF PLOT CHY55577

CHY55577

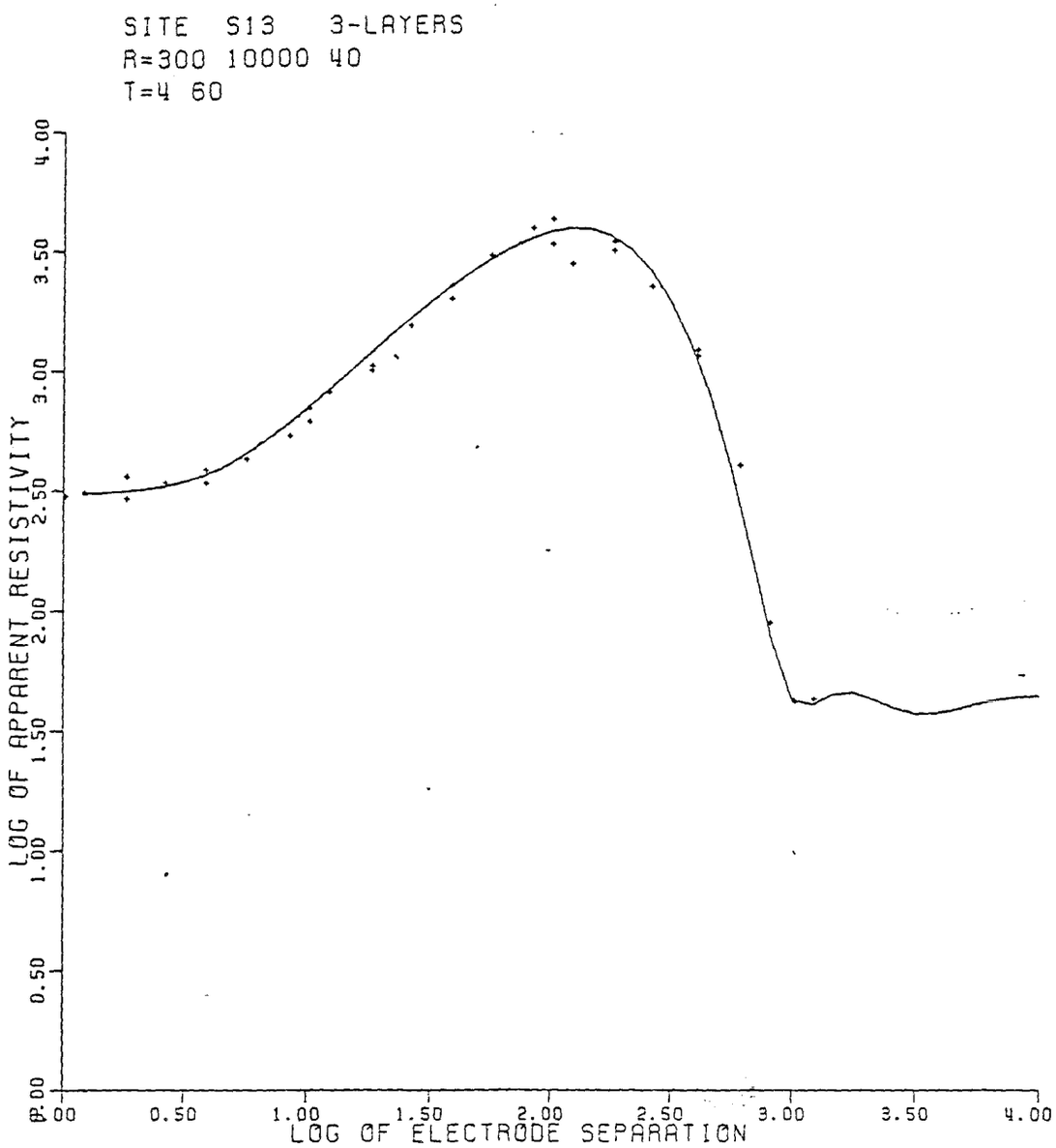

END OF PLOT CHY22269

CHY22269

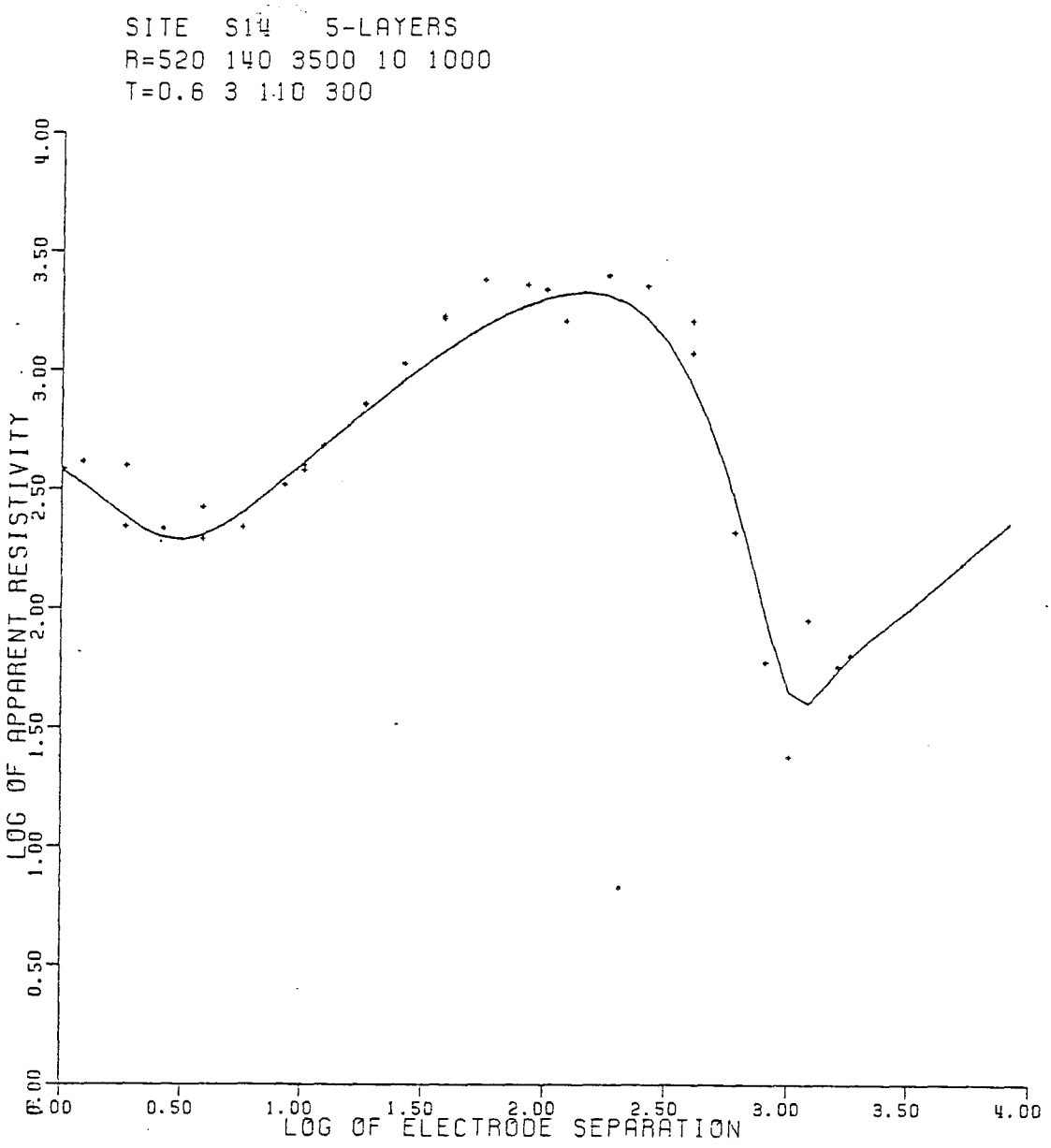

END OF PLOT CHY43068

CHY43068

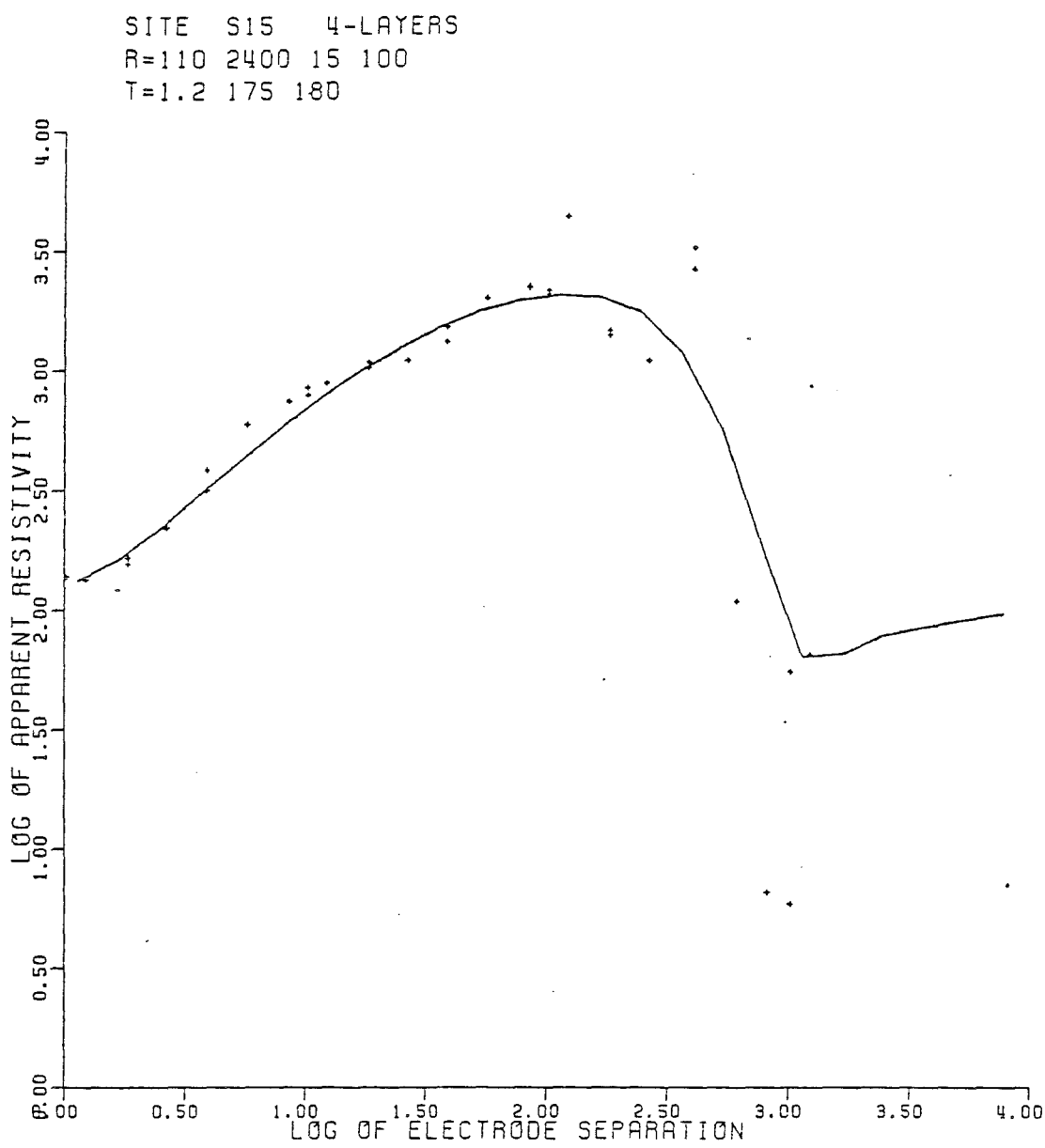

END OF PLOT CHY14526

** START OF JOB CHY24242 TUESDAY MAY 22, 1979 21:28:49 ***

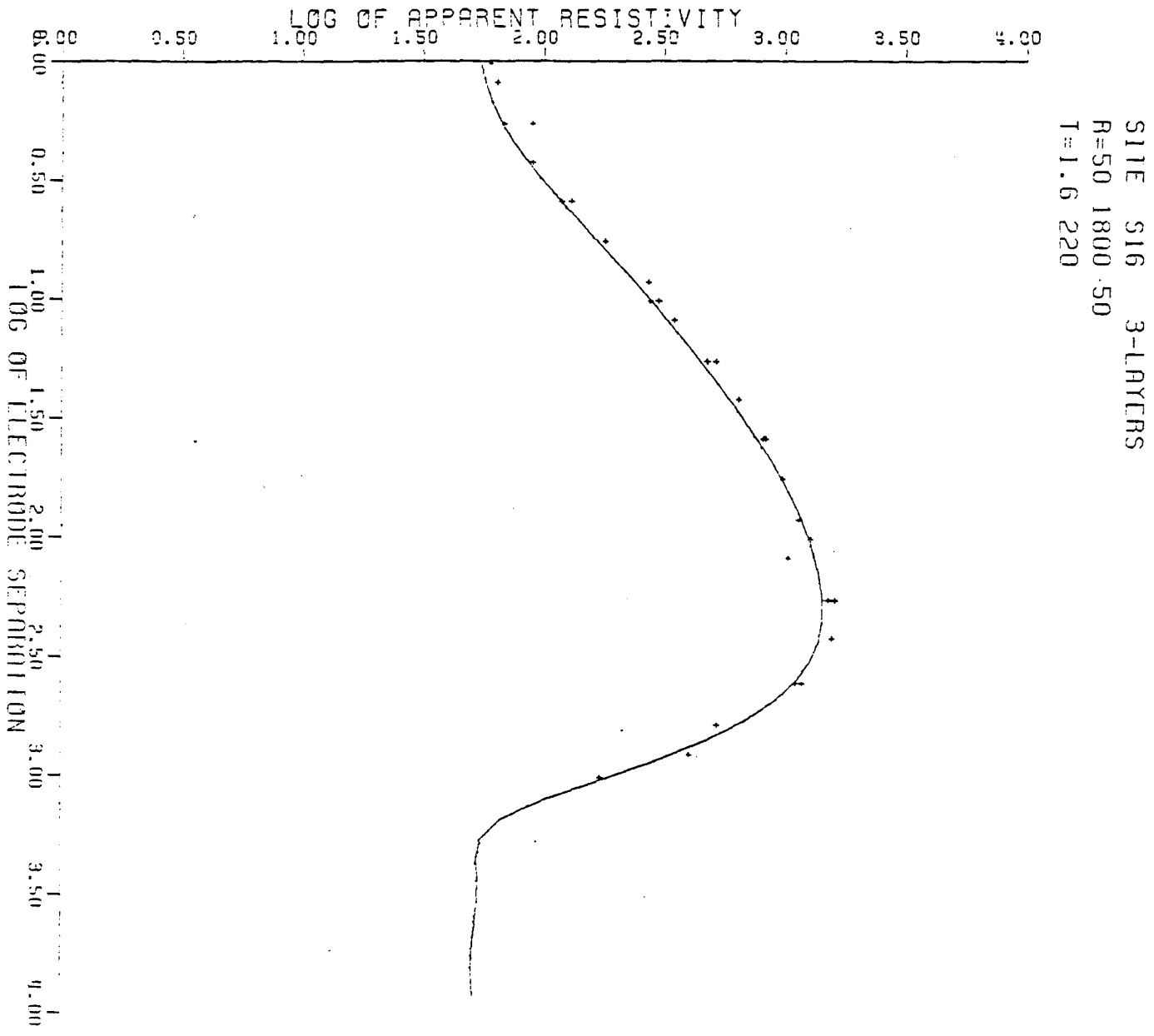

SITE S17 5-LAYERS
R=62 54 12 5 500
T=1.8 0.5 55 250

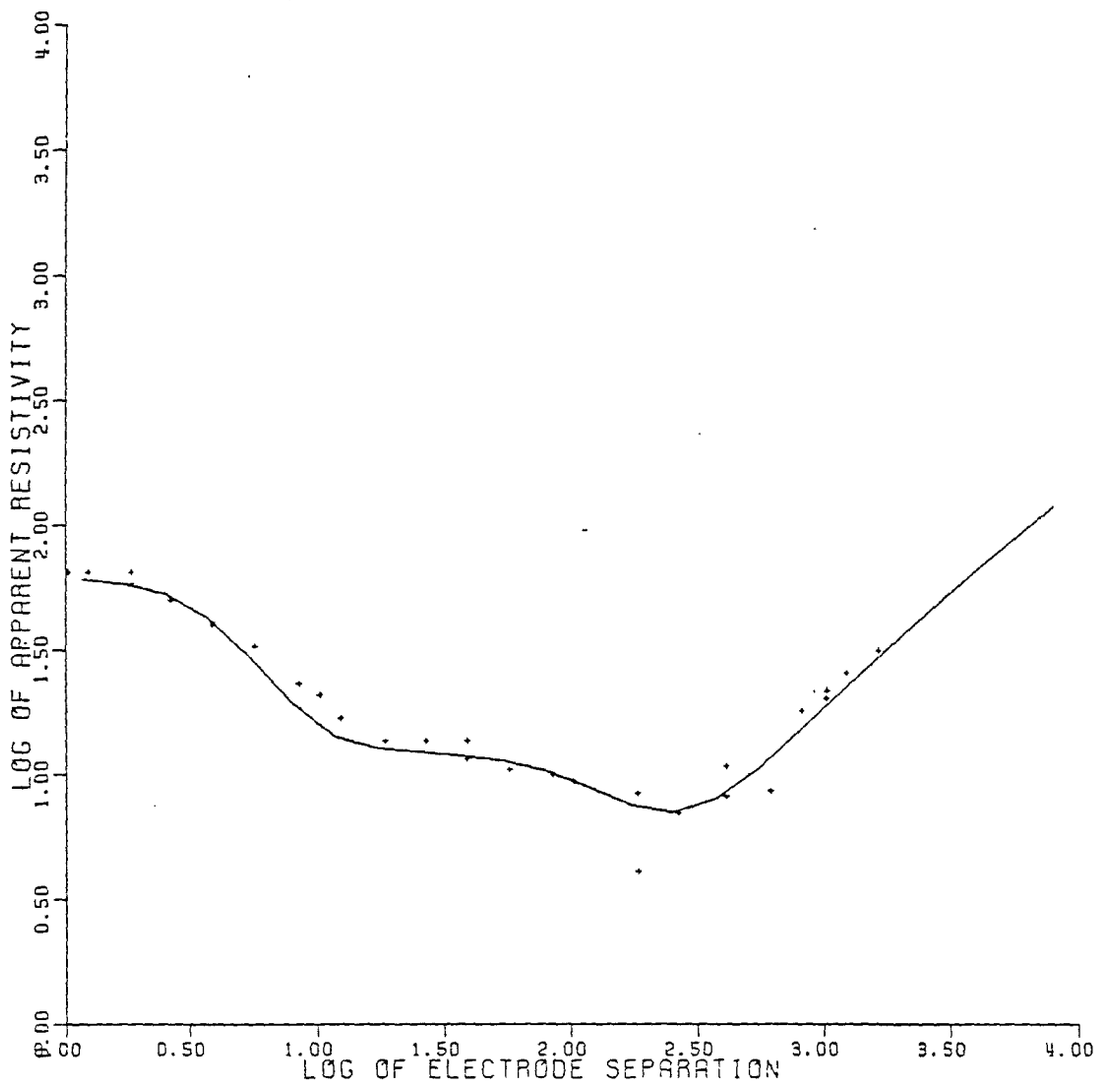

END OF PLOT CHY21106

CHY21106

SITE S18 4-LAYERS
R=65 42 7 400
T=1 19 180

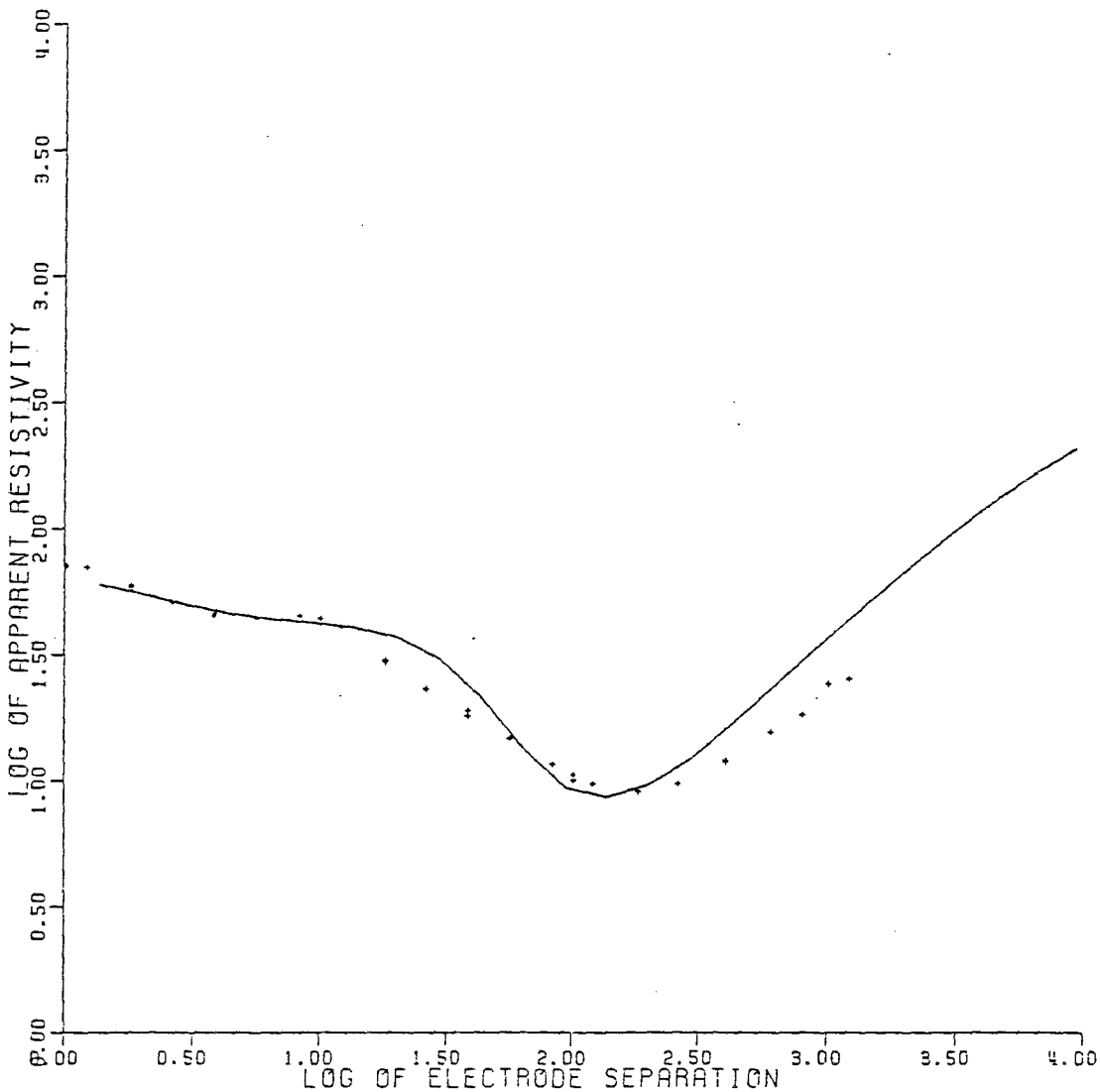

END OF PLOT CHY25178

SITE G1 3-LAYERS
R=200 2200 10
T=17 45

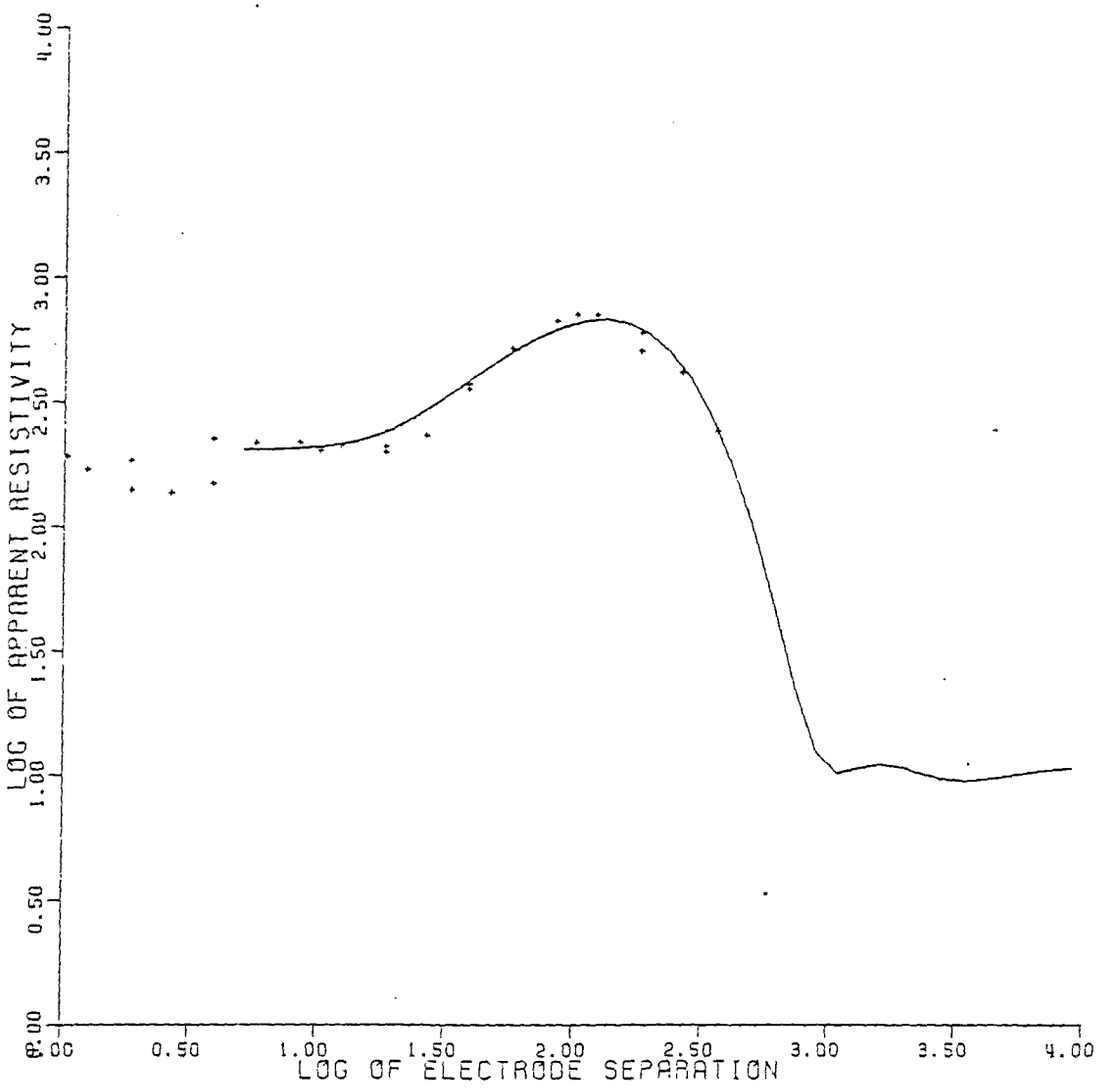

END OF PLOT CHY20287

*** START OF JOB CHY19352 TUESDAY MAY 22, 1979 21:21:27 ***

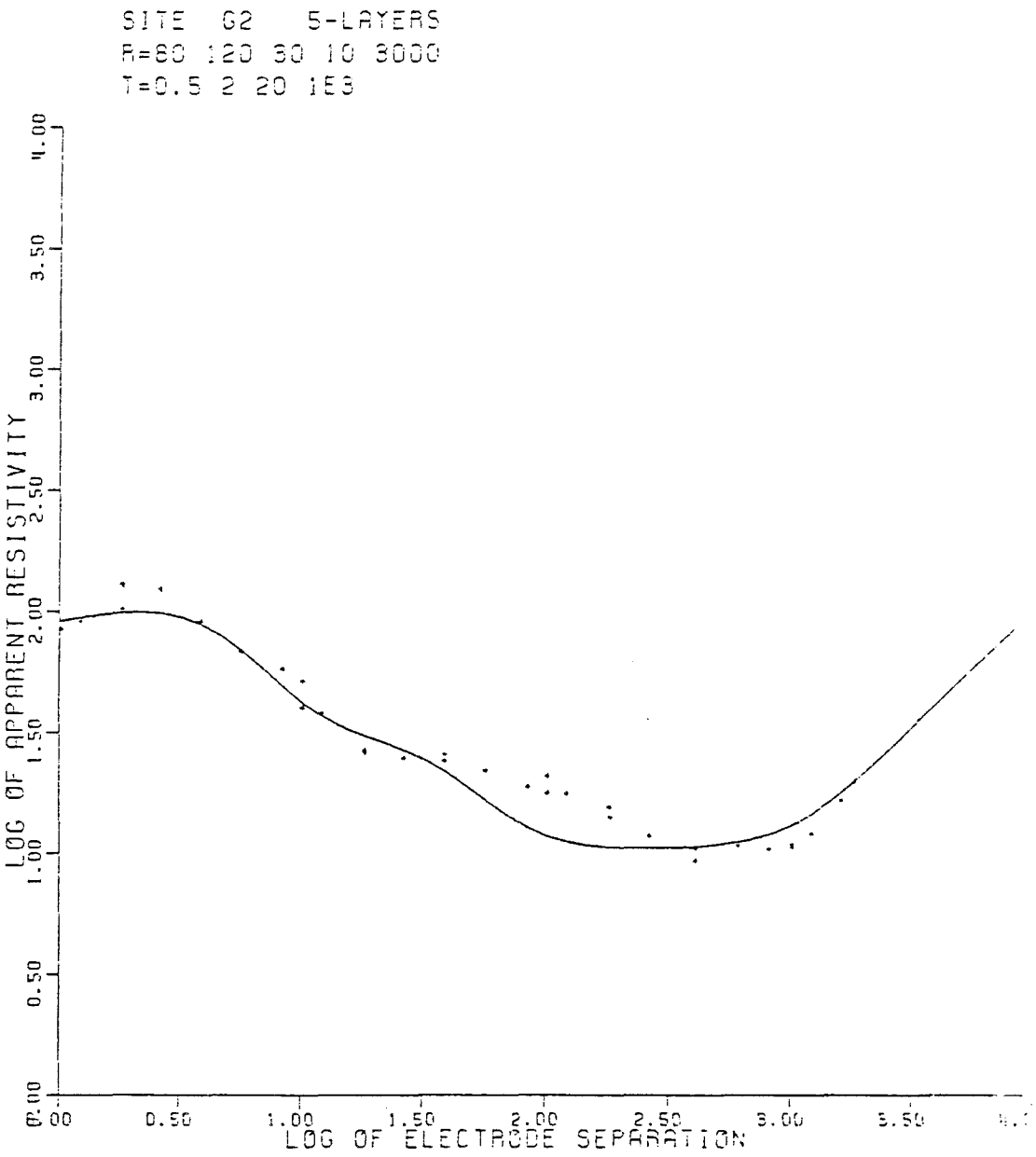

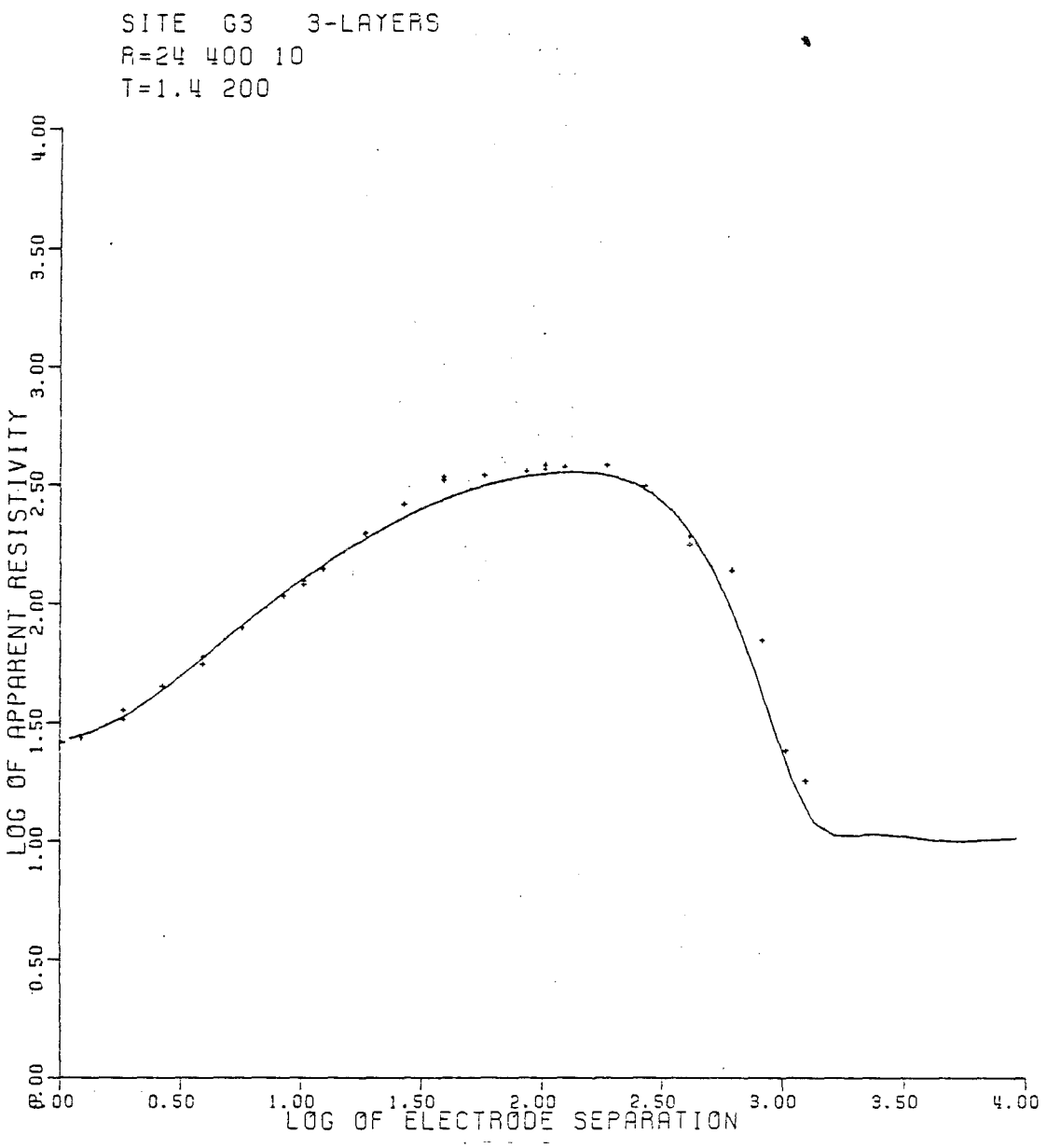
SITE G3 3-LAYERS
R=24 400 10
T=1.4 200
LOG OF APPARENT RESISTIVITY
LOG OF ELECTRODE SEPARATION
0.00
0.50
1.00
1.50
2.00
2.50
3.00
3.50
4.00

Interim Technical Report

for

Arizona Division of Geology and Mineral Technology, Geothermal Group

Implications of a Refraction Profile Study for Geothermal Potential Eastern and Central Arizona

Part of

Study of the Seismic Characteristics of Selected Areas of Geothermal Potential in Arizona

Contract Period: February 15, 1978 - January 15, 1980

Level of Support: $47,194

Principal Investigator: M.L. Sbar

Department of Geosciences

University of Arizona

Tucson, Arizona 85721

Prepared by: Dan M. Gish

Government Technical Officer: Dick Hahman

20 November 1979

--The views and conclusions contained in this documentation are those of the authors and should not be interpreted as necessarily representing the official policies, either expressed or implied, of the U.S. Government.

Interpretations and conclusions in this report are those of the consultant and do not necessarily coincide with those of the staff of the Bureau of Geology and Mineral Technology.

INTRODUCTION

The reversed refraction line currently being investigated by the University of Arizona between Globe, Arizona and Tyrone, New Mexico is now one of the most detailed studies of its kind ever done in Arizona as a result of the completion of field work this summer. Fig. 1 shows the location of this study in relation to existing available deep crustal studies. Station spacings average 3 km and consist of vertical component seismometers filtered between 5 and 12 Hz. The data will permit high resolution of details of velocity structures within the crust and upper mantle and should aid in defining important tectonic parameters such as a seismic low velocity layer (LVL), the topography of the MOHO, and correlation of the LVL to layers of low resistivity which exist in the Southwestern U.S., adding critical seismic data to research already begun (Porath and Gough, 1970; Porath, 1971; Decker and Smithson, 1975; Mitchell and Landisman, 1970; Wiggins and Helmberger, 1973). Additional seismic data is necessary because, although the Basin and Range province is characterized by high heat flow values, heat flow is a manifestation of the earlier sub-crustal thermal history. Electromagnetic studies may reveal a more accurate and current thermal status of the crust, but they possess an inherent ambiguity in the product of conductivity times depth and in modeling deep structures, since shallow lateral complexities can seriously invalidate one and two dimensional electrical modeling techniques. For this reason, independent, detailed seismic studies are required to adequately map the thermal potential of many heat flow anomalies that have been presently identified in the Basin and Range.

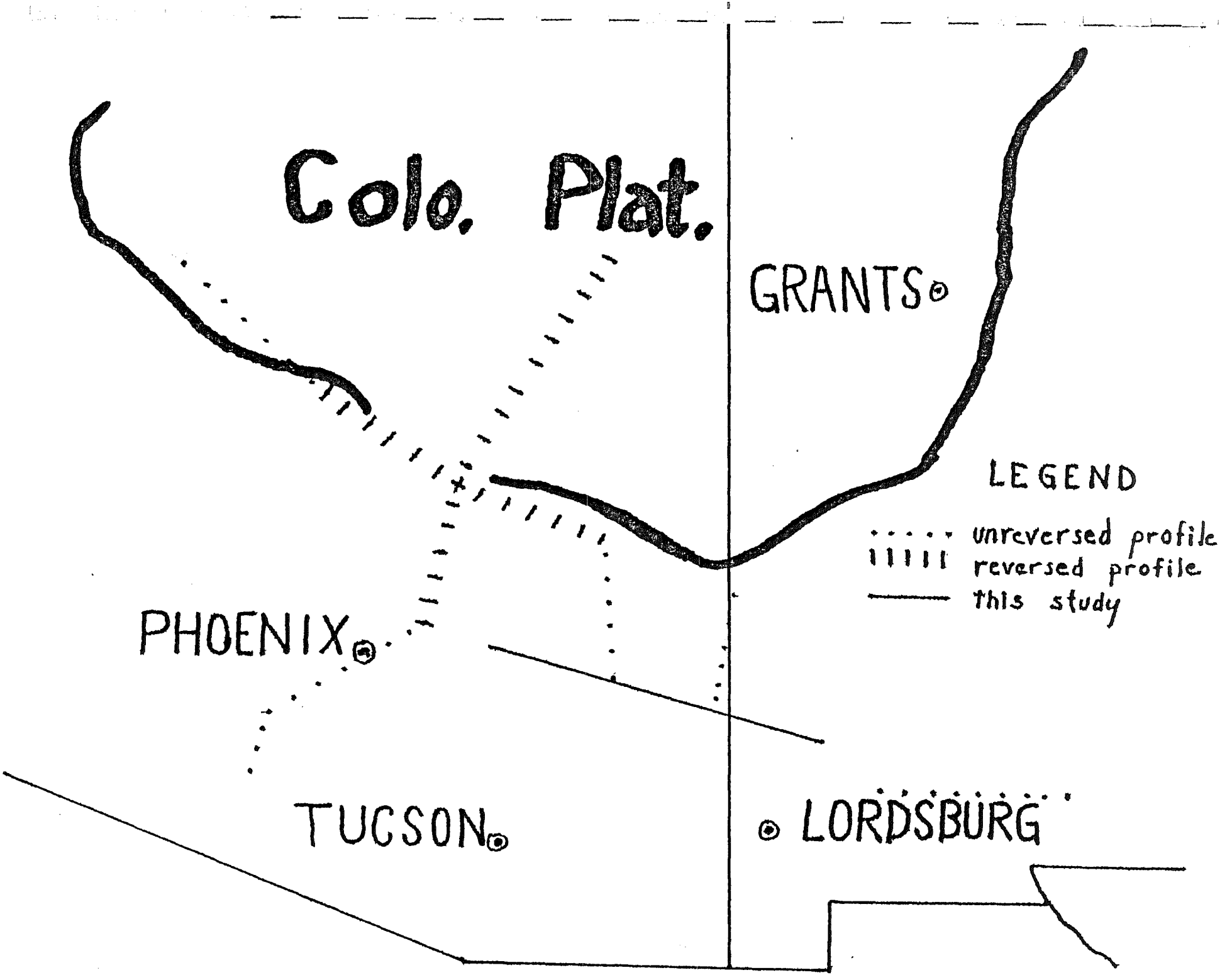
Colo. Plat.
GRANTS
LEGEND
unreversed profile
reversed profile
this study
PHOENIX
TUCSON
LORDSBURG

In addition, this reversed seismic line will tie into two other studies currently in progress at each end of this line; one extends from Parker, Arizona to Globe, Arizona, the other from Tyrone, New Mexico to Grants, New Mexico. This composite refraction line will complete an extensive deep crustal study throughout a tectonically interesting and economically valuable region of the Southwest.

The method of data collection has remained essentially the same as was outlined in previous reports (letter: Sbar, April 19, 1979) and consists of smoked-paper records that necessitate hand digitization. Some use of the Teratech digital 3-component seismometer was made in near-site recording of the blast origin time and vertical reflections, due to the instrument's large dynamic range and automatic trigger.

CURRENT WORK BEING DONE

As the method for reduction of this type of refraction data involves lengthy and complex computer programs for synthetic modeling using the reflectivity method described by Fuchs and Miller (1971), as well as bandpass filtering, scaling, migration and plotting of the data in vertical record sections, several trips to the University of Texas at El Paso, where the computer programs have been adapted to their computer and digitizer, are required.

Presently, the data reduction is at the stage involving digitization and has been slowed somewhat owing to the timeconsuming requirements of travel to El Paso and time away from classes. Once digitization procedures at El Paso have been completed, however, additional modeling can be accomplished at the University of Arizona where some of the subroutines have been rewritten to utilize the DEC-10 facilities here.

Of the approximately 100 individual records obtained for this profile, all are of digitizable quality and reveal excellent coverage of the cross-over distance, the distance at which the refracted arrival from the upper mantle (Pn phase) becomes a first arrival on the record section, preceeding the Pg phase, a direct arrival through the upper crust, which occurs for this study across the southern portion of the San Carlos Indian Reservation in Arizona. The remoteness of these areas fortunately resulted in seismically quiet records of excellent quality and justified the patience and delays involved in obtaining permission to record on Indian lands.

This section of the profile also corresponds to the transitional zone of the Moho, the apparent change in depth from 22 km under the Basin and Range to 40 km under the Colorado Plateau, as proposed by Warren (1969), and crosses the Bylas - Carrizo leg of that study. This study may provide more resolution of faint and sparse upper-mantle reflections for this region which Warren observed but was unable to interpret due to lack of quality data.

Another portion of the data reduction is to establish precise origin times. If small velocity anomalies, such as might be observed in regions of partial melting or mantle upwarps are to be detailed, then travel times must be known to within 0.2 sec. Much of the error in timing accuracies stems from ambiguities in origin times. For the blasts at the Tyrone mine, for example, the blasting area is so large that delay times from one portion of the mine to another must be known. A delay time contour map of the mine and vicinity has been constructed so that t_o, the time of blast initiation, from an observation point such as the seismological facilities at Silver City, N.M. can be calculated.

A typical example of a record section resulting from a similar (but unreversed) refraction study in New Mexico, is shown in Fig. 2. The

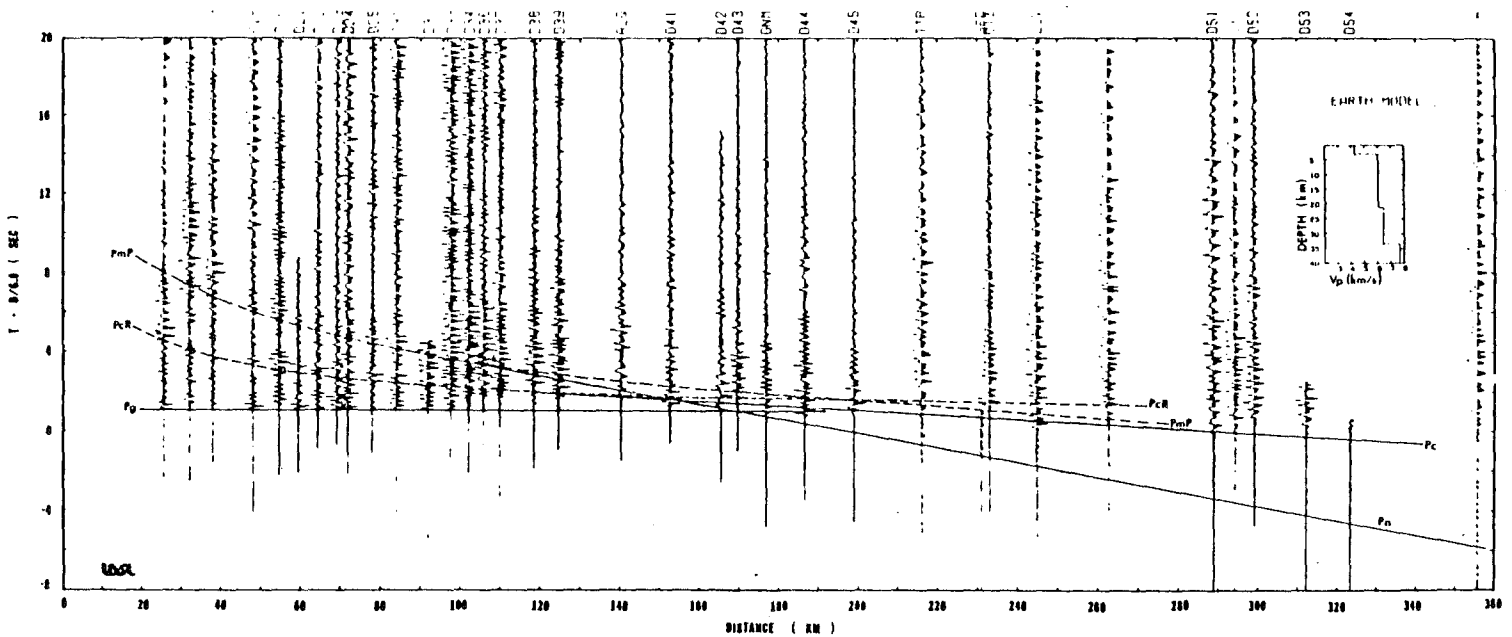
EARTH MODEL
DEPTH (km)
Vp (km/s)
PmP
PcR
Pg
Pc
Pn
DISTANCE (KM)
T - D/6.0 (SEC)

Fig. 2

A Z 3 0

6.5 SECONDS

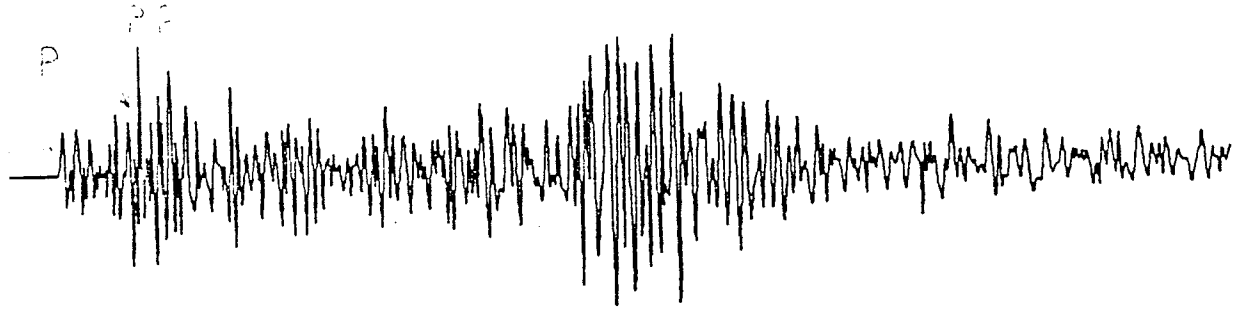

VERTICAL EXAGGERATION 1.00

Fig. 3

spacing of that study averaged 10 km with gaps of 25 km at more distant stations. The arrival times of phases for a 3 layer crust are shown. The cross-over distance occurs at 165 km. Reflections are shown as dashed lines, while refractions are indicated by solid lines. The phase PmP is a reflection from the top of the Moho and the coherency of the phase gives good control to the depth of the Moho, although the station spacing makes resolution of details smaller than 10 km impossible. The PcR phase is a reflection from a major crustal layer at a depth of about 20 km. From the slope of the Pn arrival, an upper mantle velocity of about 7.7 km/sec was calculated.

A station record from this study is shown in Fig. 3, recorded at a distance of 65 km. Tentative phases have been identified.

FUTURE WORK

Digitization of the data should be completed by the end of December, 1979, after which time, modeling of the synthetic data can be accomplished at the University of Arizona facilities. Some of the computer programs which will be used during this phase of the study are still being modified from the El Paso versions. After the best-fit modeling of the data, interpretation of the results will begin in an effort to fully utilize the available information from this study. Some of the issues that this study will address are:

a). to determine the degree with which the seismic crustal low velocity layer may coincide with zones of high conductivity within the crust, as proposed by Decker and Smithson (1975). If the conductive layer should coincide with the LVL, the requirements for extensive partial melting within the crust are not nearly as great as suggested by the seismic data alone.

b). to resolve lateral velocity gradients which might indicate potential areas of high geothermal heat flow, or other anomalous zones of potentially economic size.

c). to resolve fine structure characteristics of the crust and topography of the Moho, possibly coinciding with heat flow evidence for mantle upwarps and shallow crustal structure.

d). to establish velocity - depth model requirements from which plate tectonic reconstructions of the southwestern portion of North America can be based. Particularly important is a clearer understanding by comparison with other regions of the lateral extent and thickness of the crustal low velocity layer. This information would have important implications for intra-plate earthquake studies, interpretations based upon heat flow measurements, and for tectonophysical models.

The conclusions from these studies will be summarized in a report which will be completed by June, 1980. Results from this report to the Geothermal Group, Arizona Division of Geology and Mineral Technology, will also be used in a publication satisfying the requirements for a Master's thesis paper and presented at a professional society meeting in the Spring, 1980.

BIBLIOGRAPHY

Decker & Smithson, 1975, Heat flow and gravity interpretations across the Rio Grande Rift in southern New Mexico and west Texas: Jour. Geophys. Res. 80, p. 2542.

Fuchs & Miller, 1971, Computation of synthetic seismograms with the reflectivity method and comparison with observations: Geophy. J. R. Astro. Soc., 23, p. 417.

Mitchell & Landismann, 1971, Electrical and seismic properties of the Earth's crust in the southwestern Great Plains of the U.S.A.: Geophysics, 36, p. 363.

Porath, 1971, Magnetic variation anomalies and seismic low-velocity zone in the western United States: J. Geophys. Res. 76, p. 2643.

Porath & Gough, 1971, Mantle conductive structures in the western United States from magnetometer array studies: Geophys. J. R. Astro. Soc. 22, p. 261.

Warren, 1969, A seismic-refraction survey of crustal structure in central Arizona: Bull. Geol. Soc. Am. v. 180, p. 257.

POTENTIAL FOR GEOTHERMAL DESALINATION IN THE SOUTHWEST UNITED STATES

by

Chandler A. Swanberg
Sandra M. Rybarczyk

Interpretations and conclusions in this report are those of the consultant and do not necessarily coincide with those of the staff of the Bureau of Geology and Mineral Technology.

ABSTRACT

Combining the results of standard chemical geothermometry techniques, chemical analysis of ground water and geologic mapping of large sedimentary basins, we have delineated areas in the southwestern United States where geothermal desalination may help to augment deficient water supplies. Ten areas favorable for geothermal desalting have been located within Arizona, New Mexico, and southwest Texas.

Introduction

The southwestern United States is an area characterized by accelerating population and economic growth and water deficiency. Availability of water represents a limiting factor in the continued development of the area. Low annual precipitation, high mean annual temperatures, and low humidity with resultant loss of large amounts of water to evaporation assures a small net water yield available as runoff in streams and recharge of underground aquifers from within the area's boundaries. Much of the water presently used is obtained from ground water supplies.

Chemical quality of ground water is variable but significant amounts of previously unusable saline water (more than 1,000 parts per million total dissolved solids) may be made available for urban, industrial, and agricultural utilization in areas where geothermal resources occur in conjunction with large volumes of saline water in permeable aquifers.

This report outlines major sedimentary basins with saline water and geothermal potential in order to outline areas which may benefit from geothermal desalination. It follows from Imperial Valley studies for other major southwestern basins. A description of the techniques of geothermal desalting and its impact on fresh water resources is reported by Fernelius (1975).

Geology

The main area of interest is the Basin and Range province of California, New Mexico, Arizona, and Texas, including the Southern

Rockies province and the Rio Grande Rift. Basin and Range structure is dominated by generally north-northwest trending fault block mountains or ridges separated by sediment-filled basins.

The structural basins between the mountain ranges are filled to depths of thousands of feet with unconsolidated or weakly consolidated deposits of gravel, sand, silt, and clay (alluvium) and are the primary aquifers in most of the area. The large major basins with their great water storage capacity and high permeability are therefore prime sites for large volumes of easily accessible ground water. In the Colorado Plateau and Great Plains provinces the primary aquifers are comprised of consolidated sandstone and limestone, respectively.

Techniques

Locations of deep sedimentary basins were obtained from the work of Gerlach et al. (1975) and Swanberg (1979). Data from Hahman et al. (1978) and Swanberg (1979) were used to determine the distribution and extent of major geothermal areas (Figure 1). Figure 2 represents additional and extended potential geothermal regions (Swanberg, unpublished data). This information was not available at the time figure 1 was prepared, but is included since the results were used in forming the conclusions drawn in this report.

Over 20,000 groundwater chemical analyses from the U.S. Geological Survey's WATSTORE "water quality file", plus those of approximately 300 water samples collected in the study area were used to locate major areas of saline water occurrence. Areas of overlap between abundant

saline water, geothermal potential and major sedimentary basins are shown in Figure 3. Availability of significant volumes of water for desalination in the Colorado Plateau Province was inferred from the approximate areal extent of consolidated sedimentary aquifers shown on the Productive Aquifers and Withdrawal from Wells map of the National Atlas of the United States.

Results

Geothermal resources may originate in deep sedimentary basins where the water is heated by the geothermal gradient and rises to the surface along active faults. Figure 3 shows 10 areas of overlap of high salinity groundwater, geothermal potential and major sedimentary basins. These are the areas that we suggest be targeted for detailed evaluation for desalting of geothermal brine.

The majority of the areas favorable for geothermal desalination occur in the Basin and Range. Waters of the province are generally of low salinity, however, areas where geothermal prospects occur may have saline water at depth. Also shown are three areas in the Great Plains region where abundant saline water occurs in areas of no known geothermal potential and potential for desalination is low.

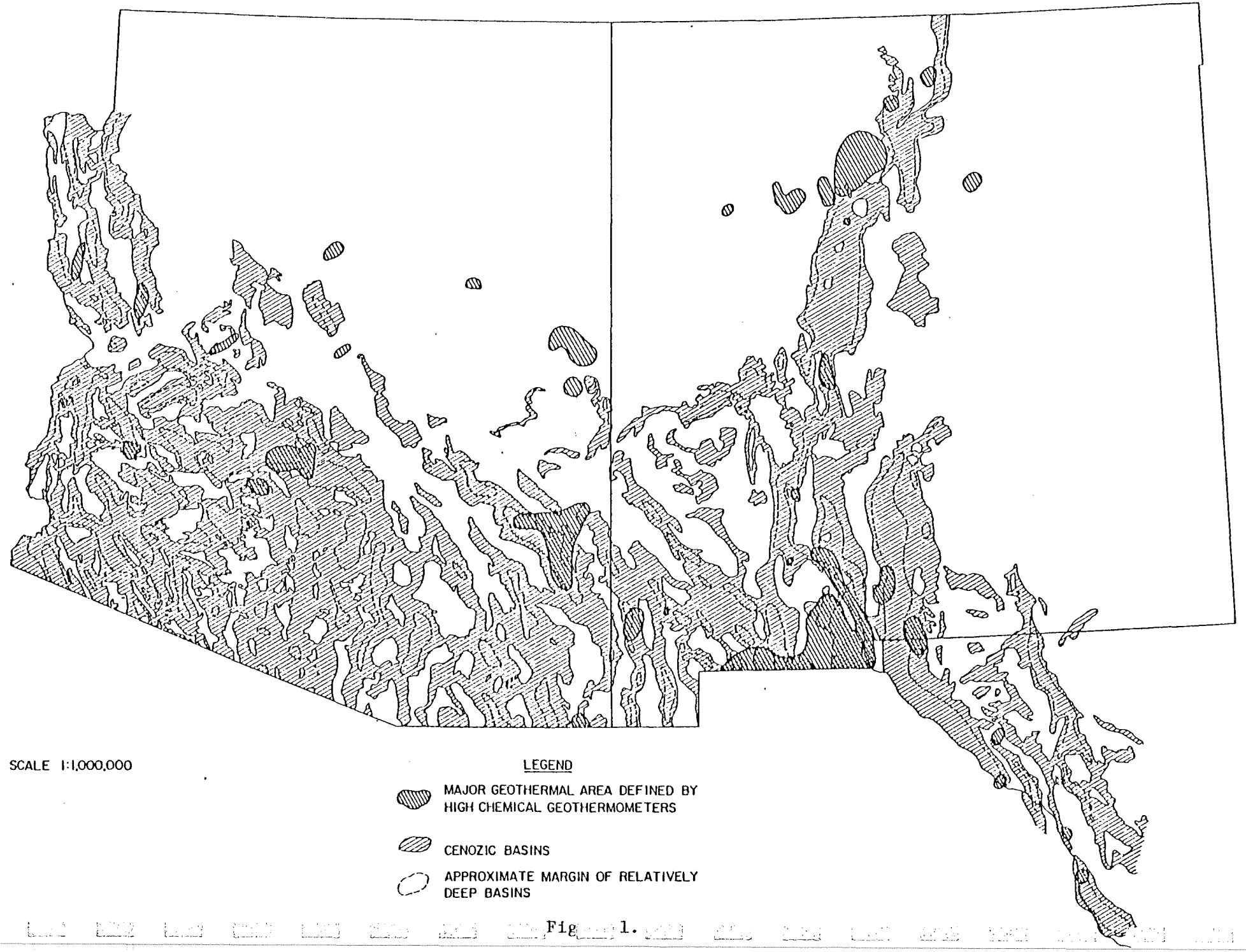
SCALE 1:1,000,000
LEGEND
MAJOR GEOTHERMAL AREA DEFINED BY HIGH CHEMICAL GEOTHERMOMETERS
CENOZIC BASINS
APPROXIMATE MARGIN OF RELATIVELY DEEP BASINS

Fig. 1.

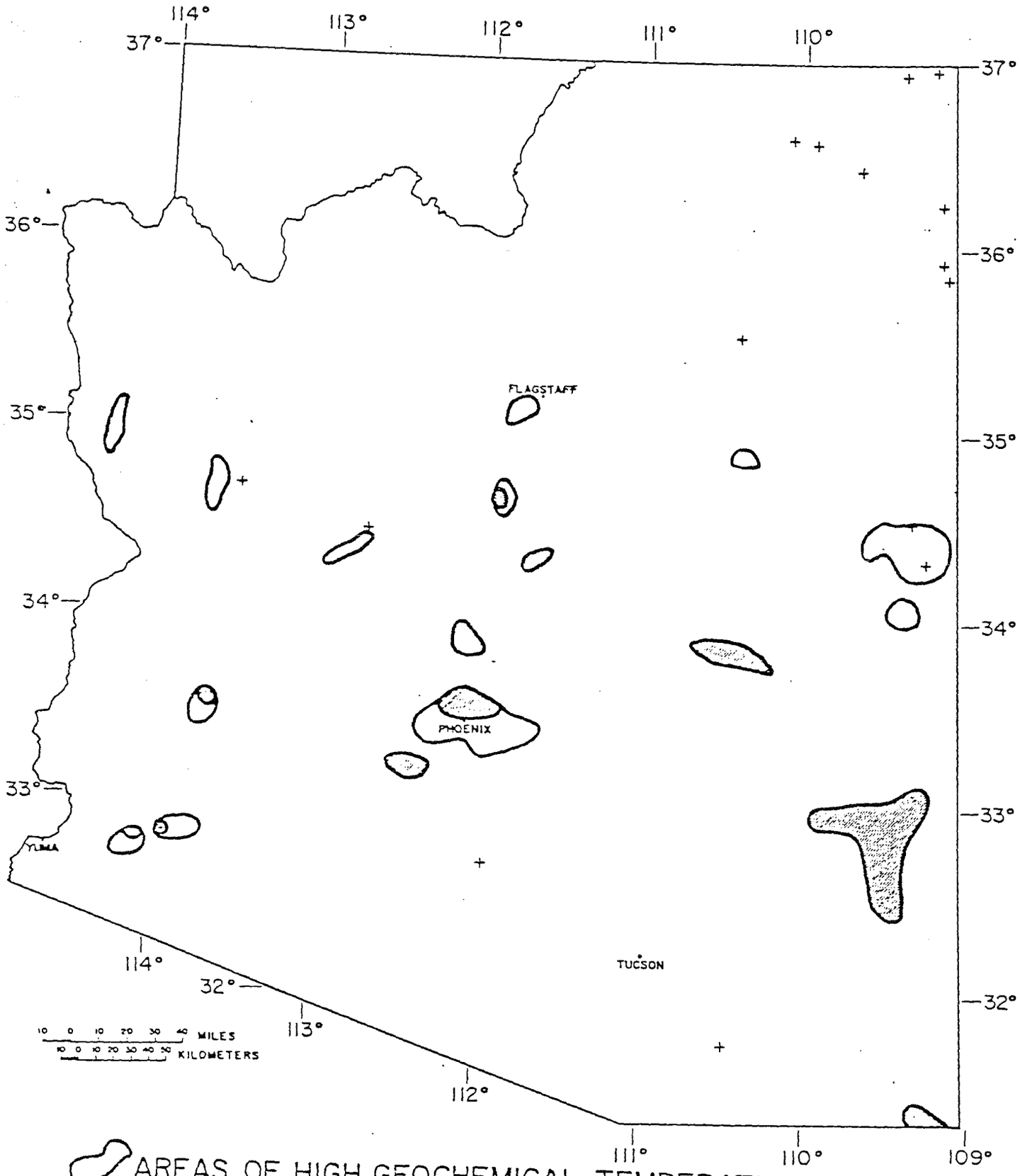

AREAS OF HIGH GEOCHEMICAL TEMPERATURES

AREAS OF HIGH GEOCHEMICAL TEMPERATURES INCLUDING Na-K-Ca-Mg

+ SINGLE HIGH Na-K-Ca-Mg GEOTHERMOMETERS

Figure 2.

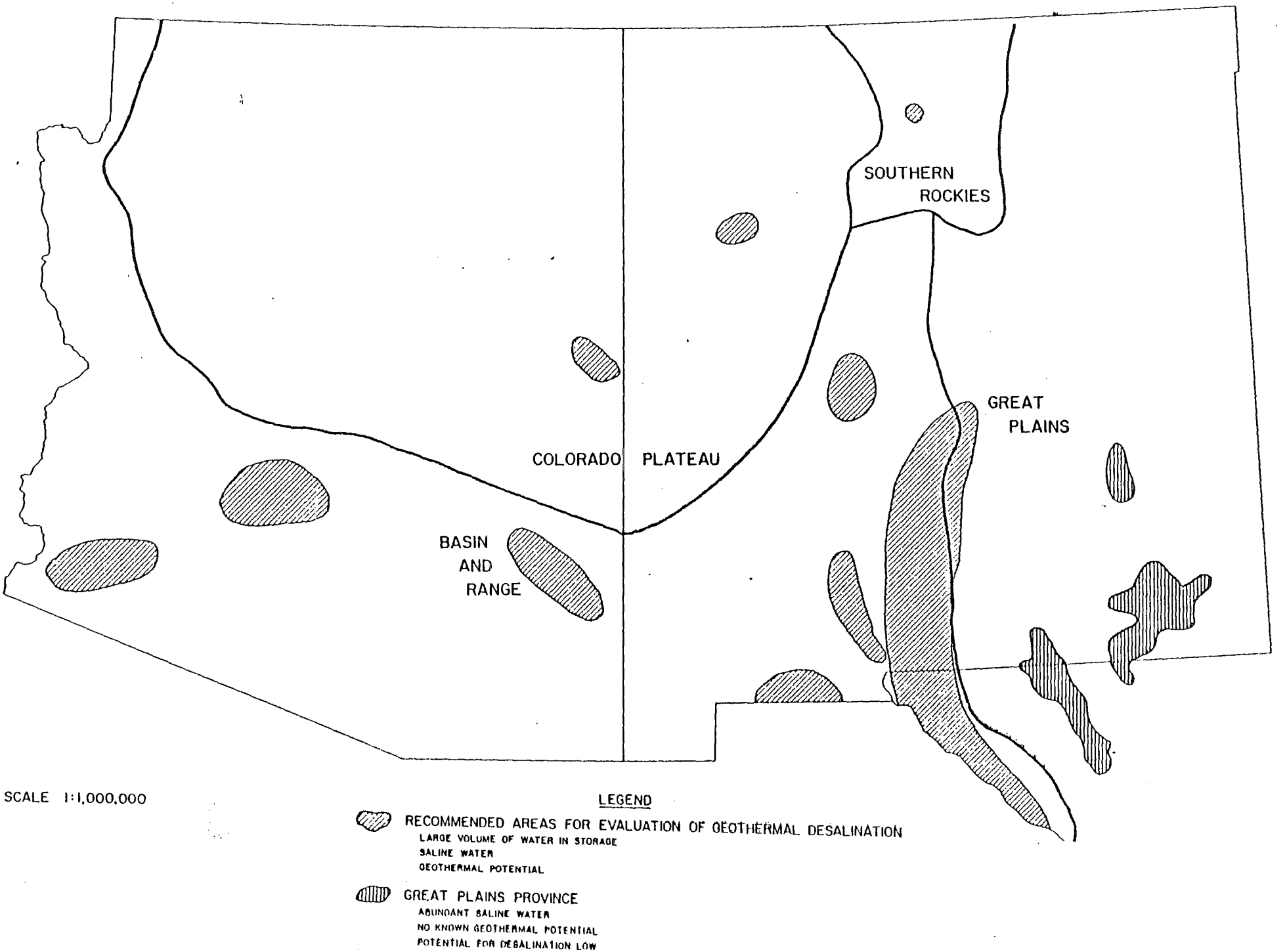
SOUTHERN
ROCKIES
GREAT
PLAINS
COLORADO PLATEAU
BASIN
AND
RANGE
SCALE 1:1,000,000
LEGEND
RECOMMENDED AREAS FOR EVALUATION OF GEOTHERMAL DESALINATION
LARGE VOLUME OF WATER IN STORAGE
SALINE WATER
GEOTHERMAL POTENTIAL
GREAT PLAINS PROVINCE
ABUNDANT SALINE WATER
NO KNOWN GEOTHERMAL POTENTIAL
POTENTIAL FOR DESALINATION LOW

Figure 3.

Acknowledgement

We would like to thank A. Viescas for help with the computer programming and J. Gilkey for assistance in map preparation. Chemical analyses were performed by Andrew Bristol and his staff at the New Mexico State University's Soil and Water Testing Laboratory in the Department of Agronomy. The study was funded in part by U.S. Department of Energy, Division of Geothermal Energy, contract no. EG-77-S-02-4362.

Swanberg, C.A., 1979, Chemistry of thermal and nonthermal groundwaters in the Rio Grande rift and adjacent tectonic provinces: in R.E. Riecher (editor), Rio Grande Rift: Tectonics and Magmatism, American Geophysical Union, Washington, D.C.

Woodward, L.A., Callender, J.F., Seager, W.R., Chapin, C.E., Gries, J.C., Shaffer, W.L., and Zilinski, R.E., 1978, Tectonic map of Rio Grande rift region in New Mexico, Chihuahua, and Texas, New Mexico Bur. Mines and Mineral Res., circ. 163.

COLLEGE OF ARTS AND SCIENCE

DEPARTMENT OF PHYSICS
Box 3D/Las Cruces, New Mexico 88003
Telephone (505) 646-3831

9 May 1979

Mr. W. Richard Hahman, Sr.
Arizona Bureau of Geology and Mineral
Technology
Geothermal Group
2045 N. Forbes Blvd, Suite 106
Tucson, AZ 85705

Dear Dick:

I am enclosing a list of all waters in Arizona that have a temperature in excess of 30°C as listed in the WATSTORE file. Also included is latitude, longitude, and well depth. This data may be of use to you in preparing your final geothermal map for the state-coupled DOE geothermal program. We have sent a similar list for New Mexico to Paul Grimm, along with the designation that the data is of sub-par quality. Assuming a 15°C surface temperature, wells having a gradient greater than 48.6°C/km should be designated as thermal, whereas wells having gradients between 38.1 - 48.6 should be designated as marginally thermal. These cutoff gradients have worked well in New Mexico, and are based on the extensive and highly accurate temperature logs of Marshall Reiter. You may also wish to note that nearly all waters in the Basin and Range are in excess of 20°C, the DOE cutoff temperature for low temperature geothermal resources. These resources should be designated with a 20°C isotherm following the C.P.-B.R. boundary, with the notation that any well south of the line that penetrates the water table will probably encounter temperatures in excess of 20°C--designating individual waters hotter than 20°C merely reflects well distribution and not geothermal resources.

The file has <u>not</u> been field checked. Beware of waters reported as °C, but measured as °F. Witcher is familiar with this problem.

Sincerely yours,

Chan

CHANDLER A. SWANBERG
Associate Professor Physics/Earth Sci.

CAS:nd
Enclosure

Interpretations and conclusions in this report are those of the consultant and do not necessarily coincide with those of the staff of the Bureau of Geology and Mineral Technology.

WATSTORE

Latitude & Longitude Degrees		°C Temp	Depth (m)
31.3928	109.2461	31.0	
31.4881	109.3194	30.0	-
31.6858	111.8250	36.0	215
31.7647	112.3019	30.0	290
31.7750	112.3017	32.0	290
31.7856	112.3092	45.5	218
31.8000	112.2986	46.5	128
31.8136	110.5942	33.0	-
31.8339	109.9081	32.2	-
31.8555	111.7917	30.0	198
31.8755	112.3094	31.5	097
31.8972	112.1736	31.0	136
31.9194	111.9775	35.5	213
31.9336	112.0128	34.0	076
31.9353	112.0153	41.5	036
31.9431	110.9706	36.5	546
31.9697	111.0747	31.1	183
31.9739	112.2811	30.0	116
31.9847	112.2547	30.0	116
31.9922	111.2700	30.0	-
31.9983	110.2842	30.0	305
31.9992	110.9978	32.2	219
31.9994	110.9978	31.1	152
32.0464	112.0617	34.0	153
32.0500	111.6530	30.0	244
32.1053	111.3017	34.0	-
32.1189	111.2150	32.0	306
32.1214	109.9361	30.0	-
32.1314	111.2155	44.5	610

Latitude & Longitude Degrees		°C Temp	Depth (m)
32.1417	110.3258	30.0	157
32.1497	111.5786	30.0	172
32.1525	110.8861	52.2	762
32.1622	111.2330	31.0	-
32.1742	111.9650	33.0	219
32.1750	110.7539	30.5	091
32.1825	110.9619	30.5	152
32.1828	110.9622	33.3	168
32.1864	111.2017	30.0	-
32.1958	109.9175	39.0	-
32.1997	109.1919	32.2	217
32.2130	110.9250	35.0	372
32.2194	111.2500	31.0	-
32.2272	111.6805	30.5	203
32.2300	111.2622	31.0	-
32.2317	109.2305	30.5	-
32.2344	111.2483	30.0	-
32.2372	109.7755	30.0	-
32.2386	110.3322	30.0	-
32.2428	109.8375	35.0	-
32.2480	111.2167	30.5	169
32.2575	110.2522	32.0	-
32.2592	109.8353	31.6	-
32.2703	111.2742	30.5	-
32.2728	109.2328	30.5	268
32.2769	111.6339	32.0	178
32.2775	111.3044	31.0	-
32.2797	109.3392	40.5	293
32.2872	109.2514	30.5	274
32.2922	111.3042	30.0	-
32.2922	111.3217	31.0	-
32.2942	109.2461	32.2	283

Latitude & Longitude Degrees		°C Temp	Depth (m)
32.3006	109.2628	35.0	297
32.3067	111.3214	30.0	-
32.3156	109.2608	32.2	290
32.3158	109.2833	33.5	274
32.3181	109.5000	31.0	213
32.3253	109.4319	31.1	255
32.3255	112.0378	30.5	119
32.3269	109.4869	37.2	253
32.3300	109.2728	33.5	262
32.3389	109.8719	31.6	098
32.3403	109.4492	30.0	218
32.3656	111.2897	30.0	-
32.3694	109.4783	31.5	201
32.3714	111.1639	35.0	110
32.4153	111.3303	35.5	-
32.4483	111.3297	30.0	-
32.5233	109.4258	40.5	587
32.5511	111.3894	34.0	224
32.5672	114.7267	33.5	-
32.5783	111.6558	30.0	210
32.5969	111.5178	34.0	162
32.6030	111.5514	31.0	366
32.6042	111.4992	30.0	185
32.6156	109.4292	36.0	474
32.6303	110.5542	31.0	265
32.6317	111.3289	32.0	332
32.6330	111.5003	30.0	183
32.6397	111.9458	30.0	208
32.6469	111.4997	30.0	305
32.6592	114.6700	39.5	-
32.6669	111.6900	30.0	244
32.6761	111.6375	35.5	396

Latitude & Longitude Degrees		°C Temp	Depth (m)
32.6983	111.5489	32.0	422
32.7053	114.9669	30.5	-
32.7105	111.9214	31.0	060
32.7342	111.4475	30.0	244
32.7417	111.6205	43.5	640
32.7422	111.4478	35.0	421
32.7544	114.9947	33.3	-
32.7558	111.7053	31.0	244
32.7558	114.8042	31.1	-
32.7564	111.6889	30.5	098
32.7633	111.5155	30.0	290
32.7633	111.6503	40.0	466
32.7632	111.7231	30.5	183
32.7639	111.7144	32.0	185
32.7678	113.3344	34.5	-
32.7739	111.7139	33.0	226
32.7747	113.3347	35.5	166
32.7750	114.8375	33.3	-
32.7761	113.3353	36.0	-
32.7780	111.4997	32.0	166
32.7780	111.7239	30.0	143
32.7825	113.3786	31.5	171
32.7828	113.3689	32.0	207
32.7828	113.3861	31.0	-
32.7897	111.8944	31.0	122
32.7928	111.4953	31.0	168
32.7997	113.5367	33.5	207
32.8028	113.3425	39.0	-
32.8042	113.4247	32.5	-
32.8047	113.4467	32.0	151
32.8069	111.5675	30.0	168
32.8094	113.4628	30.0	-

Latitude & Longitude Degrees		°C Temp	Depth (m)
32.8114	113.4433	33.5	-
32.8114	113.4561	34.0	-
32.8114	113.4628	33.5	155
32.8139	111.5153	30.0	305
32.8181	111.9722	32.0	430
32.8331	109.8147	44.0	-
32.8397	113.5397	31.0	-
32.8405	111.9794	30.0	251
32.8517	111.7211	32.0	149
32.8542	109.5458	41.0	-
32.8575	112.0136	30.0	183
32.8617	111.6180	33.0	152
32.8650	111.9639	30.0	116
32.8667	109.7489	46.5	659
32.8769	112.6869	30.5	092
32.8806	114.8625	37.0	-
32.8858	111.6272	34.0	366
32.8867	112.0136	31.0	153
32.8900	111.4630	36.5	091
32.9047	112.1975	31.0	136
32.9083	112.0669	32.0	297
32.9092	111.6053	35.0	-
32.9122	112.9553	33.5	-
32.9125	112.8405	32.0	-
32.9131	112.9467	31.0	-
32.9139	112.9378	33.0	-
32.9142	111.7633	31.5	046
32.9164	111.6555	30.0	199
32.9164	112.0661	30.0	366
32.9169	111.7661	33.5	207
32.9230	112.0822	32.0	189
32.9233	112.9467	30.5	-
32.9247	111.9530	31.0	366

Latitude & Longitude Degrees		°C Temp	Depth (m)
32.9247	112.9467	31.0	-
32.9261	112.7930	32.0	-
32.9267	112.9378	30.0	-
32.9272	112.9553	33.5	-
32.9297	112.7853	34.0	-
32.9314	112.7725	35.0	-
32.9317	112.7622	35.0	-
32.9319	111.9639	31.5	424
32.9342	112.9469	33.0	-
32.9344	112.9300	30.0	-
32.9355	112.7447	37.0	-
32.9355	112.7447	38.0	300
32.9364	111.5500	48.0	782
32.9364	112.7361	33.0	305
32.9408	112.7256	41.3	-
32.9411	111.9639	30.0	-
32.9411	112.0911	32.0	-
32.9450	113.5025	31.0	075
32.9461	111.5911	54.0	155
32.9472	112.7125	41.5	532
32.9472	112.7130	48.5	534
32.9472	112.9242	31.0	-
32.9480	112.9414	34.0	-
32.9547	112.0819	31.0	183
32.9569	112.0989	31.5	190
32.9578	112.1158	36.0	183
32.9600	111.5333	52.0	061
32.9600	111.5755	54.0	591
32.9600	113.2961	39.0	-
32.9639	113.2894	39.5	349
32.9708	112.7214	30.0	-
32.9714	112.7817	30.5	-
32.9744	112.7525	30.0	-
32.9769	113.3100	33.5	-

Latitude & Longitude Degrees		°C Temp	Depth (m)
32.9786	112.7775	33.0	-
32.9794	113.3047	32.0	-
32.9825	113.5072	33.5	079
32.9836	112.1678	33.0	154
32.9858	113.5089	34.0	187
32.9861	112.0972	31.0	306
32.9875	114.9736	30.0	-
32.9894	113.3322	34.5	-
32.9906	113.4881	34.0	145
32.9908	113.3047	32.0	-
32.9958	111.4642	33.5	121
32.9989	109.8978	48.3	183
32.9992	109.8983	47.7	-
32.9992	109.8989	47.7	018
32.9997	113.4958	33.5	122
32.9997	113.5019	35.5	-
32.9997	113.5094	37.0	100
33.0003	113.1433	35.0	-
33.0005	112.1214	33.0	207
33.0005	113.3047	45.0	-
33.0005	113.3822	35.5	-
33.0008	111.9700	33.0	398
33.0028	113.5042	42.5	-
33.0028	113.5064	41.0	-
33.0044	113.1400	32.0	-
33.0050	113.5089	42.5	-
33.0056	112.6636	31.5	-
33.0069	113.1389	33.0	187
32.0072	113.3680	36.5	-
33.0111	111.9975	36.0	114
33.0150	113.5094	31.5	-
33.0153	112.1219	32.5	290
33.0155	113.5019	36.0	-

Latitude & Longitude Degrees		°C Temp	Depth (m)
33.0175	112.6578	33.0	256
33.0189	113.5033	35.0	-
33.0192	111.9369	32.0	213
33.0200	113.5092	30.0	-
33.0244	113.5094	30.0	113
33.0255	112.6653	30.5	-
33.0272	112.9269	31.0	213
33.0272	113.5111	31.0	-
33.0286	112.9728	30.5	253
33.0289	113.5158	32.0	-
33.0292	113.0594	30.0	-
33.0294	113.3739	39.0	305
33.0297	112.6653	30.0	-
33.0314	112.6542	30.0	-
33.0328	113.0814	30.0	-
33.0333	113.0464	31.5	-
33.0339	113.0558	31.0	083
33.0405	113.0494	37.0	-
33.0411	113.0455	34.5	059
33.0575	112.8919	30.5	289
33.0586	111.9617	33.0	342
33.0589	111.6336	37.0	140
33.0589	112.1180	33.0	305
33.0619	111.9819	34.0	-
33.0647	112.6503	30.0	-
33.0650	113.4083	30.5	397
33.0725	113.3947	32.0	418
33.0728	111.9528	31.0	-
33.0728	113.4161	35.0	-
33.0730	112.6497	31.0	258
33.0761	112.1255	32.0	290
33.0794	112.0294	30.0	305
33.0800	109.3031	56.0	-

Latitude & Longitude Degrees		°C Temp	Depth (m)
33.0867	112.1339	38.5	-
33.0878	113.4083	30.0	152
33.1019	113.4250	40.0	-
33.1022	113.3481	38.0	375
33.1022	113.3567	35.0	126
33.1033	110.9536	30.5	-
33.1078	113.2714	33.5	137
33.1092	112.0292	36.0	-
33.1153	112.6564	30.0	107
33.1161	113.3561	40.0	-
33.1167	113.3128	37.5	-
33.1167	113.3228	33.5	-
33.1167	113.3736	39.0	162
33.1169	113.4256	44.5	142
33.1169	113.4297	38.5	-
33.1183	113.3072	38.0	-
33.1319	112.3653	30.0	-
33.1886	112.6758	30.5	149
33.1908	111.5105	33.0	-
33.1978	111.5286	30.0	-
33.1978	112.6761	31.0	-
33.2011	111.3911	33.0	-
33.2022	112.6764	31.5	076
33.2039	111.7628	38.0	-
33.2039	112.3653	34.0	-
33.2039	112.4333	33.0	-
33.2042	112.4158	31.6	267
33.2050	111.5283	30.0	-
33.2097	112.6933	33.0	140
33.2111	111.5000	30.0	-
33.2119	111.7289	36.0	-
33.2122	111.6339	35.0	-

Latitude & Longitude Degrees		°C Temp	Depth (m)
33.2125	111.5283	31.0	-
33.2125	111.6172	37.0	-
33.2128	112.6855	34.0	137
33.2139	112.3764	35.0	268
33.2139	112.3975	37.0	-
33.2147	111.5825	31.0	-
33.2167	111.5628	30.0	-
33.2167	112.3589	37.0	-
33.2167	112.6736	37.0	-
33.2169	112.3661	38.0	-
33.2183	112.4425	33.3	314
33.2183	112.6308	36.0	-
33.2186	111.5283	32.0	-
33.2186	112.4583	35.5	287
33.2189	112.4528	35.5	330
33.2200	111.6855	37.5	-
33.2217	111.8236	44.0	-
33.2217	112.3755	36.0	-
33.2217	112.4094	34.0	-
33.2225	112.4489	34.0	-
33.2231	112.3586	36.6	245
33.2244	112.4583	31.6	322
33.2250	112.3755	35.5	285
33.2250	112.3844	36.0	-
33.2250	112.3972	33.8	183
33.2261	111.6855	37.0	-
33.2269	111.5628	31.0	-
33.2269	112.4344	31.6	335
33.2269	112.6428	31.5	130
33.2272	111.5283	31.0	-
33.2294	111.5283	30.0	-
33.2319	112.3864	35.0	247

Latitude & Longitude Degrees		°C Temp	Depth (m)
33.2322	112.3692	38.0	-
33.2328	111.5283	33.0	-
33.2328	112.4517	30.5	381
33.2330	112.4428	30.5	385
33.2342	111.6344	30.0	-
33.2344	111.6467	30.0	-
33.2344	111.6944	34.4	274
33.2355	111.7289	30.0	-
33.2378	111.6342	30.0	-
33.2386	111.5825	34.0	-
33.2392	111.6514	31.0	-
33.2392	112.3803	35.5	219
33.2397	112.3931	32.7	-
33.2411	111.6944	30.0	-
33.2422	112.3128	37.0	-
33.2439	112.3933	38.0	-
33.2464	112.4025	33.0	-
33.2480	112.4250	32.0	-
33.2531	112.3919	35.5	292
33.2544	112.4814	30.5	305
33.2550	112.4272	31.6	302
33.2564	111.7028	31.5	-
33.2614	112.4092	32.0	-
33.2630	111.6205	30.0	-
33.2644	112.4472	30.0	-
33.2653	111.5828	32.0	-
33.2658	111.6855	30.0	183
33.2697	112.4103	30.0	-
33.2697	112.4703	30.0	-
33.2717	112.7794	32.0	-
33.2792	111.8411	31.5	-
33.2850	111.5828	31.0	-
33.2856	111.6347	30.0	-

Latitude & Longitude Degrees		°C Temp	Depth (m)
33.2908	112.0008	33.5	-
33.2911	111.6178	31.5	-
33.3061	112.7478	31.0	-
33.3080	112.8325	34.0	-
33.3186	112.7664	34.0	-
33.3255	112.8828	34.0	-
33.3333	112.9106	34.0	-
33.3481	112.9180	35.0	406
33.3489	113.1600	33.0	-
33.3558	113.1944	30.0	-
33.3578	111.6703	32.0	-
33.3594	113.1086	32.0	-
33.3597	111.4717	30.0	-
33.3617	113.0908	33.0	-
33.3628	113.1600	30.0	-
33.3633	113.1267	32.0	-
33.3636	113.2211	44.0	-
33.3639	113.1428	33.0	307
33.3647	111.6703	34.0	-
33.3647	111.8583	32.0	305
33.3717	111.6442	34.0	-
33.3717	111.6958	32.0	-
33.3755	111.6931	31.1	155
33.3781	113.1267	30.0	-
33.3781	113.2133	31.0	-
33.3789	111.6692	34.0	-
33.3789	111.6789	33.0	-
33.3797	111.7336	30.0	066
33.3850	112.8578	33.0	-
33.3878	112.6294	40.0	607
33.3919	112.7119	33.0	-

Latitude & Longitude Degrees		°C Temp	Depth (m)
33.3928	113.1872	30.5	314
33.3975	112.4250	30.0	-
33.4019	111.7089	37.0	107
33.4069	113.1961	30.0	-
33.4069	113.2133	35.0	-
33.4081	112.1019	39.5	-
33.4089	111.7475	34.5	066
33.4103	112.4647	36.1	276
33.4139	113.1961	32.0	315
33.4144	112.5639	30.0	-
33.4150	113.2292	32.0	-
33.4203	113.2130	32.0	274
33.4208	113.1255	32.0	-
33.4256	112.3628	50.0	457
33.4278	113.2128	35.5	456
33.4350	113.1353	32.0	-
33.4353	112.4597	46.0	-
33.4353	112.4778	46.0	-
33.4355	113.1436	32.0	-
33.4358	113.2219	34.0	279
33.4361	113.1431	34.0	-
33.4364	113.2308	35.0	518
33.4369	111.7014	40.0	-
33.4386	112.4789	40.5	516
33.4400	112.4767	33.0	-
33.4428	113.1264	40.5	244
33.4431	113.1433	32.0	-
33.4458	112.4611	31.0	-
33.4497	112.8922	32.0	-
33.4497	113.1108	35.0	-
33.4503	113.1608	34.0	-
33.4508	113.1303	37.0	-
33.4508	113.2300	34.5	433

Latitude & Longitude Degrees		°C Temp	Depth (m)
33.4511	112.4253	45.5	580
33.4511	112.4508	49.0	549
33.4511	113.2344	36.0	613
33.4511	113.2392	33.5	244
33.4511	113.2472	31.0	280
33.4514	112.4431	48.5	549
33.4572	113.1536	35.0	-
33.4578	113.1108	35.0	-
33.4636	113.1108	32.0	231
33.4642	112.4431	45.5	463
33.4644	113.1442	33.5	468
33.4644	113.1528	39.0	-
33.4717	112.9022	33.0	-
33.4719	112.9350	35.0	-
33.4722	112.4256	48.0	533
33.4722	113.1700	37.0	-
33.4733	113.1100	32.0	-
33.4772	113.7142	30.5	-
33.4780	112.4250	32.0	-
33.4786	112.4050	40.5	279
33.4786	112.9333	37.0	-
33.4789	112.4689	30.0	280
33.4792	112.9272	39.0	-
33.4792	113.1100	34.0	371
33.4792	113.1436	33.0	-
33.4800	111.9117	30.5	300
33.4800	112.4594	30.0	-
33.4817	113.1436	33.0	-
33.4819	111.8997	30.0	366
33.4842	111.8956	32.2	152
33.4855	112.4097	33.0	-
33.4861	112.4169	30.0	084
33.4861	113.1092	34.0	-

Latitude & Longitude Degrees		°C Temp	Depth (m)
33.4864	112.9803	32.0	-
33.4867	112.4180	31.0	-
33.4869	113.1017	38.0	-
33.4869	113.1483	38.0	-
33.4881	111.9044	36.6	168
33.4897	112.9330	40.0	-
33.4903	112.9447	37.0	-
33.4928	112.9375	48.5	063
33.4928	112.9575	33.0	-
33.4930	112.4453	40.0	488
33.4930	112.9436	44.0	-
33.4933	112.9492	35.0	-
33.4936	112.4256	32.0	-
33.4939	112.9817	33.0	-
33.4939	112.9864	33.0	-
33.4939	113.1108	35.0	-
33.4944	111.8950	31.6	404
33.4944	111.8992	32.7	366
33.4947	111.8911	33.8	366
33.4950	111.9330	30.0	192
33.4955	111.9089	30.0	366
33.4964	112.3742	56.1	226
33.4967	112.9528	34.0	-
33.5003	112.4253	32.0	-
33.5005	112.4081	32.0	294
33.5005	113.1261	35.0	-
33.5008	112.9019	30.0	-
33.5072	112.3956	32.0	-
33.5075	112.3958	31.1	220
33.5078	112.3656	48.8	318
33.5078	112.4603	30.0	364
33.5083	111.8786	30.5	-
33.5111	111.9503	30.0	-
33.5142	112.3400	33.3	-

Latitude & Longitude Degrees		°C Temp	Depth (m)
33.5147	112.9528	35.5	209
33.5150	113.0933	31.5	155
33.5169	111.8994	34.4	311
33.5192	112.1758	43.5	479
33.5214	112.4078	31.0	-
33.5217	112.4447	30.0	-
33.5225	113.1358	33.0	184
33.5230	113.1611	33.0	466
33.5242	111.9128	30.0	306
33.5258	111.8753	31.0	-
33.5286	111.9230	30.5	
33.5297	113.1608	35.0	-
33.5300	111.1883	34.0	457
33.5308	112.3744	34.4	366
33.5322	111.9014	33.3	305
33.5361	112.1844	36.5	529
33.5367	112.4003	33.3	213
33.5369	113.1694	33.5	457
33.5369	113.1786	33.5	396
33.5369	113.1883	34.5	469
33.5372	113.1614	34.5	457
33.5381	111.8217	32.0	-
33.5381	111.8306	33.0	-
33.5381	111.8392	32.0	-
33.5381	111.8422	34.0	-
33.5392	112.2208	30.0	-
33.5436	112.9019	35.0	-
33.5447	112.3833	38.0	-
33.5453	112.1928	30.0	213
33.5458	112.3292	31.5	256
33.5480	112.3369	32.2	282
33.5489	112.1928	40.0	579
33.5492	112.3822	31.1	305

Latitude & Longitude Degrees		°C Temp	Depth (m)
33.5494	112.4353	32.0	-
33.5506	112.4150	32.0	-
33.5514	112.4142	30.0	-
33.5514	112.4256	30.0	308
33.5586	112.3925	30.0	-
33.5653	112.3872	32.7	315
33.5653	112.4083	33.0	-
33.5658	112.3844	34.0	-
33.5658	112.3928	34.0	-
33.5661	112.3758	36.0	-
33.5717	112.1255	32.0	092
33.5722	112.3405	30.0	-
33.5722	112.3528	30.0	305
33.5730	112.3653	31.6	198
33.5736	112.3925	33.0	-
33.5794	112.3233	-	-
33.5794	112.3233	33.8	194
33.5797	112.3353	33.0	-
33.5797	112.3405	30.0	-
33.5797	112.4180	33.0	-
33.5800	111.9078	42.0	-
33.5800	112.3755	32.0	-
33.5800	112.3800	33.0	-
33.5803	112.3928	31.0	-
33.5811	112.1111	31.6	369
33.5903	113.7789	32.0	-
33.5930	111.8769	30.0	-
33.5947	112.3753	34.0	-
33.5950	112.3580	32.0	-
33.5950	112.3844	32.0	-
33.5958	111.9533	32.7	319
33.6019	112.3625	35.0	-
33.6019	112.3661	34.0	-

Latitude & Longitude Degrees		°C Temp	Depth (m)
33.6672	112.2372	30.0	-
33.6672	112.3586	41.0	-
33.6675	112.4017	30.0	183
33.6686	112.3900	33.5	364
33.6781	112.3928	33.0	305
33.6817	112.4025	31.0	329
33.6953	111.5167	36.0	-
33.6964	112.3503	31.0	-
33.6964	114.6775	31.1	-
33.6967	114.6575	30.6	-
33.7042	114.6436	30.6	-
33.7058	113.8022	30.0	-
33.7114	113.7969	33.5	-
33.7169	114.6869	32.8	-
33.7222	113.7017	33.0	-
33.7233	113.7719	34.0	-
33.7389	113.5411	33.0	-
33.7394	113.8778	32.5	443
33.7406	113.1492	32.5	443
33.7428	113.7517	32.5	-
33.7430	113.7519	33.5	-
33.7900	113.6278	30.0	-
33.7972	113.6328	30.0	-
33.8044	113.5714	30.0	-
33.8050	113.5917	30.0	-
33.8111	113.5997	31.0	-
33.8119	113.5861	31.0	-
33.8183	113.5917	30.0	-
33.8228	113.5750	33.0	-
33.8255	113.5831	33.0	-
33.8264	113.5561	36.0	-
33.8264	113.5656	34.0	-
33.8264	113.5914	30.0	-
33.8283	113.5425	35.0	-

Latitude & Longitude Degrees		°C Temp	Depth (m)
33.6019	112.3842	32.0	-
33.6033	114.7278	33.3	-
33.6042	114.6922	31.1	-
33.6061	112.3928	35.0	-
33.6064	114.6028	30.8	-
33.6067	112.0064	30.5	101
33.6089	112.3844	33.0	-
33.6100	112.1680	30.0	190
33.6100	112.4519	34.0	467
33.6103	112.1678	30.0	-
33.6172	112.1253	30.0	152
33.6233	112.3669	31.0	-
33.6236	112.3842	33.0	-
33.6236	112.4014	30.0	-
33.6236	112.4089	39.0	224
33.6269	114.6761	30.6	-
33.6317	112.4014	32.2	367
33.6322	112.1505	37.7	580
33.6347	112.4083	30.0	-
33.6378	112.4022	30.0	-
33.6378	112.4367	30.0	-
33.6383	112.3844	31.0	-
33.6461	114.6922	31.1	-
33.6494	112.3928	33.0	-
33.6494	112.4256	30.0	-
33.6494	114.6636	33.3	-
33.6517	111.9683	30.5	370
33.6522	112.2339	31.0	-
33.6539	112.3986	31.0	158
33.6542	112.4275	30.0	-
33.6542	113.7467	31.0	-
33.6589	112.9172	33.0	-
33.6608	114.6875	32.2	-
33.6667	112.3778	33.0	329
33.6669	112.3686	31.0	160

Latitude & Longitude Degrees		°C Temp	Depth (m)
33.8300	113.5739	35.0	-
33.8331	113.5922	30.0	-
33.8372	113.5661	36.0	-
33.8411	113.8892	30.0	335
33.8472	113.3819	30.5	305
33.8481	113.5392	35.0	-
33.8494	113.4878	30.0	287
33.8508	111.9478	30.0	-
33.8550	113.5430	34.0	-
33.8553	113.5533	33.0	-
33.8561	113.4592	35.0	-
33.8572	113.4533	35.0	-
33.8580	113.4533	37.7	365
33.8825	113.8683	30.0	-
33.9075	113.0992	32.0	-
33.9214	113.1247	32.0	-
33.9436	113.1100	36.0	-
33.9436	113.1142	36.0	-
33.9436	113.2147	31.0	-
33.9439	113.0028	30.0	177
33.9494	113.1133	37.0	-
33.9528	113.2111	31.0	-
33.9569	113.1611	35.0	219
33.9653	113.1594	30.0	-
33.9717	113.1661	30.0	-
33.9719	113.1764	30.0	-
33.9778	113.2089	33.0	-
33.9850	113.2081	34.0	-
33.9881	113.3047	39.5	021
33.9936	113.3047	33.0	022
33.9992	113.2117	35.0	-
33.9992	113.2125	33.8	412
34.0005	113.2172	32.2	306
34.0008	113.1967	33.0	-

Latitude & Longitude Degrees		°C Temp	Depth (m)
34.0008	113.2117	33.0	-
34.0008	113.2203	33.0	-
34.0611	113.6117	33.0	-
34.0780	111.7067	36.0	-
34.1322	111.7886	30.0	-
34.1622	109.3017	40.0	-
34.3550	111.7089	39.5	-
34.6953	113.5736	35.5	-
34.8147	114.1383	46.0	-
34.8755	114.1547	33.5	306
34.8775	114.1444	33.0	-
34.9350	113.6672	31.0	-
35.0389	114.3228	31.0	113
35.1222	114.2074	36.5	-
35.1528	114.5778	32.0	146
35.1844	114.2253	32.0	-
35.1861	113.7142	31.1	299
35.2278	114.2150	37.5	-
35.7967	110.9111	30.0	-
35.9836	114.7472	30.0	-
36.0003	114.7400	61.0	-
36.0005	114.7422	63.0	-
36.0028	114.7425	47.0	-
36.0028	114.7494	33.0	-
36.0128	114.7419	30.0	-
36.2069	110.4019	30.0	-
36.3775	114.4433	30.0	-
36.4153	113.9567	30.0	-
36.4155	110.4064	33.0	-
36.4403	110.3769	33.0	-
36.4464	110.4097	34.0	-
36.4836	110.3947	34.0	-
36.5014	110.4192	30.0	-
36.5019	110.3700	34.0	-
36.5072	110.4244	30.0	-

SPRINGERVILLE, ARIZONA

Results of Heat Flow Drilling

by Claudia Stone

Introduction

Eighteen sites were selected for heat flow drilling in the Springerville Geothermal Project area (Fig. 1). The site locations were selected on the basis of a preliminary site evaluation (Stone, 1979) and a reconnaissance electrical resistivity survey (Young, 1979). Justification for site locations was submitted to the Bureau of Reclamation, Boulder City, Nevada, in March, 1979. Four holes, No. 107, 114, 116, and 118, were to be drilled to 150 ft. depth; the remaining holes were to be drilled to 500 ft. Extended cold weather and snow in the project area delayed the start of drilling until May, 1979, and even by that date poor access necessitated revising some drill-site priorities.

Five heat flow holes were completed by August, 1979 (Fig. 2), at which time the drilling operation was moved to Clifton, Arizona. Drilling dates, total depths, and hole locations are presented in Table 1.

Hole Completion

All holes were drilled using conventional rotary-mud techniques except the upper 400 ft. of hole No. 116, which was drilled using an air compressor and downhole hammer. Considerable difficulty was encountered in holes No. 112, 113, and 114 as a result of the voluminous water moving through the permeable volcanic layers.

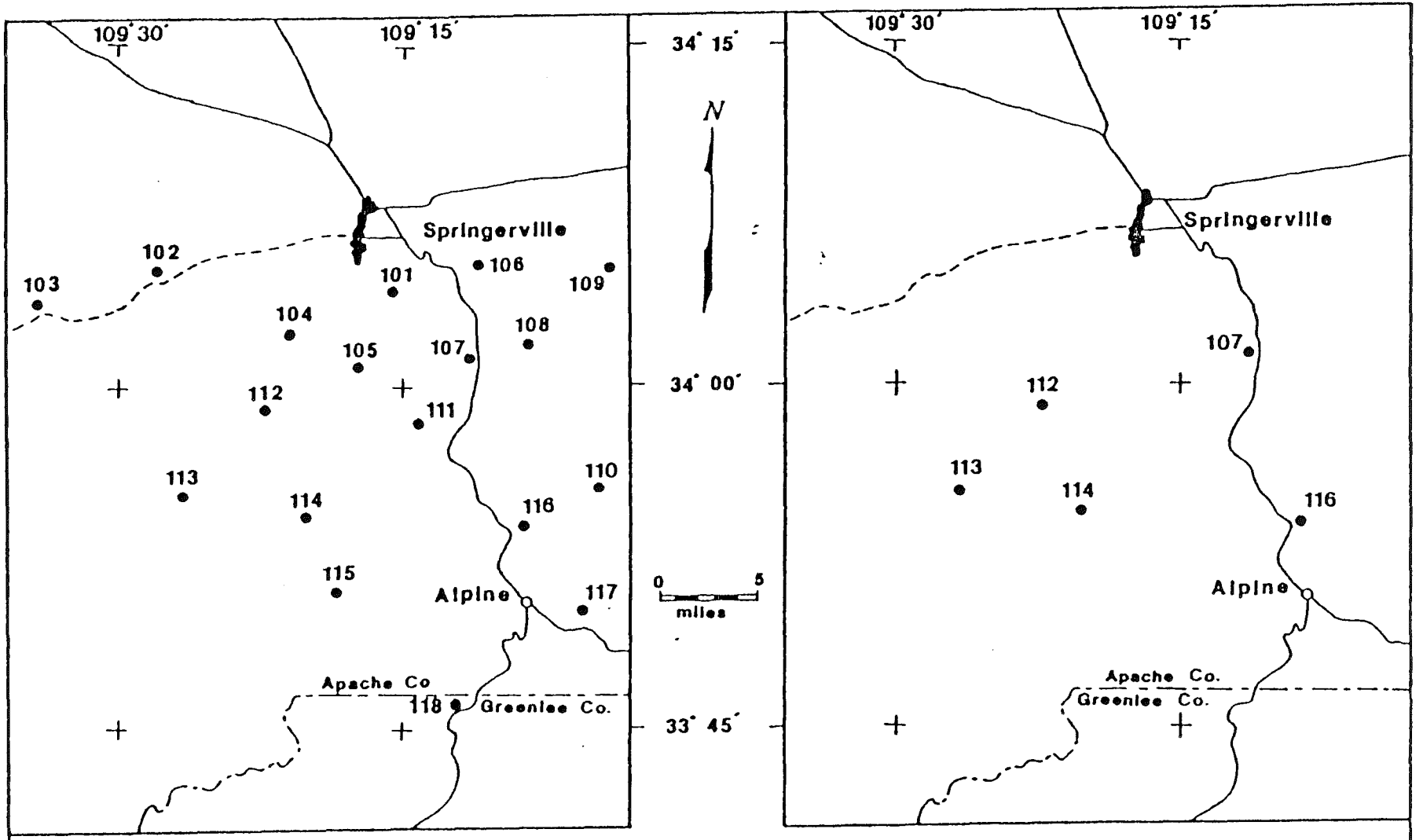

FIGURE 1. Proposed heat flow drill sites.

FIGURE 2. Completed heat flow drill sites.

TABLE 1. Heat flow hole locations, total depths, ground elevations, and drilling dates.

Hole No.	Location*	Spud Date	Completion Date	Ground Elev., ft.	Total Depth, ft.
SJ-107	(A-7-30) 7dda	5-22-79	6-15-79	7730	1145
SJ-112	(A-7-28) 27bca	7-23-79	7-26-79	9240	507
SJ-113	(A-6-27) 12cdc	7---79	7---79	9200	351
SJ-114	(A-6-28) 13aaa	6-17-79	6---79	8840	718
SJ-116	(A-6-30)	7-31-79	8-8-79	8560	1171

*Gila-Salt Meridian. "A" represents NE quadrant of state.

Each drill hole was completed by running two-inch diameter standard black iron pipe to total depth and pumping about ten sacks of cement grout through the pipe. This operation was followed by a wiping rag that cleaned the pipe. The pipe was then sealed at the bottom and filled with clear water. The rest of the annulus was backfilled with drill cuttings and drilling mud. A cement plug of variable thickness was set at the top of each hole, and the pipe was closed with a metal screw cap (Fig. 3).

Lithology

Holes No. 112, 113, and 114 were drilled in interbedded basaltic lava flows and cinder, and encountered copious amounts of water. Hole 113 bottomed in about 40 ft. of fine to coarse sandstone. Hole 107 encountered medium- to fine-grained, pinkish-tan sandstone to total depth and was dry. Hole 116 penetrated 521 ft. of medium- to fine-grained, pinkish-tan sandstone, 302 ft. of orange-red coarse-grained sandstone, and 400 ft. of red-brown to black clay, siltstone, and black (basaltic ?) lithic fragments. This hole,

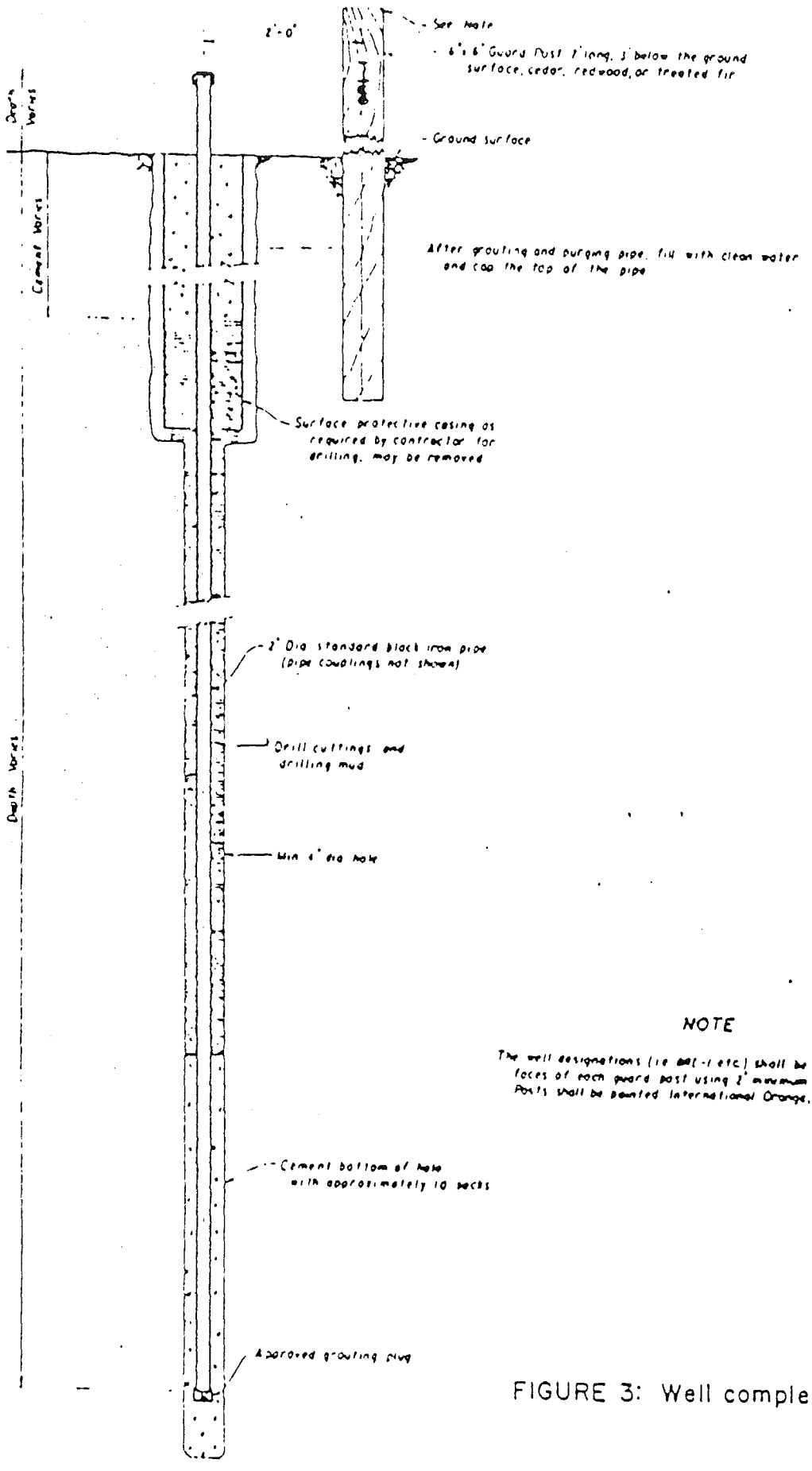

HEAT FLOW WELL (ATSI)
SCHEMATIC

NOTE

The well designations (ie 001-1 etc) shall be painted on two faces of each guard post using 2" minimum size stencils. Posts shall be painted International Orange, lettering black.

FIGURE 3: Well completion.

No. 116, produced about 10 gpm of 16.7°C water at 230 ft. A fence diagram (Fig. 4) shows the lighology of these and five other wells in the area.

Heat Flow Determinations

The heat flow holes were logged at 5-m intervals, three time each, with little apparent differences in gradients. The temperature data are shown in Figures 5 and 6. The most recent temperature logs, those measured September 5, 1979, are the thermal gradients used in the heat flow calculations.

The temperature logs of holes No. 112, 113, and 114 (Fig. 5) confirm the high volume and velocity of water moving through the permeable volcanic layers. Such rapid groundwater movement renders these holes of poor quality for reliable heat flow estimates. Had the holes been grouted from top to bottom the problem may have been minimized, but a valid conductive heat flow value still could not have been obtained due to groundwater circulation. The other two heat flow holes (Fig. 6) are essentially dry, and represent fairly reliable heat flow measurements. An additional, abandoned dry water well drilled several years ago, about three miles south of hole No. 107, has been temperature logged to a depth of 246 ft. (Fig. 7). This hole is designated DR-1 and for estimating the rock thermal conductivity, it is considered to have a lithology similar to that of hole No. 107.

The linear regression method was used to fit straight lines to the temperature data of each hole. The slope of the line is the thermal gradient and the y-intercept represents the MAT (mean annual temperature). Credible segments of data from holes No. 112, 113, and 114 yield thermal gradients that extrapolate back to reasonable MAT's for the project area, thereby providing a small degree of confidence in the gradients. The measured thermal gradients for holes No. 107, 116, and DR-1 are nearly linear (Figs. 6 and 7). The thermal gradient data are presented in Table 2.

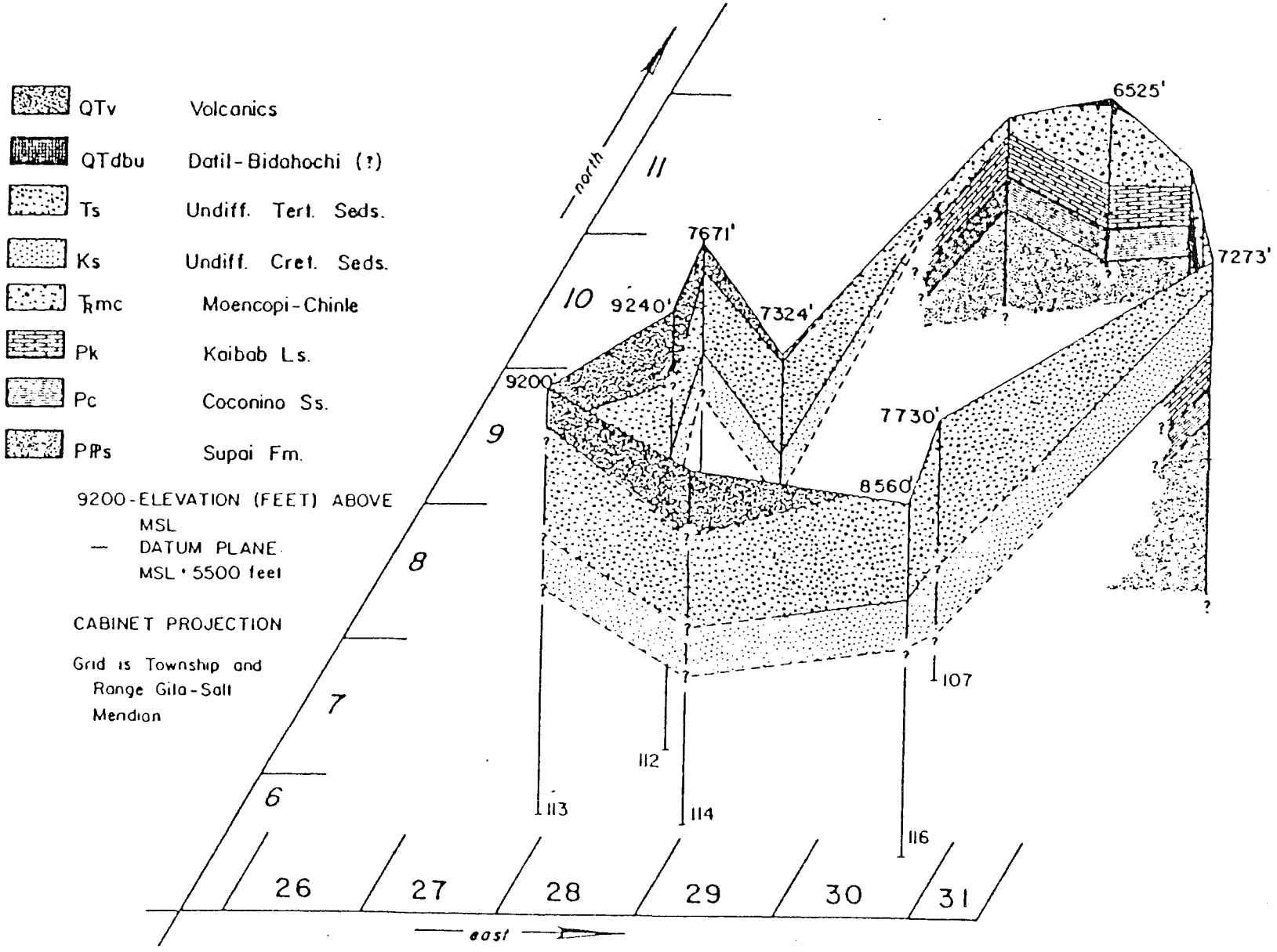

FIGURE 4: Fence diagram showing subface lithology in the Springerville Geothermal Project Area.

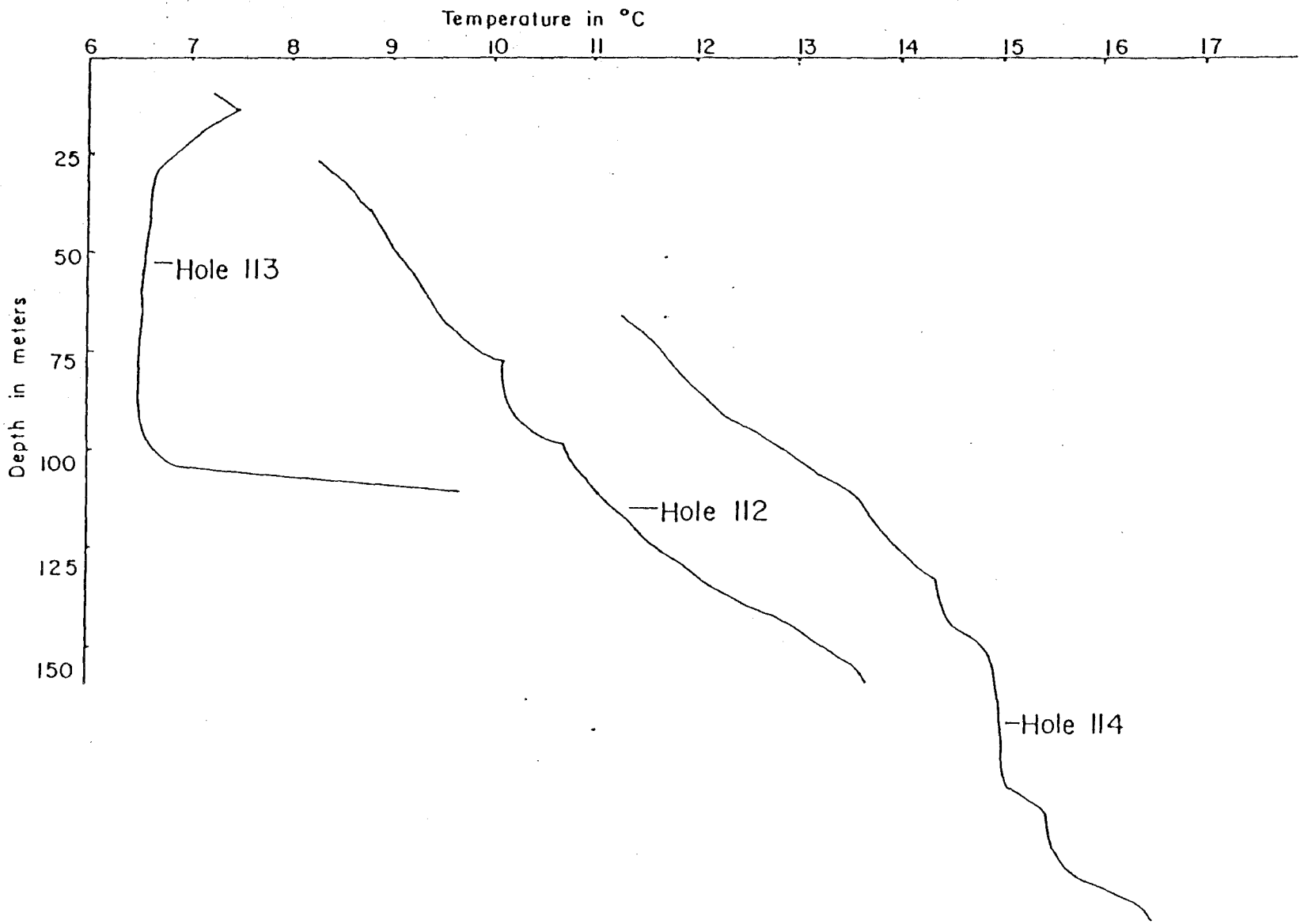

FIGURE 5: Temperatuer-depth profiles, Springerville Geothermal Project Area. (See Table 1 for hole locations.)

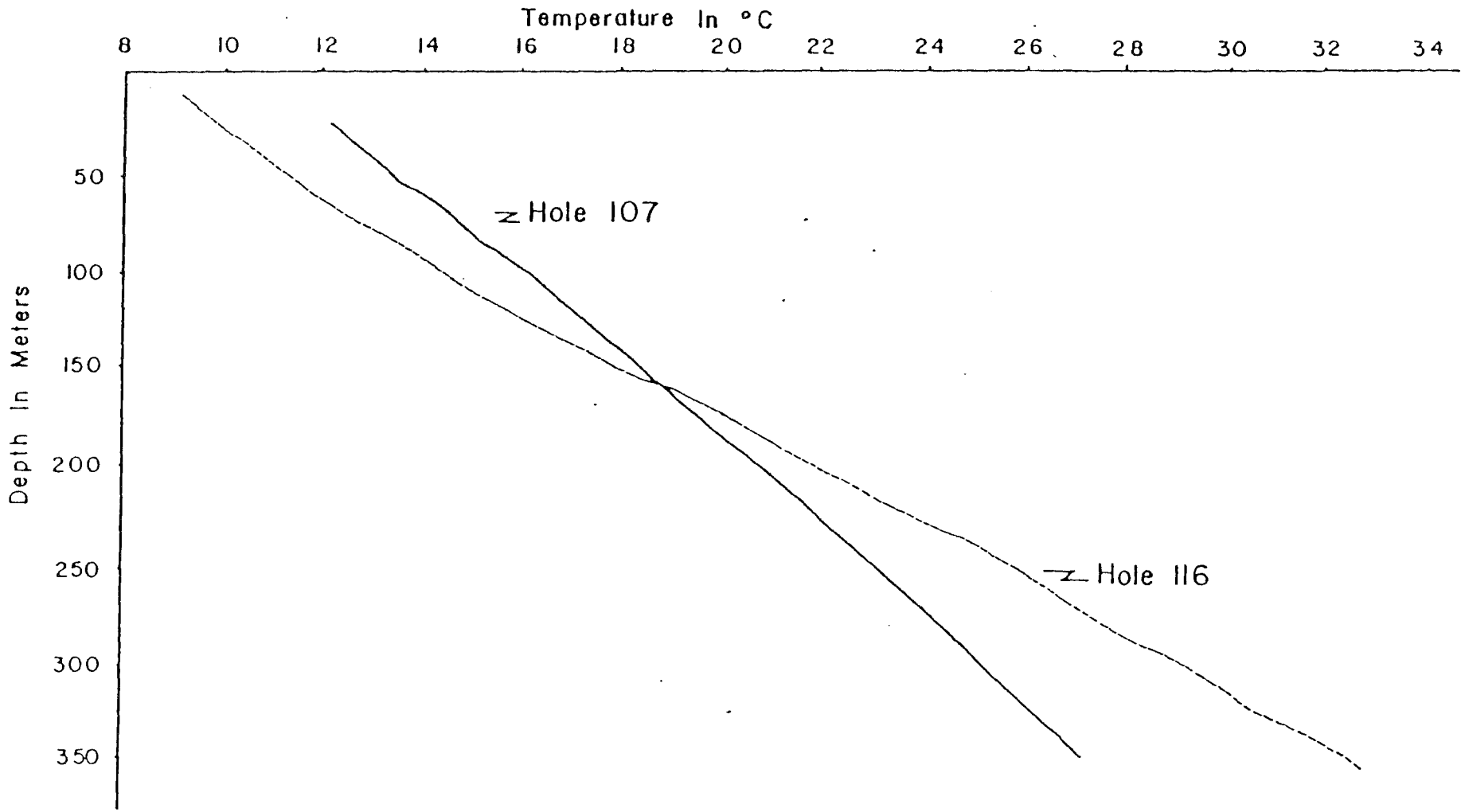

FIGURE 6: Temperature - depth profiles Springerville Geothermal Project Area. (See Table I for hole locations.)

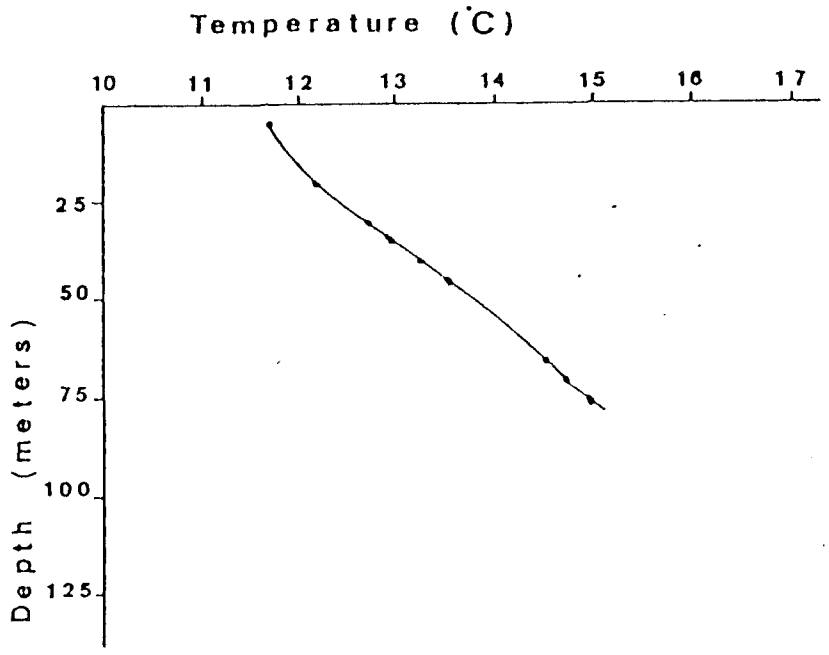

FIGURE 7: Hole DR-1

Springerville Geothermal Project Area.
(See Table 4 for location.)

TABLE 2. Thermal Gradients

Hole No.	No. of Date Pts.	Depth Intervals, m	Thermal Gradients ($^{o}C/km$)	MAT (^{o}C) y-Intercept	Correlation Coefficient
112	10	25-75	33.1	7.43	0.9944
	6	95-120	35.9	7.18	0.9975
113	3	5, 10, and 107 only	25.3	7.07	0.9982
114	5	65-85	35.4	9.03	0.9999
107	63	23-345 (excluding 55+85)	43.9	12.07	0.9414
116	69	10-355 (excluding 15+355)	71.6	7.59	0.9994
DR-1	9	30-75	51.1	11.17	0.9993

The thermal conductivity of representative drill cuttings was measured with a divided bar apparatus, using the chip method of Sass, Lachenbruch, and Munroe (1971). Measurements were made in the laboratory of Dr. Robert F. Roy, University of Texas, El Paso. Thermal conductivity values are presented in Table 3. Heat flow data are presented in Table 4.

Discussion and Conclusions

Working in southern Colorado and New Mexico, Reiter and others (1975) recognized two generalized zones of heat flow in the eastern Colorado Plateau: (1) 63 mWm^{-2} or less associated with major structural basins and (2) 84 mWm^{-2} and greater associated with some intrusions and perhaps major uplifts. Chapman and others (1978) determined a representative heat flow of 49 ± 8 mWm^{-2} for the Utah portion of the Colorado Plateau province.

Swanberg and Morgan (1978/79) found a linear relation between temperatures based on the silica content of groundwater and regional heat flow in the United States. This relationship enhances the validity of the 55 mWm^{-2} regional heat flow value determined for the Colorado Plateau province by Swanberg and others (1977) using the silica-geothermometry method.

The regional heat flow for eastern Arizona and western New Mexico, using the data from this and from published reports, is shown in Figure 8. Several observations and conclusions can be made from these data, keeping in mind that the number of heat flow values along the Arizona-New Mexico border is too few to do anything more than generalize. (1) A low-amplitude, heat-flow high does exist in the project area (Figs. 8 and 9), but the magnitude of the anomaly is insufficient to indicate an economic high-temperature geothermal resource. (2) A heat flow anomaly of significant magnitude is believed to exist within or to the west or east of the project area, but definitive identification of the exact location and size of the

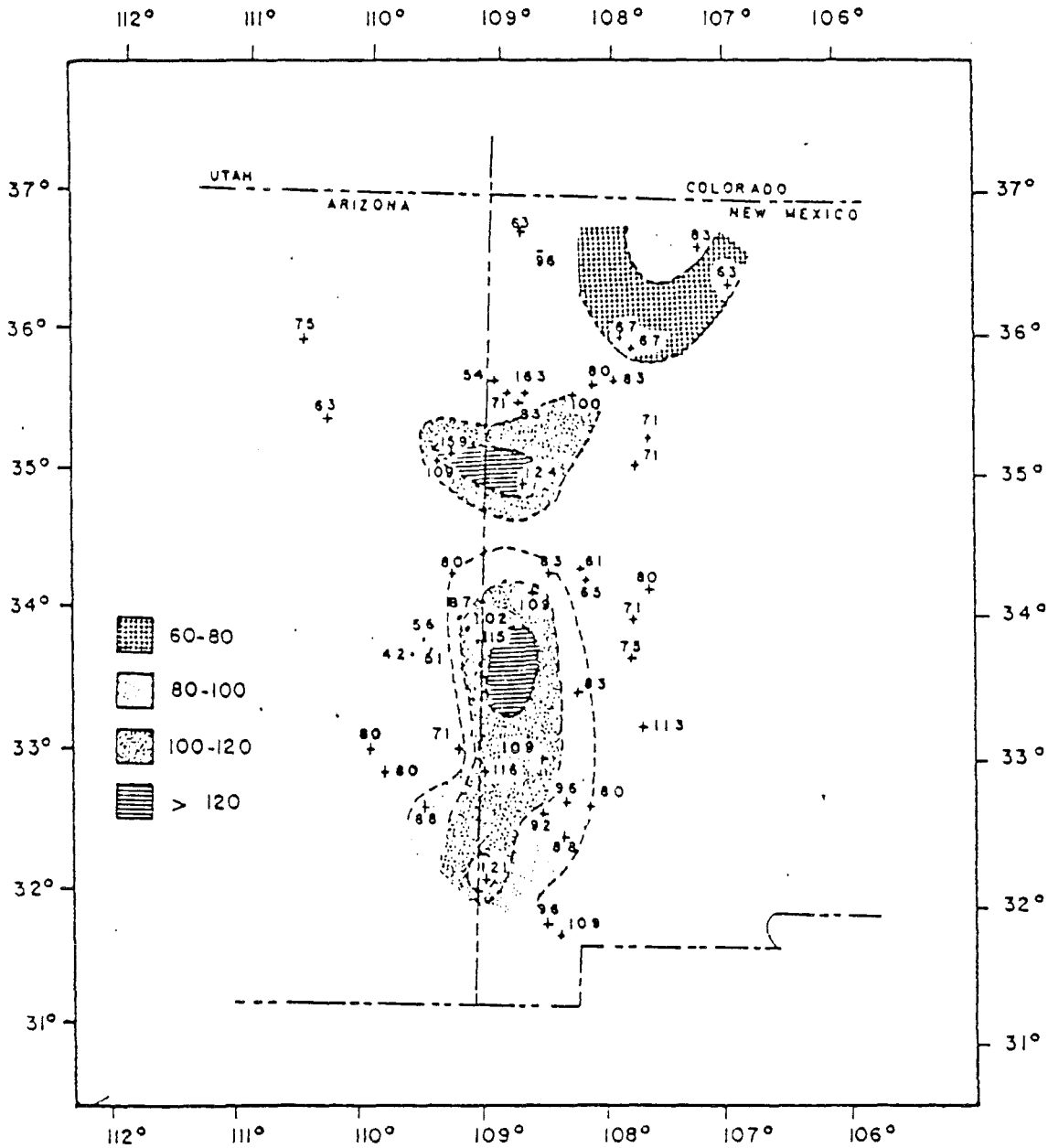

FIGURE 8: Heat flow contour map of eastern Arizona and western New Mexico (modified after Reiter and others, 1975). Dots represent sites measured for this report. Plus signs represent data from other investigators. Contour interval is 20 mWm^{-2}.

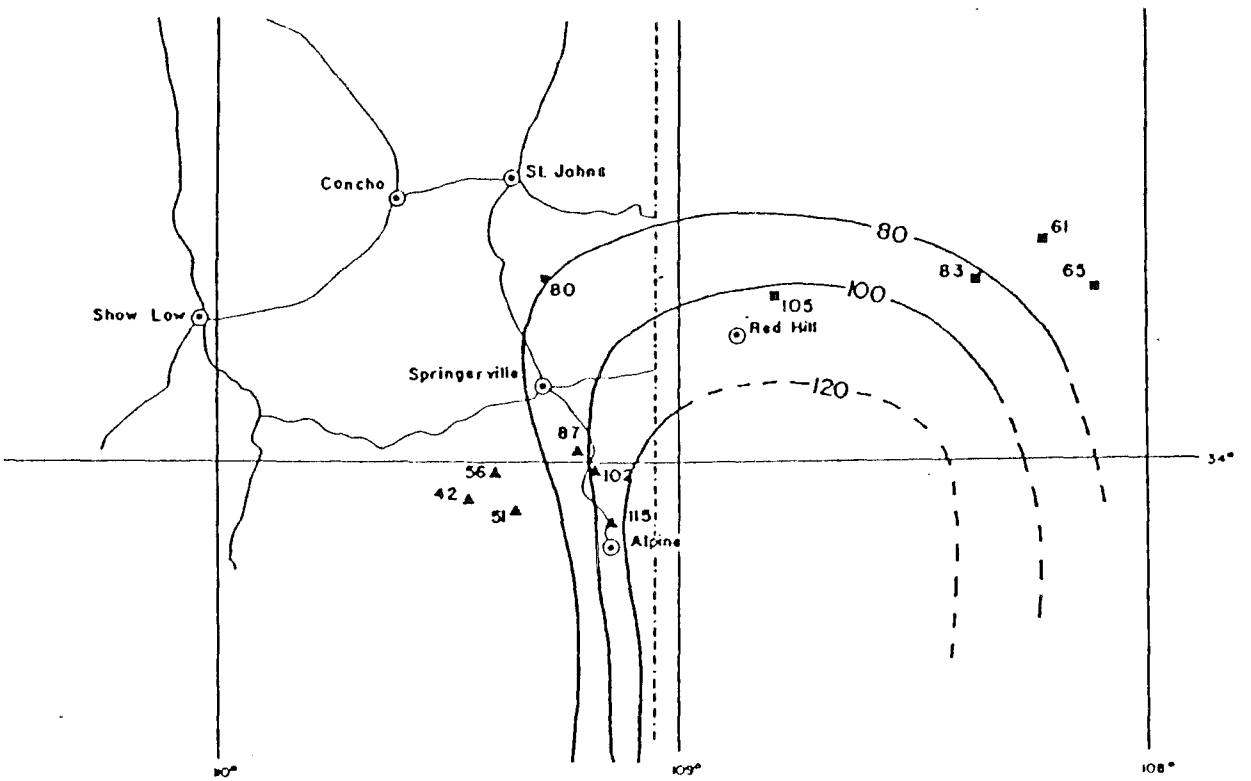

FIGURE 9: Heat flow in the Springerville Geothermal Project Area. Countour interval is 20 mWm 2. Triangles are data from this report. Squares are data from published reports, (Stone, 1979; Reiter and others, 1975).

TABLE 3. Thermal Conductivity

Hole No.	Depth Range, m	K 10^{-3} cal/cm s ^{o}C	K W/mK	Density gm/cm^3
112	6-12	4.12	1.72	2.71
	37-43	4.04	1.69	2.82
	67-73	3.87	1.62	2.81
	98-104	3.81	1.59	2.68
113	37-43	4.13	1.72	2.85
	55-61	3.90	1.63	2.81
	97-104	3.96	1.65	2.68
114	6.12	4.58	1.91	2.94
	61-67	3.75	1.57	2.61
	85-92	3.13	1.31	2.49
107	18-24	4.27	1.78	2.47
	55-61	4.41	1.84	2.50
	92-98	4.66	1.95	2.41
	122-128	4.60	1.92	2.42
	183-189	5.88	2.46	2.40
	213-220	4.77	1.99	2.47
	244-250	5.17	2.16	2.41
	305-311	4.37	1.83	2.47
116	24-31	5.76	2.41	2.52
	61-67	4.44	1.86	2.43
	116-122	4.13	1.73	2.48
	152-159	3.59	1.50	2.37
	195-201	3.36	1.41	2.34
	232-238	3.02	1.26	2.27
	274-281	3.09	1.29	2.13
	311-317	3.42	1.43	2.28

TABLE 4. Summary of new heat flow data.

Locality	Hole	N. Lat.	W. Long.	Elev. (M)	Depth Range (M)	Gradient ($^{o}C/km$)	K. mean (W/mK)	Q (mWm^{-2})
Rudd Knoll	112	33° 59'	109° 23'	2817	25-75	33.1	1.68	55.5
					95-120	35.9	1.59	57.1
Crescent Lake	113	33° 55'	109° 27'	2805	5, 10, 107	25.3	1.67	42.2
Crosby Crossing	114	33° 55'	109° 20'	2695	68-85	35.4	1.44	51.0
Riggs Creek	107	34° 01'	109° 13'	2356	25-345	43.9	1.99	87.4
Alpine Divide	116	33° 54'	109° 09'	2610	10-355	71.6	1.61	115.4
Nutrioso	DR-1	34° 00'	109° 11'	2296	30-75	51.1	1.99	101.4

anomaly will require detailed geological and geophysical exploration as discussed in the final chapter. (3) Little reliance can be placed on the three western-most heat heat flow values measured in the volcanic rocks. The importance of this area in terms of the geothermal resource is as yet undetermined, but it cannot be dismissed. Drilling must be done beneath the volcanic pile to reliably assess the heat flow in this area.

It is recommended that a flexible program for drilling additional heat flow holes be carried out south and west of the project area and to the east in New Mexico, to target the area of maximum heat.

References

Chapman, D. S., and others, 1978, Regional heat flow and geochemical studies in southwest Utah: Department of Geology and Geophysics, University of Utah, 119 p.

Reiter, M., and others, 1975, Terrestrial heat flow along the Rio Grande rift, New Mexico and southern Colorado: Geol. Soc. of Am. Bull., v. 86, p. 811-818.

Reiter, M. and Shearer, C., 1979, Terrestrial heat flow in eastern Arizona: A first report: Jour. Geophys. Res., v. 84, p. 6115-6120.

Sass, J. H., Lachenbruch, A. H., and Munroe, R. J., 1971, Thermal conductivity of rocks from measurements on fragments and its application to heat flow determinations: Jour. Geophys. Res., v. 76, p. 3391-3401.

Stone, C., 1979, An overview of the geothermal potential of the Springerville area, ARizona: in Geothermal Reservoir Site Evaluation in Arizona, Semiannual Progress Report for the Period July 15, 1979 - January 15, 1979, Arizona Bureau of Geology and Mineral Technology, pp. 1-25.

Swanberg, C. A., and others, 1977, An appraisal study of the geothermal resources of Arizona and adjacent areas in New Mexico and Utah and their value for desalination and other uses: NMEI Report No. 006, New Mexico Energy Institute, Las Cruces, N. M., 76 p.

Swanberg, C. A., Morgan, P., 1978/79, The linear relation between temperatures based on the silica content of groundeater and regional heat flow: A new heat flow map of the United States: Pure and Applied Geophysics, v. 117, pp. 227-241.

Young, C. T., 1979, Geoelectrical studies near Springerville, Arizona: unpublished report submitted to the Bureau of Geology and Mineral Technology, Tucson, Arizona.

Heat Flow and the Thermal Regime in the Clifton, Arizona Area

James C. Witcher
Claudia Stone

March 1980

Useful Conversions

HFU = 1 heat flow unit = 1×10^{-6} cal/cm^{2}sec = 41.84×10^{-3} W/m^2

TCU = 1 thermal conductivity unit = 1×10^{-3} cal/cm sec $^{\circ}$C = 0.4184 W/*m*k

Heat Flow and the Thermal Regime in the Clifton, Arizona Area

James C. Witcher
Claudia Stone

Introduction

Four heat flow measurements in the Clifton, Arizona area are available for interpretation. Three of the heat flow measurements are detailed in this report. Reiter and Shearer (1979) reported the additional heat flow measurement. Analysis of the data shows significant movement of groundwater in the area, which masks the regional heat flow. Near-surface heat-flow measurements in the drill holes less than 350 m deep have values ranging between 0.4 HFU and 2.3 HFU. The Clifton area regional heat flow is believed to be 2.25 HFU.

Hot springs in the area, with discharge temperatures up to 82°C, are surface manifestations of local geothermal convection system(s). Low measured-heat-flow values, compared to the regional heat flow, result from lateral or downward flow of water in the Clifton area, or from a combination of both; the water flow may recharge the hot spring-geothermal convection system(s). Available data suggest that the convective systems are heated by regional heat flow although a hypothetical magmatic heat source masked by water flow is not disproven.

Regional Setting

The Clifton area lies on the northern margin of the Basin and Range province near the transition zone with the Colorado Plateau province (Figure 1). The confluence of the San Francisco

River with the Gila River is just south of Clifton. In the northern part of the area, topographic relief is great because high mountains (greater than 1800 m) are cut by deep canyons. In the southern part, the elevations (1060 m) are lower and the land surface is also cut by smaller canyons related to entrenchment of the Gila and San Francisco rivers. The entrenchment of the rivers is post-Pliocene and may be due to regional uplift, to acquisition of drainage outside of the Clifton area, or to climatic change (Morrison, 1965, Harbour, 1967). All of these factors may influence local and regional heat flow.

Rainfall and the mean annual temperature are quite varied in the area. In the mountains, weather stations at Granville and Grey Peak average 50.6 cm (20 inches) of rain per year and have mean annual temperatures around 11°C to 12°C (Sellers and Hill, 1974). At lower elevations such as at Clifton, average annual rainfall is 15.4 cm (10 inches) or less and the mean annual temperatures range up to 19°C (Sellers and Hill, 1974). As a result of the climatic contrasts, the vegetative cover changes radically from low elevations to high elevations. Sparse creosote vegetation changes to dense forests of pinon, cedar, oak, manzanita, and ponderosa pine with increasing elevation. The areally variable climate and vegetative cover enchance complex hydrologic conditions. Lateral and vertical flow of water, which can profoundly change the thermal regime, may result from complex hydrologic conditions.

Geology

The geologic history of the Clifton area is complex, as evidenced by an extremely varied suite of lithologies and ages and styles of tectonic deformation (Figure 2). Crystalline rocks of Precambrian and Late Cretaceous-early Tertiary ages are exposed in the Clifton area. Granite, granodiorite,and diorite comprise the bulk of these rocks. Outcrops of Precambrian schist and metaquartzite are identified north of Clifton (Lindgren, 1905).

Paleozoic rocks unconformably overlie the Precambrian rocks and depict a time of relative tectonic quietude. A basal arkosic sandstone is overlain by interbedded shales and carbonate rocks; the carbonate rocks become dominant higher in the Paleozoic section (younger in age). Sediments from all Paleozoic periods except Silurian and Permian are exposed (Lindgren, 1905). Silurian rocks are not found in Arizona, having never been deposited or having been stripped away by erosion during Late Silurian or early Devonian (McKee, 1951). Permian rocks are not exposed in the Clifton area and are probably absent due to Mesozoic and Cenozoic erosion. North of Clifton, Permian rocks are probably present in structural lows where they were protected from erosion and are now buried beneath Mesozoic and Cenozoic sediments and volcanics. Deeply eroded Pennsylvanian carbonate rocks crop out north of Clifton along Highway 666 in the vicinity of Mitchell Peak (Ross, 1973). Prior to Mesozoic tectonism, up to 1300 m of Paleozoic rocks are believed to have overlain the Clifton area (Pierce, 1976).

The Clifton area was greatly disturbed by Mesozoic and Cenozoic tectonic events. No Triassic or Jurassic strata are observed

in the area; either they were removed by erosion during the Cretaceous Burro-Graham uplift or they were never deposited. Erosion following the Burro-Graham uplift stripped off all of the Paleozoic rocks, exposing Precambrian rocks in the region south of Clifton (Elston, 1958; Turner, 1962). Late Cretaceous fine-grained clastic rocks deposited in shallow marine and terrestrial environments unconformably overlie lower Paleozoic rocks at Clifton (Lindgren, 1905).

Late Cretaceous-early Tertiary (Laramide Orogeny) magmatic intrusion and faulting created an extensive hydrothermal system that emplaced low-grade copper mineralization into the area (Moolick and Durek, 1966; Langton, 1973).

Mid-Tertiary volcanism buried the area under thick piles of andesite and basaltic andesite that contain volumetrically minor and discontinuous silicic ash flow tuff (Lindgren, 1905; Berry, 1976). Silicic intrusions of rhyolite are observed in a northwest-striking zone north of Clifton. The rhyolites were intruded contemporaneously with the last mid-Tertiary eruptions of basaltic andesite (Berry, 1976). Major late-Tertiary faulting has uplifted the northern part of the area into a horst or up-thrown crustal block (Clifton-Morenci horst) that is itself broken into two blocks by the northeast-trending San Francisco fault (Lindgren, 1905; Langton, 1973). More than 600 m of late-Tertiary vertical displacement along the San Francisco fault is believed to separate the upthrown intrahorst Morenci block on the west from the downthrown intrahorst Clifton block on the east. The Clifton-Morenci horst is bordered on the south by the Ward Canyon fault (Lindgren, 1905; Langton, 1973). The downthrown block south

of the Ward Canyon fault comprises the basement of the Duncan basin. Late-Tertiary sedimentation has filled the Duncan basin with a thick sequence of clastic sediments derived mostly from volcanic rocks. The southern boundary of the Duncan basin is defined by the Peloncillo Mountains, a thick pile of mostly basaltic andesite volcanics of probably middle Tertiary age. A major fault is inferred to separate the mountains and the basin.

The Ward Canyon fault is inferred to have Quaternary to Recent movement. Analysis of U-2 air photos reveals a poorly defined scarp along the inferred and continued trace of the mapped portion of the fault. The inferred young movement has not been field checked to confirm the air photo interpretation.

Hot Springs

Clifton area hot springs, surface manifestations of local geothermal convective systems, discharge the hottest groundwater naturally flowing at the surface in Arizona (Figure 1). The maximum spring temperatures range from 66°C for the Clifton Hot Springs to 82°C for the Gillard Hot Springs.

Chemical geothermometry on these springs indicates subsurface reservoir temperatures over 130°C (Swanberg and others, 1977). The highest geothermometer temperatures are calculated from chemical analysis of the Clifton Hot Springs north of Clifton. Chemical and isotopic evidence suggests that mixing with cold near-surface groundwater is occurring (Mariner and others, 1977; Witcher, 1979). Mixing model calculations suggest temperatures up to 180°C for the quartz geothermometer and agree well with the Na/K/Ca geothermometers (Witcher, 1979).

The Clifton Hot Springs occur as small seeps and limited

flows on the banks of the San Francisco River. However, temperature, salinity, and increased flow of the river down stream from the hot springs indicate that a significant amount of hot water flows into the San Francisco River through the river bed (Hem, 1950; Swanberg and others, 1977). The system's total discharge is substantial and is greater than 3785 liters per minute (Hem, 1950).

The Clifton Hot Springs and Gillard Hot Springs appear to be controlled by structure and topography. Both spring systems occur near major fault zones and in the bottoms of canyons formed by the Gila and San Francisco rivers.

Heat Flow - General Discussion

Many factors influence the temperature distribution within the upper crust of the earth. Heat flow from the earth's interior is the most important factor. Daily and annual solar heating has only minor importance and affects only the uppermost few meters. Temperature differences caused by pressure changes with depth (adiabatic temperature) are insignificant and of no importance in shallow crustal studies because of the incompressibility of crustal rocks.

Heat flow is predominantly influenced by deep subsurface temperature, thermal conductivity of rock, and by groundwater flow (convection). Additional factors are also important, such as radiogenic and chemical heat production, and time (i.e., time since emplacement of a magma body or initiation of convection). Topography may also influence subsurface temperature distribution.

Conductive heat flow measurements are the easiest and most straightforward method to study the temperature distribution of

the crust. Conductive heat flow depends mostly upon the rock thermal conductivity and the subsurface temperature. The equation for vertical conductive heat flow, assuming no radiogenic heat production, groundwater convection, or inhomogeneity in crustal rock is: $q = K \frac{\partial T}{\partial Z}$ (1)

where
q is heat flow
K is the rock thermal conductivity
$\frac{\partial T}{\partial Z}$ is the temperature gradient

Temperature at depth may be extrapoltated to greater depth in a region of conductive heat flow if reasonable assumptions about rock thermal conductivity can be made. For this reason, regional heat flow studies seek drill holes that are located in nonpermeable, isotropic rock such as granite.

The objective of geothermal exploration is to locate and explore hydrothermal convection systems, at economically drillable depths. Since convective transport of heat from great to shallow (economic) depths occurs in convection systems, geothermal studies are concerned with convective heat-flow measurements in addition to conductive heat-flow measurements. Also, convective heat flow contains information concerning the movement of goundwater that may be useful for indirect estimation of flow rates, rock permeability, and heat budgets within the system. The equation for vertical heat flow with convection, but no heat production, is:

$$q = K \frac{\partial T}{\partial Z} + \rho C v \partial T \qquad (2)$$

where
ρ is the density of water,
C is the heat capacity of water,
∂T is change in temperature through interval of the heat flow measurement
v is the vertical component of water velocity,
and other terms as in Equation (1)

The velocity of convective water flow is dependent upon the pressure (head), permeability, and fluid viscosity according to Darcy's Law.

Clifton Heat Flow Data

Rotary-mud drilling commenced at the Clifton-1 drill site on 9 September, 1979 by Cowley Pump Company of Phoenix, Arizona. Funding agent for the drilling operation was the U.S. Bureau of Reclamation (Water and Power Resources Service), Boulder City, Nevada. Lost circulation due to caving and high formation permeability resulted in temporary cessation of drilling so 17.8 cm (seven inch) OD casing could be emplaced to 44 m. Drilling stopped at 305 m and the hole was completed with a 5.1 cm (two-inch) iron pipe cemented in place at the top and bottom by ten sacks of cement. The iron pipe was filled with water.

The water table at Clifton 1 is approximately 50 m deep, which approximates the level of the Gila River one-half mile away.

Figure 3 shows the lithology of the Clifton-1 drill hole. Basin-fill sediment derived mostly from volcanic rocks is penetrated by the hole. The lower 130 m appears to be a boulder fanglomerate consisting of basaltic andesite clasts. Drill chips are rounded and slightly weathered on one side as if originally part of a large cobble or boulder. Also, the cuttings contain substantial quantities of "fines", but these "fines" could be contamination or sluff from the upper parts of the drill hole.

The other heat-flow holes, HF1 and HF2, are "free" holes that Phelps Dodge Corporation, Morenci, Arizona, kindly gave permission to log and provided rock samples for thermal conductivity measurements. Figure 3 shows the lithology of these holes. HF1 is in granite and monzonite porphyry of Paleocene (?) age. HF2 is in the lower Paleozoic section exposed in the Clifton area. The upper 60 m is in the Ordovician El Paso Limestone (Longfellow Limestone of Lindgren, 1905), a sandy dolomite-to-dolomitic sandstone. The lower 70 m is in the Cambrian Coronado Sandstone, a tightly cemented arkose to orthoquartzite.

Temperature measurements at five-meter intervals were taken in HF1, HF2, and Clifton-1 with a calibrated thermister logging unit. Calibration accuracy of the temperatures is $\pm$ .001°C. The temperature data from the drill holes are shown in Figure 4.

HF1 has a straight temperature-depth profile, possibly indicative of a lithology with conductive heat flow and little change in rock thermal conductivity. HF2 has a curved temperature profile and a very low overall temperature gradient. High and variable rock thermal conductivity or water flow can explain the temperature log of HF2.

Clifton-1 temperatures were obtained a few days after drilling had stopped. The anomalous temperatures at the top and bottom of the hole on 9/29/79 represent the heating effects of newly poured cement holding the 5.1 cm (two-inch) casing in place. (As cement solidifies it generates heat). The 11/19/79 temperature log of Clifton-1 shows the hole had equilibrated

to ambient rock temperature. The temperature gradient in this hole is very low. The temperature-depth profile reveals a subtle concave-upward curvature. Downward or lateral flow of water can create the Clifton-1 temperature profile.

Heat-flow determinations are listed in Table 1, with pertinant supporting information. Rock thermal conductivities of representative drill cuttings were obtained with a divided bar apparatus, using the chip method of Sass, Lachenbruch and Munroe (1971). Measurements were made in the laboratory of Dr. Robert F. Roy, University of Texas, El Paso. Thermal conductivities are also listed in Table 1.

Reiter and Shearer (1979) published heat-flow data in the Clifton area on a hole drilled deeper than 600 m. The data are summarized in Table 1. The temperature-depth profile of their hole is concave upward, also suggesting downward water seepage or progressively decreasing rock thermal conductivity (Figure 4). The low, 1.4 HFU, value from the thickest depth interval of their hole is significantly below the 2.0 HFU average Basin and Range province heat flow, and tends to substantiate modification of the thermal regime of this hole by water flow.

Heat Flow, Interpretation and Conclusions

HF1 probably represents a regional heat flow of 2.25 HFU for the Clifton area. However, this interpretation could be in error because the thermal regime may not result strictly from conductive heat flow as the straight temperature profile would initially suggest (Figure 4). The rock thermal conduc-

tivities probably are accurate because they are consistent with the subsurface lithology. However, the heat flow values change from over 2.0 HFU to less than 1.50 HFU (Figure 5). The inconsistent section of the hole is associated with a section of monzonite porphyry between 189-293 m. The lowest heat-flow value is calculated at the middle of the monzonite interval. We believe the monzonite porphyry is an almost vertical dike that is an apophysis of a local northeast-striking monzonite intrusive(s) which is related in turn to the Paleocene magmatic activity that emplaced copper mineralization at Morenci (Langton, 1973). We hypothesize downward seepage of cold water in the dike that "washes out" the conductive heat flow in the dike. Also, the monzonite dike may not be sufficiently wide to change the temperature profile in the hole even though the monzonite has different thermal conductivity (Paul Morgan, personal commun., 1980). Figure 5 summarizes the pertinant data on HF1.

HF2 temperature gradients are very low. Figure 6 is a Temperature versus Temperature Gradient profile of the HF2 heat-flow hole. At least two conditions are influencing the temperature distribution in this hole. First, very high thermal conductivities are contributing to very low temperature gradients, shown by the fact that gradients less than 12°C/km have conductivities greater than 9 TCU and gradients greater than 16°C/km have conductivities less than 7 TCU. Second, groundwater flow at depth seems likely since the heat flow values for the hole are internally consistent but the 1.0

HFU value is far below the average basin-and-range value of 2.0 HFU.

Clifton-1 also has very low heat flow. The Temperature versus Temperature-Gradient profile (Figure 7) between 130-350 m is nearly linear, suggesting a uniform vertical flow of water that would transport heat. The Heat Flow versus Depth plot (Figure 8) shows that the heat flow increases with depth, which confirms that vertical water flow is occuring in a downward direction. Where vertical water flow exists, the heat flow contributed or removed by this convective component (Δq) can be calculated by subtracting the component of heat flow contributed by conduction.

$$\Delta q = \rho C v \partial T = (\text{Eqn. } 2 - \text{Eqn. } 1) \quad (3)$$

For Clifton-1, Δq is - 0.22 HFU* and is obtained by subtracting the heat flow at 250 m from the heat flow at 130 m. Assuming a heat capacity (C) of 1.0 cal/gm^{o}C and a density (ρ) of 1.0 gm/cm^3 for water, a one-cm^3 volume of water would require a downward velocity (v) of about 4.6 cm/year to lower the heat flow through a one-cm^2 area at the top of the 130-250 m interval by 0.22 HFU.

A column of water moving downward each year (4.6 cm/year) is 18 percent of the annual rainfall (26 cm/year). This percentage of annual rainfall recharging subsurface aquifers may be too high for an arid region because Rantz and Eakin (1971) report

* A negative sign indicates reduction of heat flow by loss of heat to downward flowing water. A positive sign indicates increased heat flow by addition of heat by upward flowing water.

recharge percentages of annual rainfall less than 7 percent in an arid and cooler region in Nevada. Therefore flow of water resulting from rainfall recharge may not account for the observed heat loss at Clifton-1. However, lateral water flow associated with a sloping water table could account for the vertical water velocities and heat loss observed by heat-flow measurements at Clifton-1. With a sloping water table in an isotropic aquifer, the lateral water flow would have a downward component of flow at shallow depths.

If the water flow is laminar and the water table is the piezometric surface for the 130 m to 250 m depth interval (unconfined), it is possible to approximate the average permeability of the sediments in the 130-250 m interval. In order to do this, the volumetric velocity calculated using convective heat flow has to be converted to the true or darcian velocity if the same volume of water flows through a porous medium. The vertical darcian velocity was calculated by dividing 4.6 cm/year (volumetric velocity) by the effective porosity or specific yield of the rock between 130 m and 250 m. Since core samples were not taken from this zone it was necessary to estimate the effective porosity from lithology logs of cuttings. Using .25 for the effective porosity, a vertical darcian velocity of 18.4 cm/year was calculated.

Assuming that the water table gradient is roughly the same as the elevation drop of the Gila River with linear map distance, a lateral velocity may be approximated by dividing the darcian vertical velocity (18.4 cm/year) by the water-table gradient (.27 percent). The approximate lateral darc-

cian water velocity is 6815 cm/year. Using this lateral darcian velocity the permeability of the sediments in Clifton 1 was calculated to be 1.0396×10^3 darcys by applying Darcy's Law.

$$k = \frac{v_d \mu}{\rho g \frac{\partial H}{\partial l}} \qquad (4)$$

where

v_d = darcian water velocity, 6815 cm/year or 1.161×10^{-4} cm/sec

μ = viscosity of water, 0.1 gm/cm sec

ρ = density of water, 1.0 gm/cm^3

g = gravity, 780 cm/sec^2

$\frac{\partial H}{\partial l}$ = water table gradient, .0027 or 14 feet/mile

k = permeability, 1.026×10^{-5} cm^2 or 1.0396×10^3 darcys

1 darcy = 9.87×10^{-9} cm^2

The permeability estimated from the heat flow data indicates that a very good aquifer exists between 130 m and 250 m.

All of the measured heat-flow values in the Clifton area except HF1 are significantly influenced by local or regional water flow. The low heat-flow values indicate lateral and downward water flow in permeable recharge areas. In order to conserve energy, the heat losses due to groundwater recharge are balanced by heat gains in discharge areas. Discharge may occur by lateral-subsurface flow out of the area, or by springs discharging at the surface or into through-flowing rivers. Conservation of mass is required too. Water that is recharging aquifers or flowing into the subsurface must exit somewhere.

The hot springs around Clifton are part of the conservation-of-mass-and-energy processes in the area.

The convective heat loss at Clifton Hot Springs is calculated using equation 5. A spring discharge temperature of 50°C is used to give a conservative figure.

$$Q = C\dot{m}\Delta T \quad \text{(Kilty and others, 1979)} \quad (5)$$

where

Q = convective heat loss, cal/sec

C = heat capacity of water, 1.0 cal/gm°C

$\dot{m}$ = mass discharge rate, 63 l/sec (Hem, 1950)

ΔT = difference of spring discharge and mean annual temperature 50°C - 19°C = 31°C, (Hem, 1950; Swanberg, other, 1977; Witcher, 1979; Sellers, and Hill, 1974)

The minimum convective heat loss is 1.95×10^6 cal/sec or 8 megawatts. Additional conductive heat loss associated with hot springs may range up to 30 percent of the convective heat loss (Kilty and others, 1979). If the 2.25 HFU observed in HF1 is used as the regional heat flow, a recharge area of 85 km^2 is required to balance the convective heat loss by the springs. However, since downward-flowing water accounts for (removes) only about 50 percent of the heat (average heat flow of 1.0 HFU versus 2.25 HFU regional value), a minimum recharge area of 170 km^2 is required to conserve heat. Therefore, the low measured-heat-flow values probably reflect part of the recharge for the geothermal systems in the area. The highly variable topography, precipitation, and permeable rock in the Clifton area result in forced convective systems that circulate water to great depth and heat it by regional heat flow.

Where the piezometric surface, topography, and vertically permeable zones coincide, these systems are visible as hot springs.

Additional heat flow, geologic and hydrologic studies are needed to adequately understand the systems in the area and determine the exact reservoir locations and heat contents. Also, radiogenic heat production data on the granite is needed to determine the source of heat for the regional heat flow.

Additional heat-flow holes should be drilled in three different geologic settings. First, shallow (30 m) holes should be drilled to profile heat flow in the hot-spring areas. Second, one or two deeper (100-300 m) holes should be drilled into Precambrian granite to confirm the 2.25 HFU regional value. Third, one or two heat-flow holes (300-500 m) should be drilled into the volcanic sequence north of Clifton to quantify regional water flow and heat loss due to recharge in the extensive volcanic sequence. These data are absolutely necessary prior to siting and drilling a production or test well in the inferred high-temperature reservoir in the Clifton area. These heat flow data will show the heat contents of the systems, provide data for estimates of potential production rates from geothermal wells, and the best locations for shallow production wells.

REFERENCES

Berry, R.C., 1976, Mid-Tertiary volcanic history and petrology of the White Mountains volcanic province, southeastern Arizona: Unpub. PhD. Thesis, Princeton University, 317 p.

Bredehoeft, J.D. and Papadopulos, I.S., 1965, Rates of vertical groundwater movement estimated from the earth's thermal profile: Water Resources Research, Vol. 1, No. 2, pp. 325-328.

Domenico, P.A. and Palciauskas, V.V., 1973, Theoretical analysis of forced convective heat transfer in regional groundwater flow: Geol. Soc. Amer. Bull., Vol. 84, pp. 3803-3814.

Elston, W.E., 1958, Burro uplift, northeastern limit of sedimentary basin of southwestern New Mexico and southeastern Arizona: Amer. Assoc. Petrol. Geol. Bull., Vol 42, pp. 2513-2517.

Harbour, J., 1967, Stratigraphy and sedimentology of the upper Safford Basin sediments: Unpub. PhD. Thesis, University of Arizona, 242 p.

Heindl, L.A., 1958, Cenozoic alluvial deposits of the upper Gila River area, New Mexico and Arizona: Unpub. PhD. Thesis, University of Arizona, 249 p.

Hem, J.D., 1950, Quality of water of the Gila River above Coolidge Dam, Arizona: U.S. Geol. Survey Water-Supply Paper 1104, 230 p.

Kilty, K.S., Chapman, D. S. and Mase, C.W., 1979, Forced convective heat transfer in the Monroe Hot Springs geothermal system: Jour. of Volcanology and Geothermal Res., Vol. 6, pp. 257-277.

Lachenbruch, A.H. and Sass, J.H., 1977, Heat Flow in the United States and the thermal regime of the crust: Amer. Geophysical Union Monograph 21, pp. 626-675.

Langton, J.M., 1973, Ore genesis in the Morenci-Metcalf District: AIME Transactions, Vol. 254, pp. 248-257.

Lindgren, W., 1905, The copper deposits of the Clifton-Morenci District, Arizona: U.S. Geol. Survey Prof. Paper 43, 375 p.

Mansure, J. and Reiter, M., 1979, A vertical groundwater movement correction for heat flow: Jour. Geophysical Res., Vol. 84, No. B7, pp. 3490-3496.

Mariner, R. H., Presser, D.D. and Evans, W.C., 1977, Chemical, isotopic, and gas compositions of selected thermal springs in Arizona, New Mexico, and Utah: U.S. Geol. Survey Open-File Report 77-654, 42 p.

McKee, E.D., 1951, Sedimentary basins of Arizona and adjoining area: Geol. Soc. Amer. Bull, Vol. 62, pp. 481-506.

Moolick, R.T. and Durek, J.J., 1966, The Morenci District, in Geology of the Porphyry Copper Deposits, Southwestern North America, Edited by S.R. Titley and C.R. Hicks: University of Arizona Press, pp. 221-233.

Morgan, P., Swanberg, C.A., and Lohse, R.L., 1979, Borehole temperature studies of the Las Alturas geothermal anomally, New Mexico in Expanding the Geothermal Frontier, Geothermal Resources Council Transactions, Vol. 3, pp. 469-472.

Morrison, R.B., 1965, Geologic map of the Duncan and Canador Peak Quadrangles and New Mexico: U.S. Geol. Survey Miscellaneous Geologic Investigations map I-442, 1:48,000, Text 7 p.

Pierce, H.W., 1976, Elements of Paleozoic tectonics in Arizona: Arizona Geological Society Tectonic Digest, Vol. X, pp. 37-57.

Rantz, S.E. and Eakin, T.E., 1971, A summary of methods for the collection and analysis of basic hydrologic data for arid regions: U.S. Geol. Survey Open-File Report, 125 p.

Reiter, M. and Shearer, C., 1979, Terrestrial heat flow in eastern Arizona, A first report: Jour. of Geophysical Res., Vol. 84, No. B11, pp. 6115-6120.

Ross, C.A., 1973, Pennsylvanian and early Permian depositional history, southeastern Arizona: Amer. Assoc. Petrol. Geologists Bull., Vo. 57, p. 887-912.

Sass, J.H., Lachenbruch, A.H. and Munroe, R.J., 1971, Thermal conductivity of rocks from measurements on fragments and its application to heat flow determination: Jour. Geophysical Res., Vol. 76, pp. 3391-3401.

Sellers, W.D. and Hill, R.H. Ed., 1974, Arizona climate 1931-1972 revised 2nd edition: University of Arizona Press, 616 p.

Swanberg, C.A., Morgan, P., Stoyer, C.H. and Witcher, J.C., 1977, An appraisal study of the geothermal resources of Arizona and adjacent areas in New Mexico and Utah and their value for desalination and other uses: New Mexico Energy Institute Report 6, New Mexico State University, 76 p.

Turner, G.L., 1962, The Deming Axis, southeastern Arizona, New Mexico and Trans-Pecos, Texas: New Mexico Geological Society Guidebook-Mogollon Rim, 13th Field Conference, 1962, pp. 59-71.

Witcher, J.C., 1979, A progress report of geothermal investigations in the Clifton area in Geothermal Site Evaluation in Arizona, semi annual progress report for period July 1978-January 1979, D.O.E. contract EG-77-S-02-4362, pp. 26-41.

Table 1 Heat Flow Data in the Clifton, Arizona Area

Heat Flow Hole	Morenci[1]	HF1	HF2	Clifton 1
Latitude Degrees	33° 05'	33° 5.9'	33° 2.7'	32° 56.7'
Longitude Degrees	109° 22'	109° 21.1'	109° 22.0'	109° 13.8'
Township section, township, range	sec. 16 T. 4S., R. 29E	NW¼, SE¼ sec. 10, T. 4S., R. 29E.	NE¼, NW¼, sec. 33, T. 4S., R. 29E.	NE¼, NE¼, sec. 1, T. 6S., R. 30E.
Elevation Meters	1296	1445	1341	1097
Mean Annual* Temperature °C	17.4	16.0	16.6	19.0
Thermal Gradient °C/km (Depth Interval)	22.7 ± 0.1 (340–580 m) 22.2 ± 0.6 (600–660 m)	25.8 (70–185 m) 23.0 (300–365 m)	9.4 (60–100 m) 16.1 (105–140 m)	12 (135–140 m) 20.0 (250–255 m)
Thermal Conductivity 10^{-3} cal/cm-sec-°C (Depth Interval)	6.1 ± 0.2 (340–580 m) 7.7 ± 0.9 (600–660 m)	8.73 ± .47 (70–185 m) 9.93 ± 1.7 (300–365 m)	10.4 (60–100 m) 6.5 (105–140 m)	4.3 (135–140 m) 4.5 (250–255 m)
Heat Flow 10^{-6} cal/cm^2-sec (Depth Interval)	1.4 (340–580 m) 1.7 (600–660 m)	2.25 (70–185 m) 2.28 (300–365 m)	0.98 (60–100 m) 1.05 (105–140 m)	0.51 (135–140 m) 0.98 (250–255 m)
Type Sample	Core	Fragments	Fragments	Fragments
Lithology	granite ?	granite	orthoquartzite, dolomitic sandstone, granite	Coarse clastic sediment derived mostly from intermediate volcanics.

(1) Data from Reiter and Shearer, 1979.

*Obtained by interpolating mean annual temperatures from drill hole elevations using local weather station elevations and average temperatures.

Figure 2

P-€	Precambrian granite and granodiorite some schist and metaquartzite
P	Paleozoic sediment lower section consists of arkose and orthoquartzite grading upward into sandy dolomite interbedded with shale, middle and upper section is mostly limestone or dolomite with minor shale
K	Late Cretaceous sediment
Ki	Late Cretaceous to early Tertiary (Laramide) intrusives diorite, monzonite and granite associated with copper mineralization at Morenci
Tdl	Tertiary calc-alkaline volcanics, mostly andesite with some rhyolite, rhyolite breccia and ash flow tuff, Datil Group equivalent (40-28 my)
Tba	Tertiary basaltic andesite, Bearwallow Mountain equivalent (post 28 my)
Ts	Tertiary, mostly volcanoclastic sediment, includes some ash and tuff, and some basaltic andesite flows, nearly flat lying to moderate dips.
Tr	Tertiary rhyolite, rhyolite breccias and tuffs, contemporaneous with the latest basaltic andesite flows
Tg	Tertiary "Gila Conglomerate," basin fill sediment includes Quaternary alluvial sediment

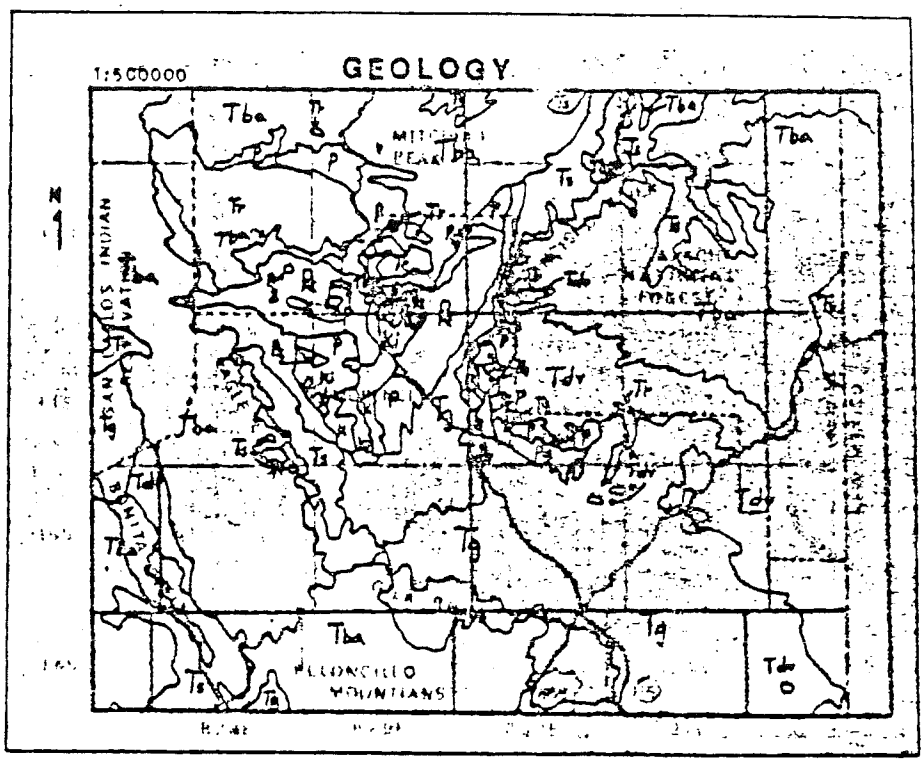

	Normal fault (dashed where inferred)
	Low angle fault, thrust or gravity fault (teeth point to upper plate)
	Possible ring fracture zone of Enebro Mountain caldera (Berry, 1976)
	Tertiary rhyolite, rhyolite breccias and tuffs (early Miocene)
	Clifton-Morenci horst

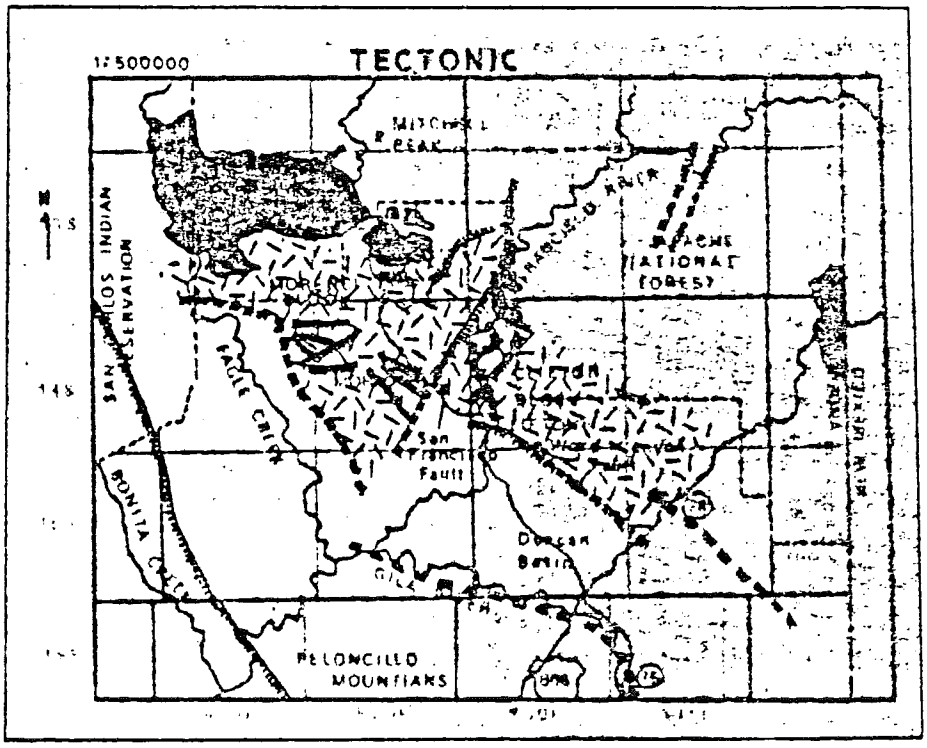

Figure 3

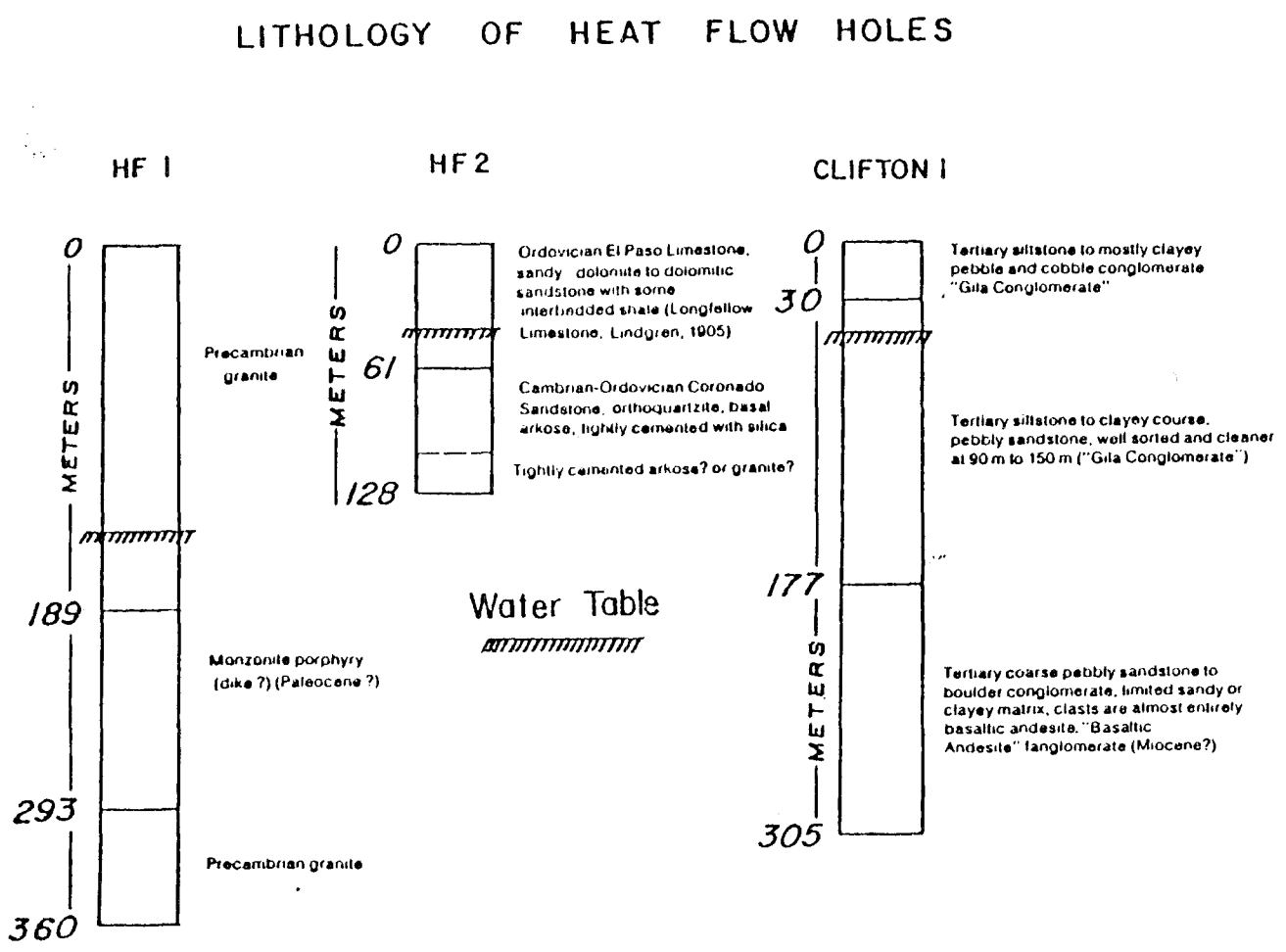
LITHOLOGY OF HEAT FLOW HOLES
HF 1
HF 2
CLIFTON I
METERS
0
189
293
360
Precambrian granite
Monzonite porphyry (dike ?) (Paleocene ?)
Precambrian granite
0
61
128
Ordovician El Paso Limestone, sandy dolomite to dolomitic sandstone with some interbedded shale (Longfellow Limestone, Lindgren, 1905)
Cambrian-Ordovician Coronado Sandstone, orthoquartzite, basal arkose, highly cemented with silica
Tightly cemented arkose? or granite?
Water Table
0
30
177
305
Tertiary siltstone to mostly clayey pebble and cobble conglomerate "Gila Conglomerate"
Tertiary siltstone to clayey course, pebbly sandstone, well sorted and cleaner at 90 m to 150 m ("Gila Conglomerate")
Tertiary coarse pebbly sandstone to boulder conglomerate, limited sandy or clayey matrix, clasts are almost entirely basaltic andesite. "Basaltic Andesite" fanglomerate (Miocene?)

Figure 4

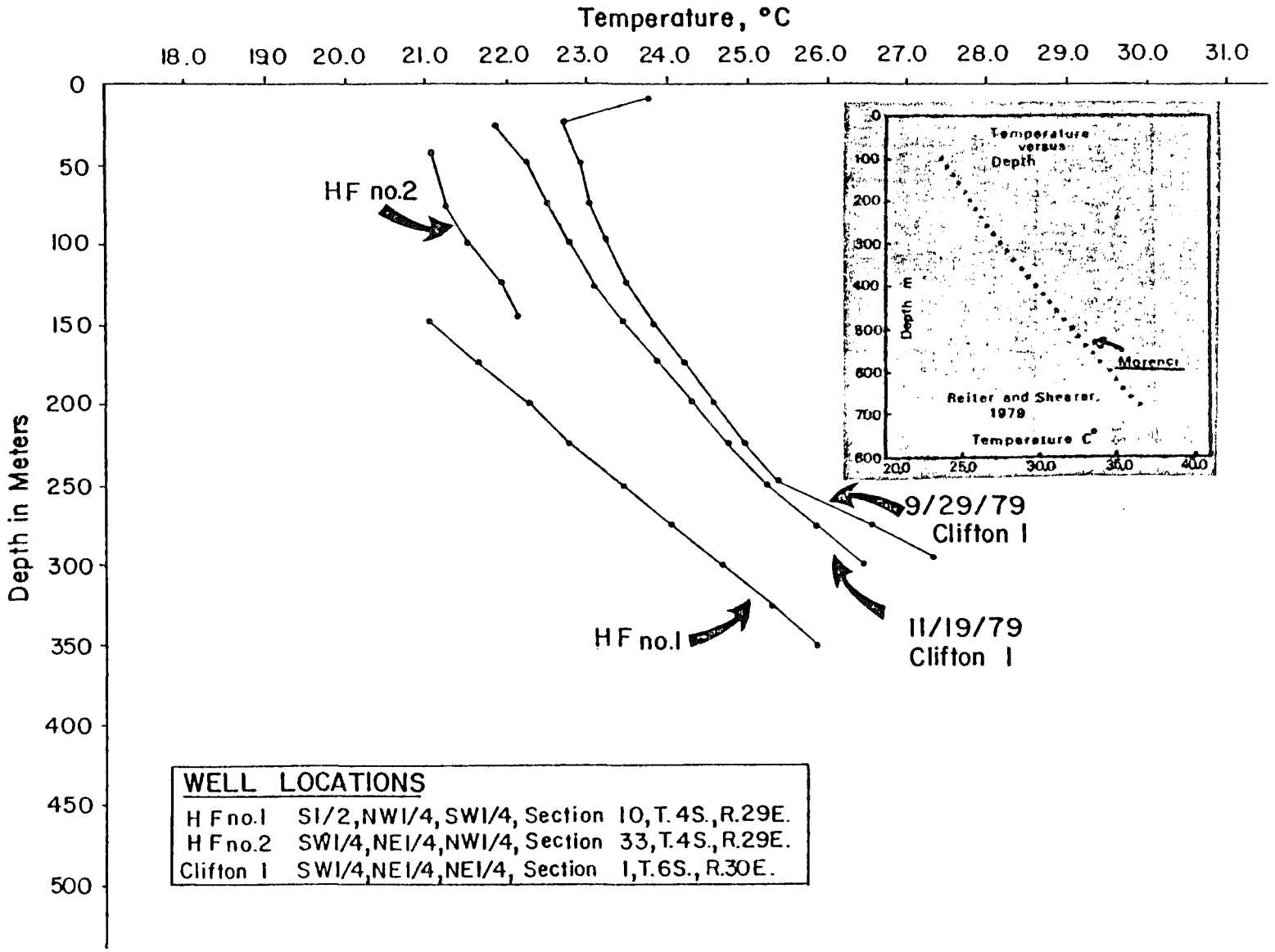

Temperature logs of drill holes in the Clifton, Arizona area.

Figure 5

Heat Flow Data for HF1 Drill Hole

Depth Meters	Temperature Gradient °C/km	Temperature °C	Thermal Conductivity 10^{-3}cal/cm-sec-°C	Heat Flow 10^{-6}cal/cm^2-sec
75	28.7	19.07	8.74	2.10
105	24.0	19.80	8.26	1.98
180	25.7	21.78	7.48	1.92
220	22.7	22.62	8.24	1.87
240	24.3	23.09	5.92	1.44
280	25.3	24.18	7.04	1.78
290	24.7	24.43	6.52	1.61
320	23.7	25.19	8.72	2.06
355	20.0	25.89	11.13	2.23

Cross section of Hypothesized Geology in HF1

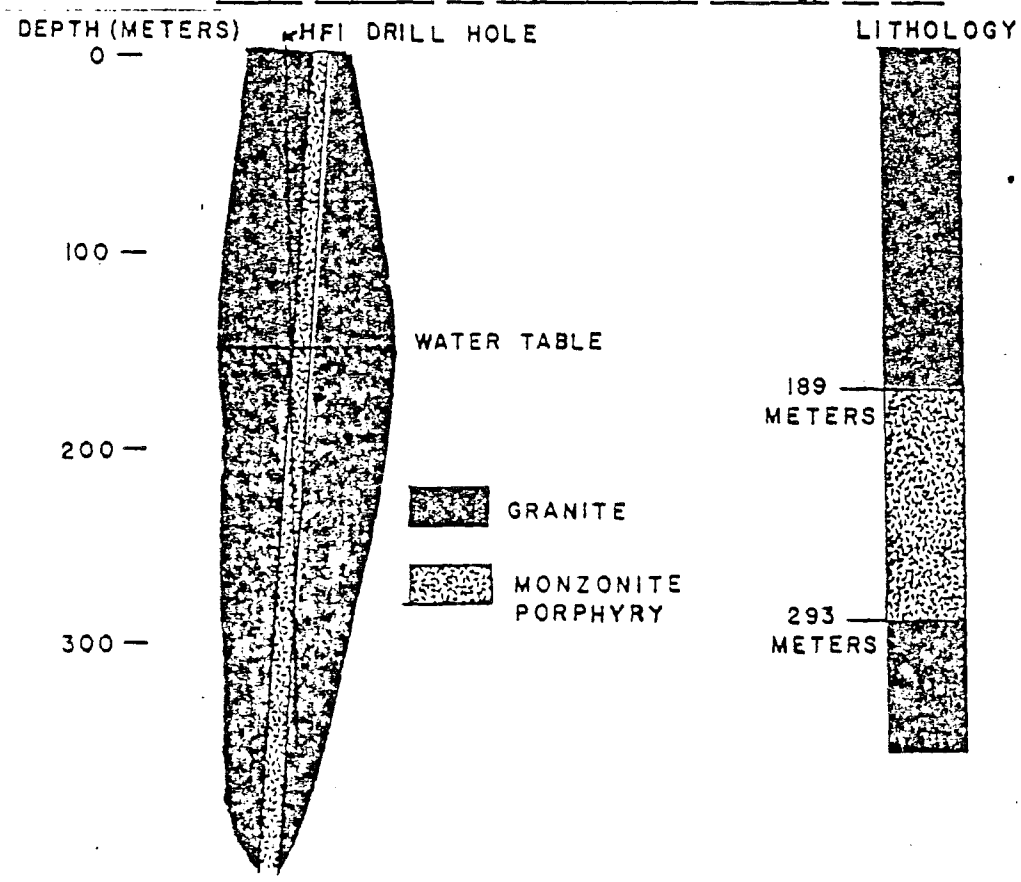

Note: The HF1 heat flow data in Table 1 are mean values for conductivities and temperature gradients calculated over the reported depth intervals. The heat flows in this figure are slightly different because they were calculated for each depth interval without averaging the data.

Figure 6

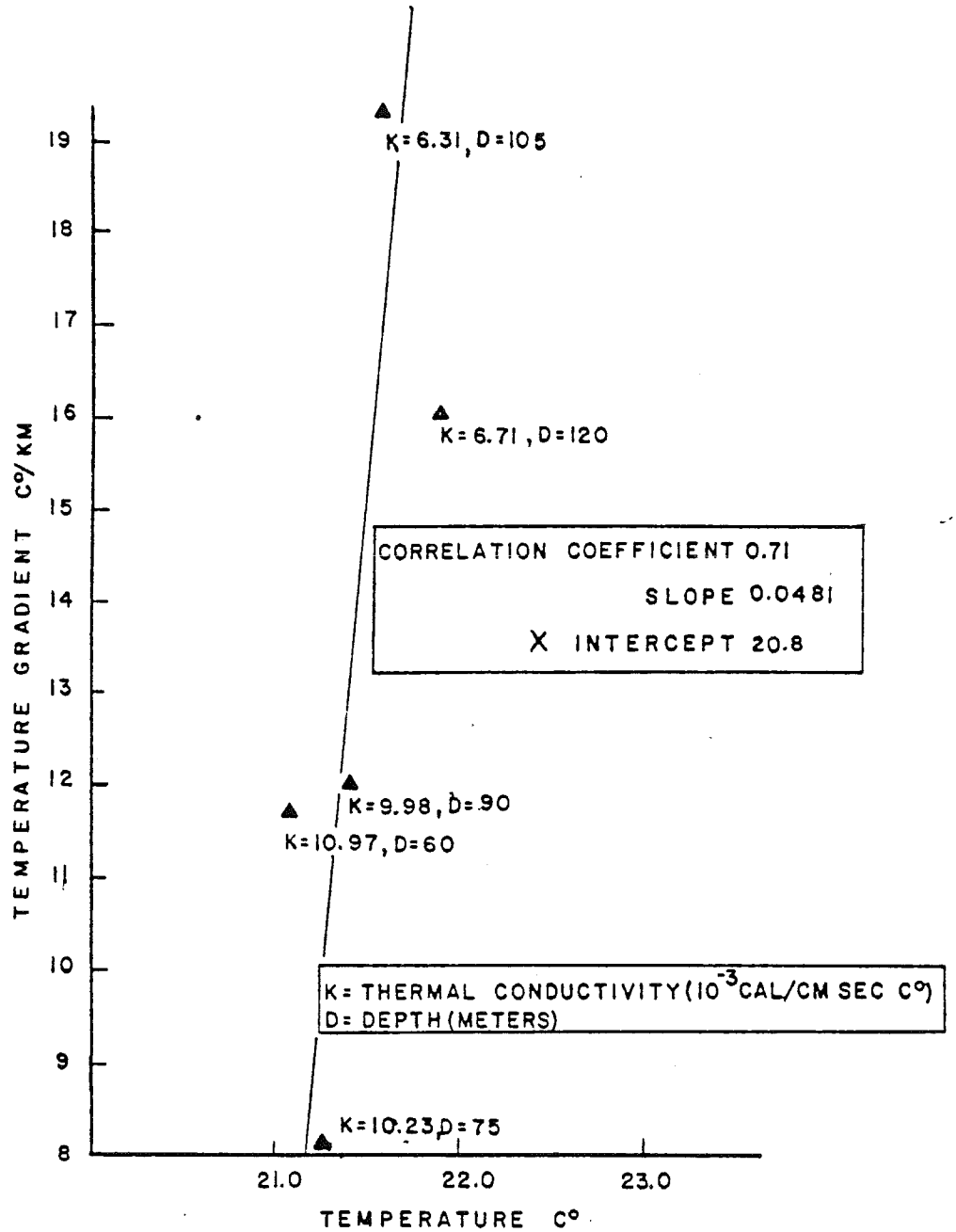

TEMPERATURE VERSUS TEMPERATURE GRADIENT
HF 2

Figure 7

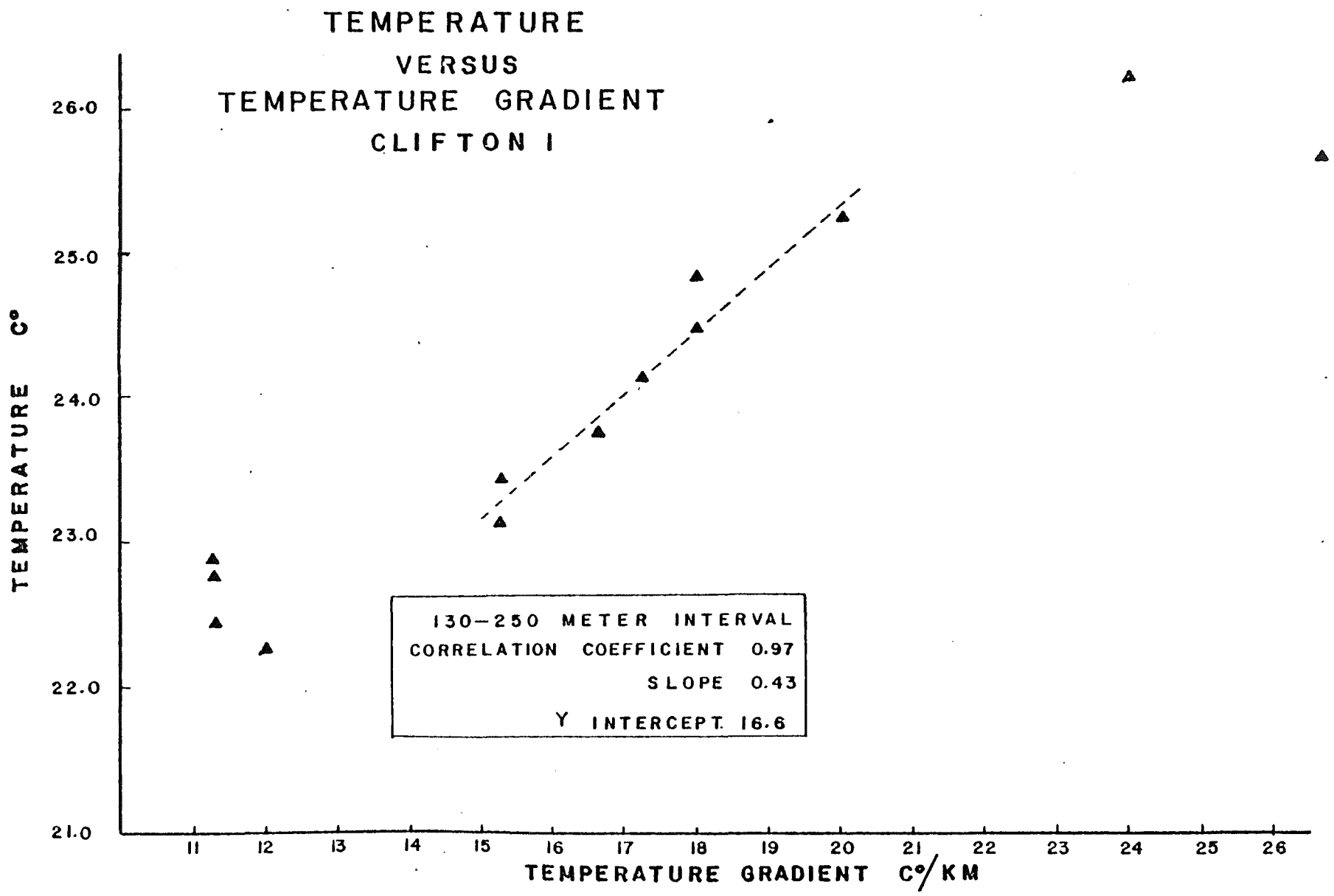
TEMPERATURE
VERSUS
TEMPERATURE GRADIENT
CLIFTON I
TEMPERATURE C°
26.0
25.0
24.0
23.0
22.0
21.0
11
12
13
14
15
16
17
18
19
20
21
22
23
24
25
26
TEMPERATURE GRADIENT C°/KM
130–250 METER INTERVAL
CORRELATION COEFFICIENT 0.97
SLOPE 0.43
Y INTERCEPT 16.6

Figure 8

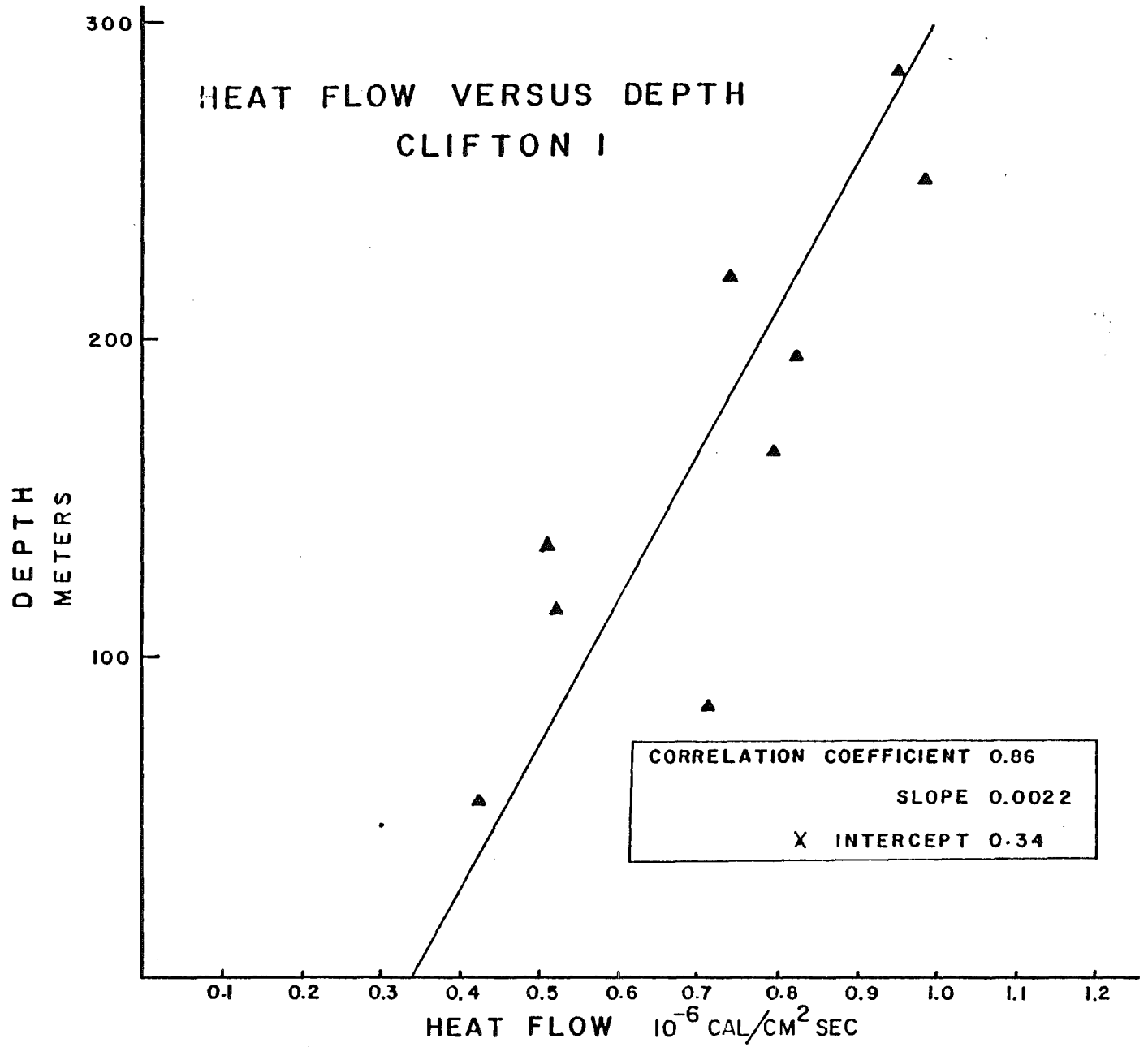
HEAT FLOW VERSUS DEPTH
CLIFTON I
DEPTH
METERS
300
200
100
0.1
0.2
0.3
0.4
0.5
0.6
0.7
0.8
0.9
1.0
1.1
1.2
HEAT FLOW 10^{-6} CAL/CM^2 SEC
CORRELATION COEFFICIENT 0.86
SLOPE 0.0022
X INTERCEPT 0.34